TECHNICAL UNIVERSITY OF CRETE
ELECTRONIC & COMPUTER ENGINEERING DEPARTMENT
TELECOMMUNICATIONS DIVISION
2009-2010

Study of OFDM-SDMA Systems and Implementation in SDR

By:
Georgios L. Sklivanitis
gsklivanitis@telecom.tuc.gr

Submitted on October 6th, 2010 in partial fulfilment of the requirements for the Electronic and Computer Engineering diploma degree.

Advisor: Professor Athanasios Liavas
Co-advisor: Assistant Professor Georgios Karystinos
Co-advisor: Assistant Professor Aggelos Bletsas

Abstract

The combined OFDM/SDMA approach has raised significant research interests recently as it appears to be quite suitable for future broadband wireless transmission. In order to build practical OFDM/SDMA systems, we need to evaluate such systems under real-world conditions. The presence of carrier frequency offsets, caused by inaccuracies of local oscillators between transmitter and receiver stations, which destroy the orthogonality among OFDM sub-carriers and induce inter-carrier-interference in conjunction with MIMO transmission where different users interfere with each other, strongly degrades the signal detection performance if it is not compensated appropriately. In this thesis, the impact of CFO on the performance of an uplink OFDM/SDMA system is analyzed. We describe a combined scheme for joint CFO and channel estimation, CFO correction and multi-user signal detection in frequency domain. Finally, we explore the viability of using GNU Radio; an open source Software Defined Radio (SDR) implementation and the Universal Software Radio Peripheral (USRP); an SDR hardware platform, to transmit and receive the OFDM radio signals with 4-QAM modulation. Bit error rate (BER) in terms of Signal to Noise Ratio (SNR) in an indoor environment is investigated and analyzed.

Acknowledgements

I would like to take some time here and thank people who made the completion of this work possible.

First of all, my parents, who supported me morally and financially throughout all my undergraduate studies. Additionally, I am deeply grateful to my advisor Professor Athanasios Liavas, who has oriented and supported me with promptness and care and have always been patient and encouraging in times of difficulties. I also feel very privileged to get to know and collaborate with Assistant Professor Aggelos Bletsas, whose technical excellence and tremendous grasp of experimental issues had a great impact on me.

I am also indebted to the postgraduate students, Manolis Matigakis and Ioannis Kardaras with whom I had the pleasure to work with. Their support has been invaluable and also helped me learn how to tackle new problems and develop techniques to solve them.

"Innovation distinguishes between a leader and a follower." - Steve Jobs

Contents

List of Figures

List of Tables

Preface

Most of the code in Matlab and Python used to generate the figures in this thesis, along with some documentation, is available at `http://users.isc.tuc.gr/~gsklivanitis/`.

A Note on Notation

Bold lowercase letters denote column vectors, e.g.:

$$\mathbf{d} = \begin{bmatrix} d[0] & d[1] & \dots & d[N_c-1] \end{bmatrix}^T.$$

The superscript $(\cdot)^H$ means "Hermitian transpose", $(\cdot)^{-1}$ denotes the matrix inverse while the superscript $(\cdot)^T$ means "transpose".

Bold uppercase letters denote matrices, e.g.:

$$\tilde{\mathbf{H}}[n] = \begin{bmatrix} h_1^1[n] & h_1^2[n] & \dots & h_1^U[n] \\ h_2^1[n] & h_2^2[n] & \dots & h_2^U[n] \\ \vdots & \ddots & \vdots & \\ h_A^1[n] & h_A^2[n] & \dots & h_A^U[n] \end{bmatrix}.$$

Calligraphic uppercase letters denote sets, e.g.:

$$\mathcal{Y}' = \{y'[0], y'[T_s], \dots, y'[(N_c+2L-2)T]\}.$$

The $\square$ symbol is used as an end-of-lemma symbol.

Operator vec$(\cdot)$ account for column-by-column vectorization of a matrix.

Operator $\odot$ denotes the Hadamard product which is defined as the element-by-element multiplication between either two matrices or vectors of the same dimensions.

Operator $\otimes$ denotes Kronecker product.

We write $\mathrm{diag}(\mathrm{a}_1, \dots, \mathrm{a}_\mathrm{n})$ for a diagonal matrix whose diagonal entries starting in the upper left corner are $a_1, \dots, a_n$.

Chapter 1

Introduction

Wireless local access networks (WLANs) provide user mobility, inexpensive network installation and significant reconfiguration capabilities compared to their wired counterparts. However, the growing demand for high speed wireless Internet access has led to extensive research on systems with fine ability to combat channel multipath and to provide high spectral efficiency [3].

Orthogonal frequency division multiplexing (OFDM) has become a popular technique in broadband wireless communications due to its capability to mitigate channel selectivity while providing a high spectrum efficiency. The wireless channel features multipath propagation, characterized by its delay spread. Due to the envisaged high data rates, the multiple paths give rise to intersymbol interference (ISI), which distorts the signal. In OFDM, data is carried over a large number of parallel sub-carriers instead of a single carrier.

OFDM modulation with cyclic prefix insertion mitigates ISI by extending the symbol period as the data are multiplexed on orthogonal sub-carriers [3]. As such, it converts a frequency selective channel into a number of parallel flat fading channels which can be easily equalized. Furthermore, the demodulation can be executed efficiently via the fast Fourier transform (FFT).

OFDM is the preferred modulation type for high-rate WLAN applications and has been adopted in WLAN applications such as IEEE 802.11a. The specific modulation type has also been successfully applied to a wide variety of digital communication applications over the past several years including TV broadcasting, digital audio broadcasting, Asynchronous Digital Subscriber Line (ADSL) modems and wireless networking worldwide. Its application in mobile communication is more complex especially because of the mobility of the user; thus more exact symbol timing and frequency offset control must be used to ensure that sub-carriers remain orthogonal.

Space division multiple access (SDMA) provides high bandwidth efficiency which is crucial because of spectral limitations. It is well known that system capacity can be further increased by spatial division multiple access (SDMA), in which more than one user can be accommodated on the same sub-carrier at the same time. Due to the wide angular spread of the received signals in indoor environments, we cannot rely on beamforming and wideband SDMA is needed. Essentially, SDMA can further improve spectrum efficiency by reusing the bandwidth among different users with independent spatial signatures. Moreover, the inherent parallelism of the

OFDM systems allows per-sub-carrier SDMA processing, resulting in a considerably lower implementation cost than the single-carrier SDMA systems. Hence, the OFDM-SDMA systems are considered quite suitable for future wireless broadband networks, for the combined OFDM-SDMA approach can benefit from the advantages of both OFDM and SDMA [4].

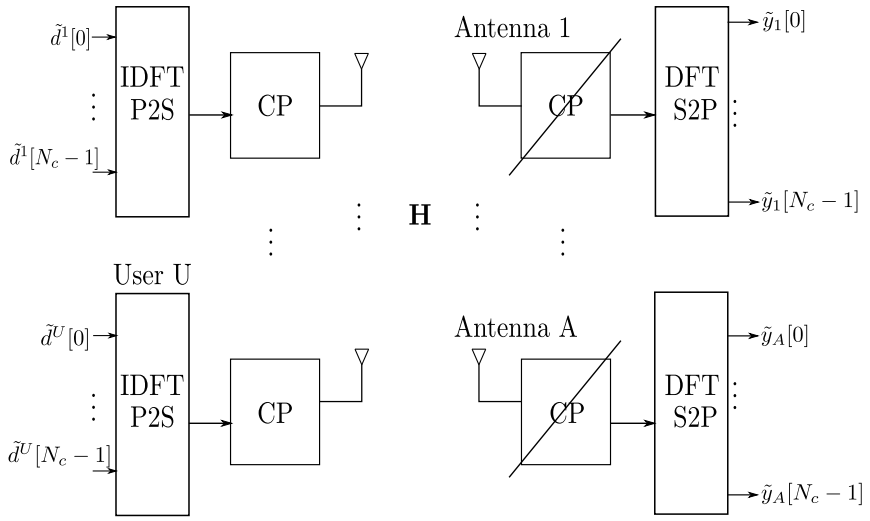

Figure 1.0.1: OFDM-SDMA block diagram.

Furthermore, OFDM-SDMA does not require perfect synchronization among user. However, while making use of the benefits, the combination of OFDM and SDMA also inherits the disadvantages from each technique. In such systems, separate base stations and mobile terminals suffer from inaccuracies in terms of synchronization mismatches in time and frequency. Timing offsets are caused by propagation delays through transmission channels. Carrier frequency offsets (CFOs) exist between user terminals and the base station (BS) because of the precision limitation of oscillators and the Doppler effect. It has been shown that OFDM systems are very sensitive to CFO, which leads to performance degradation by introducing inter-carrier-interference (ICI) [5]. For uplink OFDM-SDMA systems, different CFO from multiple users should be considered, and analysis can be found in [15]. Additionally, in an uplink OFDM-SDMA system, channel output received signals from different users should be separated by multi-user detection, where its performance relies on channel estimation accuracy, which can also be affected by the CFO. Therefore, when consider channel estimation, without compensating the CFO impact, the system's performance degradation may be significant. Although various works on studying the impact of CFO in OFDM-SDMA systems [15], [16], [8] have been carried out and results over systems' performance degradation have been presented, all of them were based on simulation and not on experimental procedure.

In this thesis, we first introduce OFDM systems. Next, we derive the system model for the Single-Input Single-Output (SISO) case as well as for the Single-Input Multiple-Output (SIMO) case. The impact of CFO on both system models is our next checkpoint, with which the chapter concludes.

In the following chapter, we consider the OFDM-SDMA system setup. After defining the sys-

tem model, we also examine in this case the CFO's impact which is expected to be significant.

The problem of time synchronization is considered next. We introduce simple packet synchronization problem solutions for the simple OFDM SISO case for ideal and non-ideal channels. The chapter continues with a further analysis of the problems mentioned before in the case we deal with OFDM-SDMA systems where a number of multiple users U transmit and a base station equipped with A antennas receive. Chapter 3, is concluded with a report about the impact of CFO on our attempt to estimate the output packet at the receiver.

In the sequel, we present joint maximum likelihood CFO and channel estimation for OFDM-SDMA systems based on CFO estimation for transmissions over selective channels [6].

Our discussion of OFDM-SDMA systems is concluded in chapter 6, where CFO compensation and detection algorithms such as zero-forcing and maximum likelihood are described.

The next chapter, introduces us the terms "Software Defined Radio" (SDR) and "Universal Software Radio Peripheral" (USRP). Information relative to the hardware as well as the software which was used in order to interface the USRP to a personal computer is also provided. In the final section of this chapter, we focus on the experimental setup of the SDR testbed we set, in order to make feasible the implementation of all algorithms mentioned above.

In the last chapter, simulation and experimental results are given along with all the necessary parameters used in terms of evaluating our system's performance. We also discern the case where the users U transmitting are synchronized or not.

Chapter 2

Basic Concepts

In this chapter, we introduce Orthogonal Frequency Division Multiplexing (OFDM) systems, as well as the Single-Input Single-Output (SISO) case and Single-Input Multiple-Output (SIMO) case. Moreover, we derive some fundamental principles as far as the transmitter and the receiver are concerned for both of the cases above.

2.1 Basic OFDM

In wideband wireless communications, the channel's power spectrum is not constant in the entire frequency band. OFDM divides a frequency selective channel into many pieces by frequency called sub-channels, with each of the sub-channels consisting of sub-carriers. The sub-carrier spacing is carefully selected so that each carrier is located on all the other carrier's spectra zero crossing points, and each sub-channel's power spectrum is constant. This is explained in 2.1.1. OFDM utilizes the transmission channel more efficiently than Frequency Division Multiplexing Access which is its predecessor.

The main advantage of OFDM is that it converts a wideband channel into N_c parallel narrowband channels. The sub-carriers are flat fading which enables them to overcome frequency selective multipath fading. As a result, no-equalization is required which is a rather computational costly procedure but only symbol-by-symbol detection.

Additionally, it offers spectral efficiency, resiliency to RF interference and mitigates multipath distortion, which lead to simplified processing at the receiver.

However, OFDM is subject to the system's linearity and synchronization. It needs more exact frequency offset controlling to ensure that the sub-carriers are orthogonal. Otherwise, the interference of different sub-carriers will lead to a high bit error probability. In mobile communication, schemes that deliver exact synchronization are hard to implement, especially in high data rate at high moving speed.

In OFDM systems, multiple signals are sent out at the same time but on different frequencies. When multiple versions of the signal interfere with each other (intersymbol interference (ISI)),

it becomes hard to extract the original information.

2.1.1 Transmitter

2.1.1.1 Sub-carrier Allocation

Many signals are analog or time continuous in nature. Such signals can be converted to digital or discrete form in order to improve the noise resistance. Consequently, many transmission systems make use of digital modulation techniques. QAM is one of such techniques. It utilizes the mathematical property that input signals are divided and carried on different components of a single carrier wave, and at the receiver they are resolved successfully into inputs. It is also desirable for high data rate performance.
The data symbols are then mapped into OFDM symbols, i.e., they are assigned to different sub-carriers on an OFDM symbol such that they are evenly spaced.
It will definitely become more clear from the following sections that our channel input will be the augmented sequence we get from the cyclic prefix added to the vector

$$\mathbf{d} = \mathbf{U}\tilde{\mathbf{d}} \tag{2.1}$$

where $\mathbf{U}$ is the matrix which implements the Inverse Discrete Fourier Transform (IDFT). More specifically the (k, l) element of the matrix $\mathbf{U}$ is

$$[\mathbf{U}]_{k,l} = \frac{1}{\sqrt{N_c}} e^{\frac{j2\pi(k-1)(l-1)}{N_c}}, \qquad k, l = 1, \ldots, N_c. \tag{2.2}$$

If we define as $\mathbf{U}_l$ the lth column of the matrix $\mathbf{U}$ then $\mathbf{d}$ can be expressed as

$$\mathbf{d} = \sum_{l=1}^{N_c} \mathbf{U}_l \tilde{d}[l]. \tag{2.3}$$

If we write analytically $\mathbf{U}_l$ we get

$$\mathbf{U}_l = \begin{bmatrix} 1 & e^{\frac{2\pi(l-1)}{N_c}} & e^{\frac{2\pi 2(l-1)}{N_c}} & e^{\frac{2\pi 3(l-1)}{N_c}} & \ldots & e^{\frac{2\pi(N_c-1)(l-1)}{N_c}} \end{bmatrix}^T. \tag{2.4}$$

As a consequence, $\mathbf{U}_l$ is part of a discrete time sinusoid signal of infinite length and frequency $f_l = \frac{(l-1)}{N_c}$. If $\mathbf{U}_l$ are of infinite length, then our channel output would be a sinusoidal signal with the same frequency but probably with different phase and amplitude. On the contrary, we have to deal with finite length, therefore, in order to have the same result, we have to add the cyclic prefix at the transmitter.
Thereupon, we can assume the input $\mathbf{d}$ as a linear combination of orthogonal codes $\mathbf{U}_l$ with coefficients the transmitted symbols $\tilde{d}[l]$. Because our system input is expressed with the multiplication of the transmitted symbols $\tilde{d}[l]$ with the vector $\mathbf{U}_l$, we can say that the symbol $\tilde{d}[l]$ is carried by the sub-carrier f_l.

When the OFDM symbols are stacked up into the frame, they are then converted to time domain using the Inverse Discrete Fourier Transform (IDFT). An efficient way of implementing

IDFT is IFFT (Inverse Fast Fourier Transform). IFFT is useful for OFDM because it generates samples of a waveform with frequency components satisfying orthogonality conditions, i.e., the IFFT modulates each sub-channel onto a precise orthogonal carrier.

The IDFT of the input vector $\tilde{\mathbf{d}} = \left[\begin{array}{ccc} \tilde{d}[0] & \dots & \tilde{d}[N_c-1] \end{array} \right]^T$ is given by

$$d[n] = \frac{1}{N_c} \sum_{m=0}^{N_c-1} \tilde{d}[m] e^{\frac{2\pi j}{N_c} mn}, \qquad n = 0, \dots, N_c - 1. \tag{2.5}$$

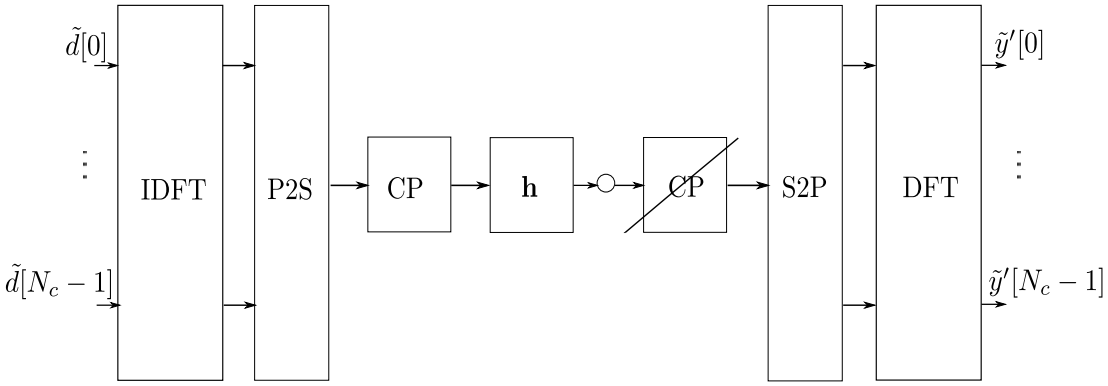

Figure 2.1.1: OFDM SISO block diagram.

2.1.1.2 Cyclic Prefix (CP)

Cyclic prefix is used in OFDM to combat intersymbol interference (ISI). The basic idea is to copy part of the OFDM time-domain waveform from the back of the signal to the front to create a guard period where the duration of the guard time is chosen such that it is longer than the worst-case delay spread of the targeted multipath environment.

Studying the discrete model case, given a block of time-domain data length N_c

$$\mathbf{d} = \left[\begin{array}{c} d[0] \\ \vdots \\ d[N_c-1] \end{array} \right], \tag{2.6}$$

we construct the vector $\mathbf{x}$

$$\mathbf{x} = \left[\begin{array}{c} d[N_c-L+1] \\ \vdots \\ d[N_c-1] \\ d[0] \\ \vdots \\ d[N_c-1] \end{array} \right] = \left[\begin{array}{c} x[1] \\ \\ \\ \vdots \\ \\ \\ x[N_c+L-1] \end{array} \right]. \tag{2.7}$$

CP makes the channel appear circular and permits low-complexity frequency domain equalization. However, a disadvantage is that it introduces overhead which reduces bandwidth efficiency.

2.1.2 Receiver

2.1.2.1 Single-Input Single-Output Case

Making use of the vector $\mathbf{x}$ as an input, the channel output would be

$$y[m] = \sum_{l=0}^{L-1} h[l]x[m-l] + w[m], \qquad m = 1, \ldots, N_c + L - 1. \tag{2.8}$$

A typical OFDM receiver first removes the cyclic prefix (the first $L-1$ channel output symbols). Using the N_c output symbols $y[m], m = 0, \ldots, N_c + L - 1$, we construct the vector

$$\mathbf{y}' = \begin{bmatrix} y'[0] \\ \vdots \\ y'[N_c - 1] \end{bmatrix} = \begin{bmatrix} y[L] \\ \vdots \\ y[N_c + L - 1] \end{bmatrix}. \tag{2.9}$$

***Lemma* 1.** *It holds that*

$$\mathbf{y}' = \mathbf{d} \otimes_{N_c} \mathbf{h} + \mathbf{w}, \tag{2.10}$$

where $\mathbf{w} = \begin{bmatrix} w[L] & \ldots & w[N_c + L - 1] \end{bmatrix}^T$, $\mathbf{h} = \begin{bmatrix} h[0] & h[1] & \ldots & h[L-1] \end{bmatrix}^T$ *and* $\mathbf{a} \otimes_{N_c} \mathbf{b}$ *is the length-*N_c *circular convolution of the vectors* $\mathbf{a}$ *and* $\mathbf{b}$.

Proof. In order to prove the above statement, we write

$$y'[0] = y[L] = \sum_{l=0}^{L-1} h[l]x[L-l] = h[0]d[0] + \sum_{l=1}^{L-1} h[l]d[N_c - l]. \tag{2.11}$$

Respectively, the first term of the circular convolution can be expressed as it follows

$$(\mathbf{d} \otimes_{N_c} \mathbf{h})[0] = h[0]d[0] + \sum_{l=1}^{L-1} h[l]d[N_c - l]. \tag{2.12}$$

In the same way, for the second term, we write

$$\begin{aligned} y'[1] = y[L+1] &= \sum_{l=0}^{L-1} h[l]x[L+1-l] \\ &= h[0]d[1] + h[1]d[0] + \sum_{l=2}^{L-2} h[l]d[N_c - l + 1]. \end{aligned} \tag{2.13}$$

The second term of the circular convolution can be expressed

$$(\mathbf{d} \otimes_{N_c} \mathbf{h})[1] \quad = h[0]d[1] + h[1]d[0] + \textstyle\sum_{l=2}^{L-2} h[l]d[N_c - l + 1]. \tag{2.14}$$

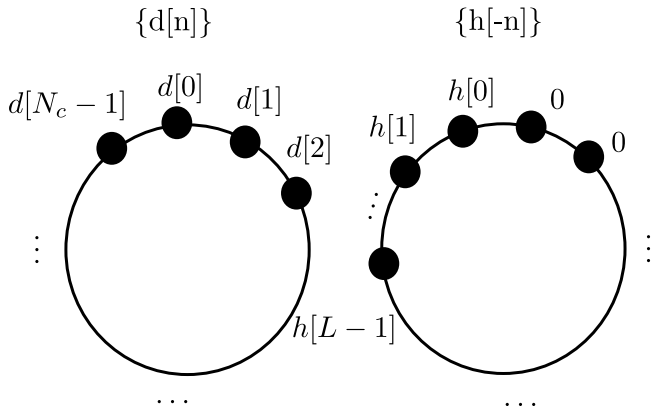

Figure 2.1.2: Graphical computation of $\mathbf{d} \otimes_{N_c} \mathbf{h})[0]$.

The same happens for the other terms. For example, for the $(N_c - 1)$th term we write

$$\begin{aligned} y'[N_c - 1] = y[N_c + L - 1] &= \sum_{l=0}^{L-1} h[l]x[N_c + L - 1 - l] \\ &= h[0]d[N_c - 1] + h[1][N_c - 2] + \cdots + h[L - 1]d[N_c - L]. \end{aligned} \tag{2.15}$$

and the corresponding term of the circular convolution can be expressed as it follows

$$(\mathbf{d} \otimes_{N_c} \mathbf{h})[N_c - 1] = h[0]d[N_c - 1] + h[1][N_c - 2] + \cdots + h[L - 1]d[N_c - L]. \tag{2.16}$$

We understand from the above equations that (2.10) holds. □

Then, the data is passed through the serial to parallel converter and fed to the Fast Fourier Transform (FFT) for frequency domain transformation.
We remind that the Discrete Fourier Transform (DFT) of the vector $\mathbf{y}'$ is given as below

$$\tilde{y}'[n] = \frac{1}{\sqrt{N_c}} \sum_{m=0}^{N_c-1} y'[m] e^{\frac{-2\pi j}{N_c} mn}, \qquad n = 0, \ldots, N_c - 1. \tag{2.17}$$

Applying DFT at (2.10), we derive

$$\begin{aligned} \mathrm{DFT}(\mathbf{y}') &= \mathrm{DFT}(\mathbf{d} \otimes_{\mathrm{N_c}} \mathbf{h} + \mathbf{w}) = \mathrm{DFT}(\mathbf{d} \otimes_{\mathrm{N_c}} \mathbf{h}) + \mathrm{DFT}(\mathbf{w}) \\ &= \sqrt{N_c}\mathrm{DFT}(\mathbf{h}) \odot \mathrm{DFT}(\mathbf{d}) + \mathrm{DFT}(\mathbf{w}). \end{aligned} \tag{2.18}$$

In order to reconstruct the original data from the received data which are distorted by the channel, channel estimation operations are performed. For this purpose, pilot sub-carriers

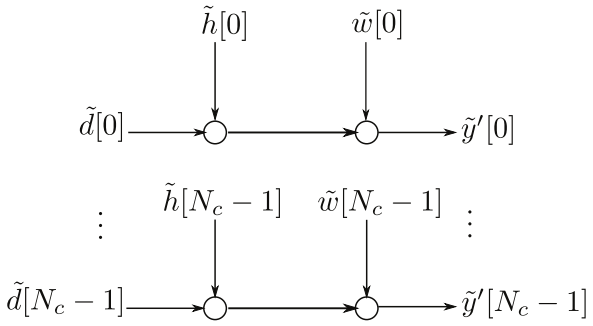

Figure 2.1.3: Analysis of a frequency selective channel into N parallel flat channels

$n = 0, \ldots, N_{tr} - 1$, are used.

In the presence of time dispersive channel and additive noise, the OFDM signal at the receiver for the SISO case is

$$\tilde{y}'[n] = \tilde{h}[n]\tilde{d}[n] + \tilde{w}[n], \qquad n = 0, \ldots, N_c - 1 \tag{2.19}$$

where $\tilde{h}[n] = \sum_{l=0}^{L-1} h[l] e^{\frac{-j2\pi ln}{N_c}}, n = 0, \ldots, N_c - 1$, coincides with the discrete channel frequency response at the frequency $f = \frac{n}{N_c}$, $\tilde{w}[n]$ is additive complex Gaussian noise.

2.1.2.2 Single-Input Multiple-Output Case

Consider the case of using a BS which has A antennas, and is illustrated in 2.1.4.
If we denote the channel from the transmitter to the a-th antenna as $\mathbf{h}_a = \left[\begin{array}{ccc} h_a[0] & \ldots & h_a[L-1] \end{array} \right]^T$ and $y_a[k]$ the output at the a-th antenna at time instant k, for $k = 1, \ldots, N_c + L - 1$, then the channel output is

$$y_a[k] = \sum_{l=0}^{L-1} h_a[l]x[k-l] + w_a[k], \qquad k = 1, \ldots, N_c + L - 1, \quad a = 1, \ldots A \tag{2.20}$$

where $x[k], k = 1, \ldots, N_c + L - 1$, are the transmitted symbols with added cyclic prefix and $w_a[k] = \left[\begin{array}{ccc} w_1[k] & \ldots & w_A[k] \end{array} \right]^T$ is the additive Gaussian noise at the a-th antenna at time instant k.

Making use of equation (2.20) we derive

$$\underbrace{\begin{bmatrix} y_1[k] \\ \vdots \\ y_A[k] \end{bmatrix}}_{\mathbf{y}[k]} = \underbrace{\begin{bmatrix} \mathbf{h}_1^T \\ \vdots \\ \mathbf{h}_A^T \end{bmatrix}}_{\mathbf{H}^T} \underbrace{\begin{bmatrix} x[k] \\ \vdots \\ x[k-L+1] \end{bmatrix}}_{x[k:(k-L+1)]} + \underbrace{\begin{bmatrix} w_1[k] \\ \vdots \\ w_A[k] \end{bmatrix}}_{\mathbf{w}[k]}, \qquad k = 1, \ldots, N_c + L - 1. \tag{2.21}$$

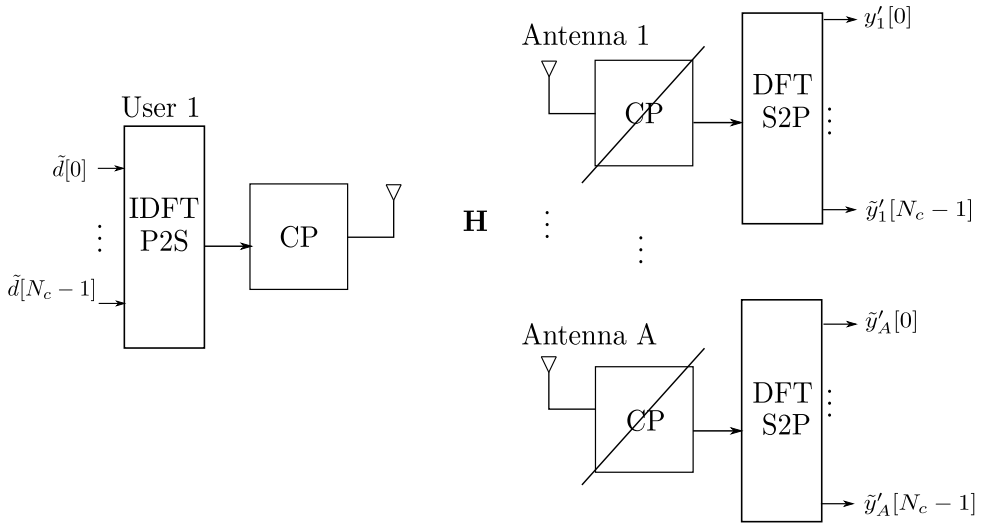

Figure 2.1.4: OFDM SIMO block diagram

.

The receiver then removes the $L-1$ symbols of cyclic prefix which is added by constructing the following matrix

$$\mathbf{Y}' = \begin{bmatrix} y'_1[0] & \dots & y'_A[0] \\ \vdots & \ddots & \vdots \\ y'_1[N_c-1] & \dots & y'_A[N_c-1] \end{bmatrix} = \begin{bmatrix} y_1[L] & \dots & y_A[L] \\ \vdots & \ddots & \vdots \\ y_1[N_c+L-1] & \dots & y_A[N_c+L-1] \end{bmatrix} \tag{2.22}$$

***Lemma* 2.** *: Generalizing* Lemma 1*, it holds that*

$$\mathbf{Y}' = \mathbf{H} \otimes_{N_c} \mathbf{d} + \mathbf{W} \tag{2.23}$$

where $\mathbf{W} = \begin{bmatrix} w_1[L] & \dots & w_A[L] \\ \vdots & \ddots & \vdots \\ w_1[N_c+L-1] & \dots & w_A[N_c+L-1] \end{bmatrix}$ *and* $\mathbf{H} \otimes_{N_c} \mathbf{d} = \begin{bmatrix} \mathbf{h}_1 \otimes_{N_c} \mathbf{d} & \dots & \mathbf{h}_A \otimes_{N_c} \mathbf{d} \end{bmatrix}$ *is the circular convolution of length* N_c *of the matrix* $\mathbf{H}$ *and vector* $\mathbf{d}$*.*

Proof. In order to prove the above statement we write

$$\begin{aligned} \begin{bmatrix} y'_1[0] & \dots & y'_A[0] \end{bmatrix} &= \begin{bmatrix} y_1[L] & \dots & y_A[L] \end{bmatrix} = \begin{bmatrix} \sum_{l=0}^{L-1} h_1[l]x[L-l] & \dots & \sum_{l=0}^{L-1} h_A[l]x[L-l] \end{bmatrix} \\ &= \begin{bmatrix} h_1[0]d[0] + \sum_{l=1}^{L-1} h_1[l]d[N_c-l] & \dots & h_A[0]d[0] + \sum_{l=1}^{L-1} h_A[l]d[N_c-l] \end{bmatrix}. \end{aligned} \tag{2.24}$$

Respectively, the first term of the circular convolution can be expressed as

$$\begin{aligned}(\mathbf{H} \otimes_{N_c} \mathbf{d})[0] &= \left[\begin{array}{ccc} (\mathbf{h}_1 \otimes_{N_c} \mathbf{d})[0] & \dots & (\mathbf{h}_A \otimes_{N_c} \mathbf{d})[0] \end{array} \right] \\ &= \left[\begin{array}{ccc} h_1[0]d[0] + \sum_{l=1}^{L-1} h_1[l]d[N_c - l] & \dots & h_A[0]d[0] + \sum_{l=1}^{L-1} h_A[l]d[N_c - l] \end{array} \right]. \end{aligned} \tag{2.25}$$

In the same way, for the second term, we write

$$\begin{aligned}\left[\begin{array}{ccc} y_1'[1] & \dots & y_A'[1] \end{array} \right] &= \left[\begin{array}{ccc} y_1[L+1] & \dots & y_A[L+1] \end{array} \right] \\ &= \left[\begin{array}{ccc} \sum_{l=0}^{L-1} h_1[l]x[L+1-l] & \dots & \sum_{l=0}^{L-1} h_A[l]x[L+1-l] \end{array} \right] \\ &= h_1[0]d[1] + h_1[1]d[0] + \sum_{l=2}^{L-2} h_1[l]d[N_c - l + 1]. \end{aligned} \tag{2.26}$$

The second term of the circular convolution for the first antenna can be expressed as it follows

$$(\mathbf{h}_1 \otimes_{N_c} \mathbf{d})[1] = h_1[0]d[1] + h_1[1]d[0] + \sum_{l=2}^{L-2} h_1[l]d[N_c - l + 1] \tag{2.27}$$

and for the Ath antenna at the receiver

$$(\mathbf{h}_A \otimes_{N_c} \mathbf{d})[1] = h_A[0]d[1] + h_A[1]d[0] + \sum_{l=2}^{L-2} h_A[l]d[N_c - l + 1]. \tag{2.28}$$

Finally, for the $(N_c - 1)$th term we write

$$\begin{aligned}\left[\begin{array}{ccc} y_1'[N_c-1] & \dots & y_A'[N_c-1] \end{array} \right] &= \left[\begin{array}{ccc} y_1[N_c+L-1] & \dots & y_A[N_c+L-1] \end{array} \right] \\ &= \left[\begin{array}{ccc} \sum_{l=0}^{L-1} h_1[l]x[N_c+L-1-l] & \dots & \sum_{l=0}^{L-1} h_A[l]x[N_c+L-1-l] \end{array} \right] \\ &= h_1[0]d[N_c-1] + h_1[1][N_c-2] + \cdots + h_1[L-1]d[N_c-L]. \end{aligned} \tag{2.29}$$

then, the corresponding terms of the circular convolution can be expressed as it follows

$$(\mathbf{h}_1 \otimes_{N_c} \mathbf{d})[N_c-1] = h_1[0]d[N_c-1] + h_1[1][N_c-2] + \cdots + h_1[L-1]d[N_c-L] \tag{2.30}$$

and for the Ath antenna at the receiver

$$(\mathbf{h}_A \otimes_{N_c} \mathbf{d})[N_c-1]h_A[0]d[N_c-1] + h_A[1][N_c-2] + \cdots + h_A[L-1]d[N_c-L]. \tag{2.31}$$

We understand from the above equations that (2.23) holds. □

Applying DFT at (2.23) we derive

$$\begin{aligned}
\mathrm{DFT}(\mathbf{Y}') &= \mathrm{DFT}\left[\begin{array}{cccc} \mathbf{h}_1 \otimes_{N_c} \mathbf{d} + \mathbf{w}_1 & \dots & \mathbf{h}_A \otimes_{N_c} \mathbf{d} + \mathbf{w}_A \end{array}\right] \\
&= \left[\begin{array}{cccc} \mathrm{DFT}(\mathbf{h}_1 \otimes_{\mathrm{N_c}} \mathbf{d} + \mathbf{w}_1) & \dots & \mathrm{DFT}(\mathbf{h}_\mathrm{A} \otimes_{\mathrm{N_c}} \mathbf{d} + \mathbf{w}_\mathrm{A}) \end{array}\right] \\
&= \left[\begin{array}{cccc} \mathrm{DFT}(\mathbf{h}_1 \otimes_{\mathrm{N_c}} \mathbf{d}) + \mathrm{DFT}(\mathbf{w}_1) & \dots & \mathrm{DFT}(\mathbf{h}_\mathrm{A} \otimes_{\mathrm{N_c}} \mathbf{d}) + \mathrm{DFT}(\mathbf{w}_\mathrm{A}) \end{array}\right] \\
&= \left[\begin{array}{cccc} \sqrt{N_c}\mathrm{DFT}(\mathbf{h}_1) \odot \mathrm{DFT}(\mathbf{d}) + \mathrm{DFT}(\mathbf{w}_1) & \dots & \sqrt{N_c}\mathrm{DFT}(\mathbf{h}_\mathrm{A}) \odot \mathrm{DFT}(\mathbf{d}) + \mathrm{DFT}(\mathbf{w}_\mathrm{A}) \end{array}\right] \\
&= \sqrt{N_c}\mathrm{DFT}\underbrace{\left[\begin{array}{ccc} \mathbf{h_1} & \dots & \mathbf{h_A} \end{array}\right]}_{\mathbf{H}} \odot \mathrm{DFT}\underbrace{(\mathbf{1}_A^T \otimes \mathbf{d})}_{\mathbf{D}} + \mathrm{DFT}\underbrace{\left[\begin{array}{ccc} \mathbf{w}_1 & \dots & \mathbf{w}_A \end{array}\right]}_{\mathbf{W}} \\
&= \sqrt{N_c}\mathrm{DFT}(\mathbf{H}) \odot \mathrm{DFT}(\mathbf{D}) + \mathrm{DFT}(\mathbf{W}) \qquad (2.32)
\end{aligned}$$

The OFDM signals at the receiver for the SIMO case are

$$\begin{aligned}
\tilde{\mathbf{y}}'[n] &= \left[\begin{array}{cccc} \tilde{y}'_1[n] & \dots & \tilde{y}'_A[n] \end{array}\right] \\
&= \left[\begin{array}{cccc} \tilde{h}_1[n] & \dots & \tilde{h}_A[n] \end{array}\right] \tilde{d}[n] + \left[\begin{array}{cccc} \tilde{w}_1[n] & \dots & \tilde{w}_A[n] \end{array}\right] \\
&= \tilde{\mathbf{h}}[n]\tilde{d}[n] + \tilde{\mathbf{w}}[n], \qquad n = 0, \dots, N_c - 1 \qquad (2.33)
\end{aligned}$$

where $\tilde{\mathbf{h}}[n] = \left[\begin{array}{cccc} \sum_{l=0}^{L-1} h_1[l] e^{\frac{-j2\pi ln}{N_c}} & \dots & \sum_{l=0}^{L-1} h_A[l] e^{\frac{-j2\pi ln}{N_c}} \end{array}\right], n = 0, \dots, N_c - 1.$
Note also that $\tilde{\mathbf{y}}[n]$, $\tilde{\mathbf{d}}[n]$ and $\tilde{\mathbf{w}}[n]$ denote frequency domain SIMO transmit, receive signals and additive Gaussian noise vectors respectively, for the nth sub-carrier.

2.1.3 Impact of CFO on System Model

2.1.3.1 Single-Input Single-Output Case

In this case, we take into account the presence of carrier frequency offset between the transceivers due to the frequency skew of their clock crystals. Firstly, we are going to examine the SISO case which is depicted in 2.1.5.
Considering the above, the channel output is

$$y[m] = e^{j\Delta\phi^{R,T}[m]} \sum_{l=0}^{L-1} h[l]x[m-l] + w[m], \quad m = 1, \dots, N_c + L - 1 \qquad (2.34)$$

where $\Delta\phi^{R,T} = \phi^T - \phi^R$ denotes the phase rotation error between the up and the down conversion process on the link between the transmitter and the receiver. ϕ is in general referred to as phase noise, but in our model we only investigate the CFO impact such that $\Delta\phi^{R,T}[m]$ can be defined as a linear phase process for the SISO link:

$$\Delta\phi^{R,T}[m] = 2\pi\Delta f^{R,T} m T_s + \phi^{R,T}. \qquad (2.35)$$

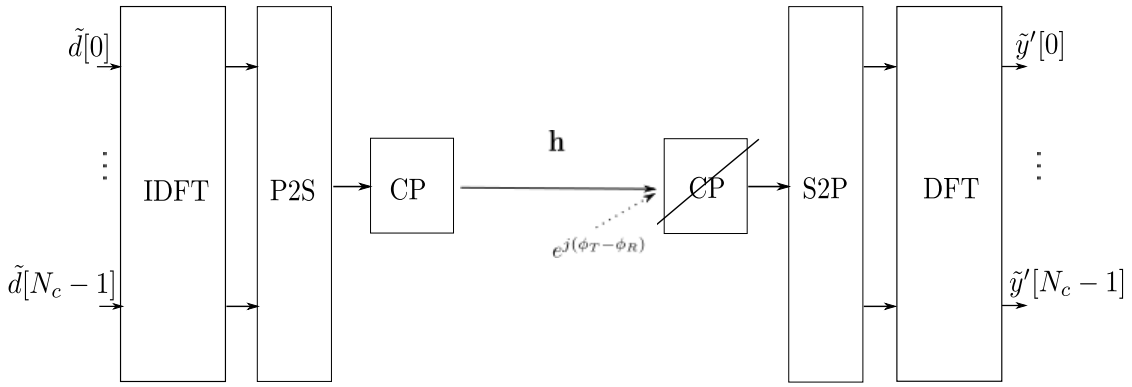

Figure 2.1.5: OFDM SISO block diagram with CFO.

For a general system model the CFO $\Delta f^{R,T}$ is normalized to sub-carrier spacing B_{SC} which leads with $mT_s = \frac{m}{N_c B_{SC}}$ to

$$\Delta\phi^{R,T}[m] = 2\pi\Delta\nu^{R,T}\frac{m}{N_c} + \phi^{R,T} \tag{2.36}$$

with $\Delta\nu^{R,T} = \Delta f^{R,T}/B_{SC}$.
Note also that in this thesis it is not going to be studied the case of different frequency offsets between each of the multiple users and is the reason why we make use of notation R for the receiver and T for the transmitter instead of u and a for the number of users and antennas respectively.
After removing the first $L-1$ output symbols, we get

$$\mathbf{y}' = \mathbf{\Gamma}(\nu)(\mathbf{d} \otimes_{N_c} \mathbf{h}) + \mathbf{w} \tag{2.37}$$

where $\mathbf{\Gamma}(\nu) = \mathrm{diag}(1, \mathrm{e}^{\mathrm{j}\Delta\phi^{\mathrm{R,T}}[1]}, \mathrm{e}^{\mathrm{j}\Delta\phi^{\mathrm{R,T}}[2]}, \ldots, \mathrm{e}^{\mathrm{j}\Delta\phi^{\mathrm{R,T}}[\mathrm{N_c}-1]})$ is the link CFO matrix.
Applying DFT at equation (2.37) we derive

$$\begin{aligned}
\mathrm{DFT}(\mathbf{y}') = \tilde{\mathbf{y}'} &= \mathrm{DFT}(\mathbf{\Gamma}(\nu)(\mathbf{d} \otimes_{\mathrm{N_c}} \mathbf{h}) + \mathbf{w}) = \mathrm{DFT}(\mathbf{\Gamma}(\nu)(\mathbf{d} \otimes_{\mathrm{N_c}} \mathbf{h})) + \mathrm{DFT}(\mathbf{w}) \\
&= \mathbf{F}(\mathbf{\Gamma}(\nu)(\mathbf{d} \otimes_{N_c} \mathbf{h}) + \mathbf{F}\mathbf{w} = \mathbf{F}\mathbf{\Gamma}(\nu)\underbrace{\mathbf{F}^H\mathbf{F}}_{=\mathbf{I}}(\mathbf{d} \otimes_{N_c} \mathbf{h}) + \mathbf{F}\mathbf{w} \\
&= \mathbf{F}\mathbf{\Gamma}(\nu)\mathbf{F}^H(\tilde{\mathbf{d}} \odot \tilde{\mathbf{h}}) + \mathbf{F}\mathbf{w} = \mathbf{F}\mathbf{\Gamma}(\nu)\underbrace{\mathbf{F}^H\tilde{\mathbf{D}}\mathbf{F}_L}_{=\mathbf{A}}\mathbf{h} + \mathbf{F}\mathbf{w} \\
&= \mathbf{F}\mathbf{\Gamma}(\nu)\mathbf{A}\mathbf{h} + \tilde{\mathbf{w}},
\end{aligned} \tag{2.38}$$

where $[\mathbf{F}]_{i,l} = \frac{1}{\sqrt{N_c}} e^{\frac{-j2\pi(i-1)(l-1)}{N_c}}$, for $i = 1, \ldots, N_c, \quad l = 1, \ldots, N_c$, denotes an $N_c \times N_c$ DFT matrix, $[\mathbf{F}_L]_{i,l} = e^{\frac{-j2\pi(i-1)(l-1)}{N_c}}, \quad i = 1, \ldots, N_c, \quad l = 1, \ldots, L$, denotes an $N_c \times L$ DFT matrix and $\tilde{\mathbf{D}} = \mathrm{diag}(\tilde{\mathbf{d}})$ denotes a $N_c \times N_c$ diagonal matrix having as main diagonal the symbols to be transmitted. Additionally, $\mathbf{h} = \begin{bmatrix} h[0] & h[1] & \ldots & h[L-1] \end{bmatrix}^T$ stands for channel impulse response and $\tilde{\mathbf{w}}$ is additive complex Gaussian noise in the frequency domain.

2.1.3.2 Single-Input Multiple-Output Case

In this study, we take into consideration the presence of carrier frequency offset in a SIMO system which is pictured in 2.1.6.

Accordingly, we get the following channel ouput

$$y_a[m] = e^{j\Delta\phi^{R,T}[m]} \sum_{l=0}^{L-1} h_a[l]x[m-l] + w_a[m], \quad m = 1, \ldots, N_c + L - 1, \tag{2.39}$$

where $a = 1, \ldots, A$ denotes the a-th antenna at the BS and $\Delta\phi^{R,T}$ has been expressed in detail in the previous section for the SISO system model. It is also necessary to remind here that we do not consider different carrier frequency offsets between the a-th antenna of the receiver and the transmitter.

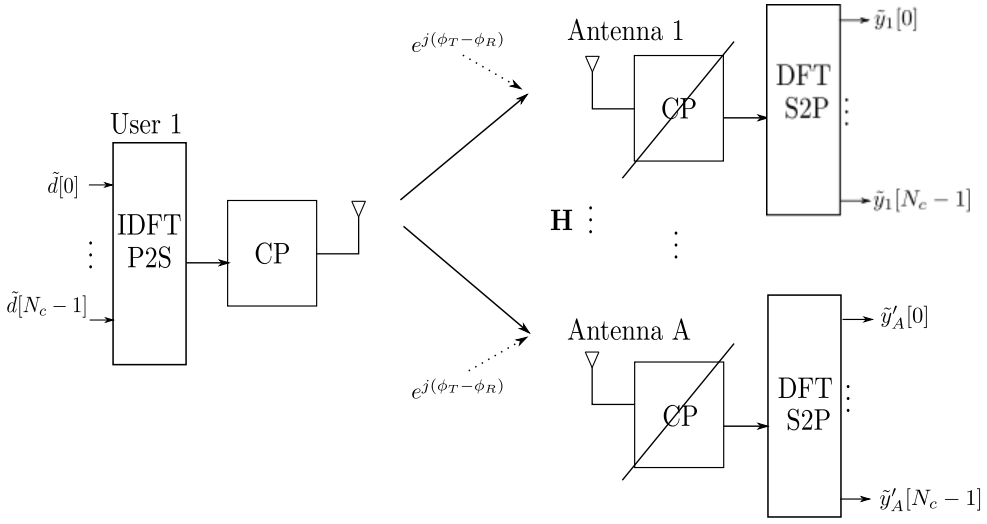

Figure 2.1.6: OFDM SIMO block diagram with CFO.

After removing the cyclic prefix at the receiver, at the a-th antenna we get

$$\mathbf{y}'_a = \mathbf{\Gamma}(\nu)(\mathbf{d} \otimes_{N_c} \mathbf{h}_a) + \mathbf{w}_a \tag{2.40}$$

where $\mathbf{\Gamma}(\nu) = \mathrm{diag}(1, \mathrm{e}^{\mathrm{j}\Delta\phi^{\mathrm{R,T}}[1]}, \mathrm{e}^{\mathrm{j}\Delta\phi^{\mathrm{R,T}}[2]}, \ldots, \mathrm{e}^{\mathrm{j}\Delta\phi^{\mathrm{R,T}}[\mathrm{N_c}-1]})$ is the link CFO matrix.
Applying DFT at equation (2.40) we derive

$$\begin{aligned}
\mathrm{DFT}(\mathbf{y}'_{\mathrm{a}}) = \tilde{\mathbf{y}}'_{\mathrm{a}} &= \mathrm{DFT}(\mathbf{\Gamma}(\nu)(\mathbf{d} \otimes_{\mathrm{N_c}} \mathbf{h}_{\mathrm{a}}) + \mathbf{w}_{\mathrm{a}}) = \mathrm{DFT}(\mathbf{\Gamma}(\nu)(\mathbf{d} \otimes_{\mathrm{N_c}} \mathbf{h}_{\mathrm{a}})) + \mathrm{DFT}(\mathbf{w}_{\mathrm{a}}) \\
&= \mathbf{F}(\mathbf{\Gamma}(\nu)(\mathbf{d} \otimes_{N_c} \mathbf{h}_a)) + \mathbf{F}\mathbf{w}_a = \mathbf{F}\mathbf{\Gamma}(\nu)\underbrace{\mathbf{F}^H\mathbf{F}}_{=\mathbf{I}}(\mathbf{d} \otimes_{N_c} \mathbf{h}_a) + \mathbf{F}\mathbf{w}_a \\
&= \mathbf{F}\mathbf{\Gamma}(\nu)\mathbf{F}^H(\mathbf{d} \odot \mathbf{h}_a) + \mathbf{F}\mathbf{w}_a = \mathbf{F}\mathbf{\Gamma}(\nu)\underbrace{\mathbf{F}^H\tilde{\mathbf{D}}\mathbf{F}_L}_{=\mathbf{A}}\mathbf{h}_a + \mathbf{F}\mathbf{w}_a \\
&= \mathbf{F}\mathbf{\Gamma}(\nu)\mathbf{A}\mathbf{h}_a + \tilde{\mathbf{w}}_a,
\end{aligned} \tag{2.41}$$

where $\mathbf{F}$, $\mathbf{F}_L$ and $\tilde{\mathbf{D}}$ are matrices which have been defined above for the SISO case, $\tilde{\mathbf{y}}'_a = \left[\begin{array}{cccc} \tilde{y}'_a[0] & \tilde{y}'_a[1] & \dots & \tilde{y}'_a[N_c-1] \end{array} \right]^T$ denotes an $N_c \times 1$ vector containing the output information for each of the $a = 1, 2, \dots, A$ antennas, $\mathbf{h}_a = \left[\begin{array}{cccc} h_a[0] & h_a[1] & \dots & h_a[L-1] \end{array} \right]^T$ denotes an $L \times 1$ vector referring to that channel response that the transmitter uses to communicate with the corresponding antenna at the receiver and $\tilde{\mathbf{w}}_a = \left[\begin{array}{cccc} \tilde{w}_a[0] & \tilde{w}_a[1] & \dots & \tilde{w}_a[N_c-1] \end{array} \right]^T$ denotes an $N_c \times 1$ vector of Gaussian noise owing to the a-th antenna at the BS.

As a result, as far as the SIMO case is concerned, the system model with the impact of CFO is

$$\begin{aligned} \left[\begin{array}{ccc} \tilde{\mathbf{y}}'_1 & \dots & \tilde{\mathbf{y}}'_A \end{array} \right] = \tilde{\mathbf{Y}}' &= \left[\begin{array}{ccc} \mathbf{F}\mathbf{\Gamma}(\nu)\mathbf{A}\mathbf{h}_1 & \dots & \mathbf{F}\mathbf{\Gamma}(\nu)\mathbf{A}\mathbf{h}_A \end{array} \right] + \left[\begin{array}{ccc} \tilde{\mathbf{w}}_1 & \dots & \tilde{\mathbf{w}}_A \end{array} \right] \\ &= \mathbf{F}\mathbf{\Gamma}(\nu)\mathbf{A} \left[\begin{array}{ccc} \mathbf{h}_1 & \dots & \mathbf{h}_A \end{array} \right] + \left[\begin{array}{ccc} \tilde{\mathbf{w}}_1 & \dots & \tilde{\mathbf{w}}_A \end{array} \right] \\ &= \mathbf{F}\mathbf{\Gamma}(\nu)\mathbf{A}\mathbf{H} + \tilde{\mathbf{W}}. \end{aligned} \tag{2.42}$$

Chapter 3

OFDM-SDMA System Model

In this chapter, we will study Orthogonal Frequency Division Multiplexing - Space Division Multiple Access (OFDM-SDMA) systems. We will derive a general system model in the case we have $u = 1, \ldots, U$ users transmitting and $a = 1, \ldots, A$ antennas at the base station (BS). The impact of carrier frequency offset owing to the frequency skew of both the transmitter's and receiver's oscillator, over the system model is also examined in detail.

3.1 OFDM-SDMA System Setup

The system under consideration, which illustrates an uplink OFDM-SDMA system with $u = 1, \ldots, U$ user terminals and one BS, is depicted in 3.1.1. Each user terminal has a single antenna for low cost, while the BS has A antennas.
Each user u feeds its data $\tilde{d}^u[n]$ in blocks of N_c symbols into a length-N_c inverse FFT (IFFT) operator to obtain the time-domain sequence $d^u[n]$.
A cyclic extension of length L is inserted into the sequence, which is then converted into a serial stream.
The resulting sequence $\mathbf{x}^u = \left[\begin{array}{cccccc} d^u[N_c - L + 1] & \ldots & d^u[N_c - 1] & d^u[0] \ldots & d^u[N_c - 1] \end{array} \right]^T$ where $u = 1, 2, \ldots U$ is transmitted through the A convolutional channels $h_a^u[n]$ with $h_a^u[n]$ the baseband representation of the multipath channel from user $u = 1, 2, \ldots U$ to antenna $a = 1, 2, \ldots, A$.
At the BS, each antenna receives the convolutional mixture

$$y_a[n] = \sum_{u=1}^{U} h_a^u[n] \star x^u[n] + w_a[n], \quad n = 0, \ldots, N_c + L - 1. \tag{3.1}$$

Subsequently, the operations of the transmitter are inverted.

After discarding the cyclic prefix and the length-N_c FFT of each received signal, we end up with A received sequences $\tilde{y}_a[n]$ on each sub-carrier $n = 0, \ldots, N_c - 1$. The signals $\tilde{y}_a[n]$ are then postprocessed by the BS to separate the distinct users and to provide estimates $\hat{\tilde{d}}^u[n]$ for the transmitted symbols $\tilde{d}^u[n]$.

If L is larger than the channel length, the linear convolution channel is observed as cyclic at

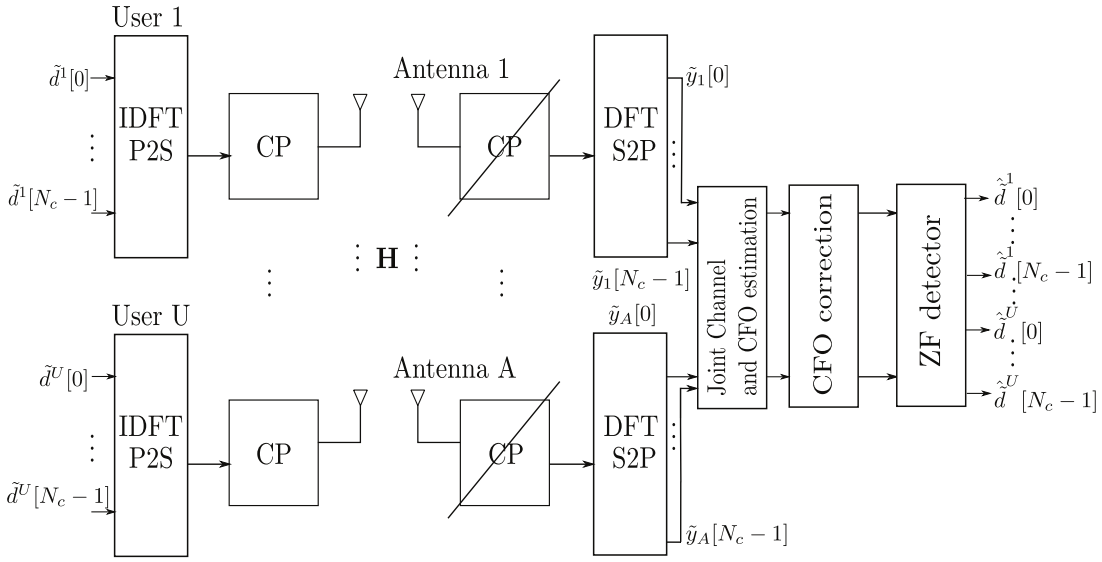

Figure 3.1.1: Uplink OFDM-SDMA system model.

the basestation. Thus, in the frequency domain, it becomes equivalent to multiplication with the discrete Fourier Transform of the channel, $\tilde{h}_u^a[n]$. Then, we can write for the sub-carrier n

$$\underbrace{\begin{bmatrix} \tilde{y}_1[n] \\ \vdots \\ \tilde{y}_A[n] \end{bmatrix}}_{\tilde{\mathbf{y}}[n]} = \underbrace{\begin{bmatrix} \tilde{h}_1^1[n] & \dots & \tilde{h}_1^U[n] \\ \vdots & \ddots & \vdots \\ \tilde{h}_A^1[n] & \dots & \tilde{h}_A^U[n] \end{bmatrix}}_{\tilde{\mathbf{H}}[n]} \underbrace{\begin{bmatrix} \tilde{d}^1[n] \\ \vdots \\ \tilde{d}^U[n] \end{bmatrix}}_{\tilde{\mathbf{d}}[n]} + \underbrace{\begin{bmatrix} \tilde{w}_1[n] \\ \vdots \\ \tilde{w}_A[n] \end{bmatrix}}_{\tilde{\mathbf{w}}[n]}, \quad n = 0, \dots, N_c - 1 \tag{3.2}$$

where the nth $A \times U$ block $\tilde{\mathbf{H}}[n]$ is the MIMO channel matrix for the nth sub-carrier, $\tilde{\mathbf{d}}[n]$ denotes the $U \times 1$ frequency domain MIMO transmit signal vector for the nth sub-carrier and $\tilde{\mathbf{y}}[n]$ denotes the $A \times 1$ frequency domain MIMO receive signal vector for the nth sub-carrier. The BS uses both the Zero-Forcing (ZF) and Maximum Likelihood (ML) schemes so as to separate the signals of the u users, based on the channel knowledge obtained by Maximum Likelihood (ML) channel estimation, a processing which will be explained in more detail in later chapters of our thesis.
Without CFO, the ideal frequency domain signal model is given by

$$\tilde{\mathbf{y}}' = \tilde{\mathbf{H}}'\tilde{\mathbf{d}}' + \tilde{\mathbf{w}}', \tag{3.3}$$

where

1. The $N_cA \times 1$ received MIMO OFDM vector is given by

$$\tilde{\mathbf{y}}' = \begin{bmatrix} \tilde{\mathbf{y}}[0]^T & \tilde{\mathbf{y}}[1]^T & \dots & \tilde{\mathbf{y}}[N_c-1]^T \end{bmatrix}^T. \tag{3.4}$$

.

2. $\tilde{\mathbf{H}}' = \mathrm{diag}(\tilde{\mathbf{H}}[0], \tilde{\mathbf{H}}[1], \dots, \tilde{\mathbf{H}}[\mathrm{N_c} - 1])$ denotes a $N_cA \times N_cU$ block diagonal matrix.

3. The $N_cU \times 1$ transmitted MIMO OFDM vector is given by

$$\tilde{\mathbf{d}}' = \left[\begin{array}{cccc} \tilde{\mathbf{d}}[0]^T & \tilde{\mathbf{d}}[1]^T & \dots & \tilde{\mathbf{d}}[N_c-1]^T \end{array} \right]^T. \tag{3.5}$$

4. The $N_cA \times 1$ vector $\tilde{\mathbf{w}}'$ represents the receiver noise, with i.i.d zero-mean, complex Gaussian elements of variance σ_N^2.

Clearly, due to the OFDM modulation, the SDMA problem falls apart in multiple parallel SDMA problems, which can be solved independently per sub-carrier, as depicted in 3.1.1. Hence, the SDMA processing is transformed into N_c SDMA processors running $N_c + L$ times slower than the time-domain symbol rate. Our SDMA processor calculates estimates $\hat{\tilde{d}}^u[n]$ for the transmitted symbols $\tilde{d}^u[n]$, using the received $\tilde{y}_a[n]$ and frequency domain joint Maximum Likelihood (ML) frequency offset and channel estimator.

3.2 Impact of CFO on System Model

Even after carrier frequency synchronization, we assume that each user still has the same normalized residual CFO jitter $\Delta f^{R,T}$ which is defined relative to the sub-carrier spacing $\Delta\nu^{R,T} = \Delta f^{R,T}/B_{SC}$. Hence, with over the oversampling rate, it corresponds to an absolute frequency offset of $\frac{over\Delta f^{R,T}}{N_c}$Hz.
In the presence of CFO, the contribution of user u to the data symbol $\tilde{y}_a[n]$ that the BS receives on the nth sub-carrier at the a-th antenna during an OFDM symbol is given by

$$\tilde{\mathbf{y}}' = \tilde{\mathbf{F}}\tilde{\mathbf{\Gamma}}\tilde{\mathbf{A}}\mathbf{h} + \tilde{\mathbf{w}}', \tag{3.6}$$

where $\tilde{\mathbf{F}} = \mathbf{I}_{A\times A} \otimes \mathbf{F}$ denotes a $N_cA \times N_cA$ block diagonal matrix having main diagonal block $N_c \times N_c$ DFT matrices, $[\mathbf{F}]_{i,l} = \frac{1}{\sqrt{N_c}} e^{\frac{-j2\pi(i-1)(l-1)}{N}}$ for $i = 1, \dots, N_c$ and $l = 1, \dots, N_c$.

Furthermore, $\tilde{\mathbf{\Gamma}} = \mathbf{I}_{A\times A} \otimes \mathbf{\Gamma}(\nu)$ denotes a $N_cA \times N_cA$ block diagonal matrix having main diagonal, $N_c \times N_c$ diagonal $\mathbf{\Gamma}(\nu)$ matrices where

$$\mathbf{\Gamma}(\nu) = \mathrm{diag}(1, \mathrm{e}^{\mathrm{j}\Delta\phi^{\mathrm{R,T}}[1]}, \mathrm{e}^{\mathrm{j}\Delta\phi^{\mathrm{R,T}}[2]}, \dots, \mathrm{e}^{\mathrm{j}\Delta\phi^{\mathrm{R,T}}[\mathrm{N_c}-1]}) \tag{3.7}$$

is the link CFO matrix. In addition, we have to remind that $\Delta\phi^{R,T}[n] = 2\pi\Delta\nu^{R,T}\frac{n}{N_c} + \phi^{R,T}$, $n = 0, \dots, N_c - 1$ denotes the linear combination of the phase rotation error and the phase noise in our link. We need also to emphasize in this section that we assumed the presence of one oscillator for producing carrier frequency for all the users and another one for the group of antennas at the BS. Consequently, there is no significant difference in carrier frequency offset computation between the multiuser case and the SISO or SIMO case. The only difference is the expression of the link CFO matrix for each of the cases described above.

Moreover, $\tilde{\mathbf{A}} = \mathbf{I}_{A\times A} \otimes \left[\begin{array}{ccc} \mathbf{A}_1 & \dots & \mathbf{A}_U \end{array} \right]$ denotes a $AN_c \times AUL$ matrix where

$$\mathbf{A}_u = \mathbf{F}^H \tilde{\mathbf{D}}'_u \mathbf{F}_L, \qquad u = 1, \dots, U, \tag{3.8}$$

1. $[\mathbf{F}]_{i,l} = \frac{1}{\sqrt{N}} e^{\frac{-j2\pi(i-1)(l-1)}{N_c}}$, for $i = 1, \ldots, N_c, \quad l = 1, \ldots, N_c$, denotes a $N_c \times N_c$ Discrete Fourier Transform matrix.
2. $[\mathbf{F}_L]_{i,l} = e^{\frac{-j2\pi(i-1)(l-1)}{N_c}}$, for $i = 1, \ldots, N_c, \quad l = 1, \ldots, L$, denotes a $N_c \times L$ Discrete Fourier Transform submatrix.
3. $\tilde{\mathbf{D}}'_u = \mathrm{diag}(\tilde{\mathbf{d}}_\mathrm{u})$ denotes an $N_c \times N_c$ diagonal matrix having main diagonal the transmitted symbols of each user.

Finally, $\mathbf{h} = \mathrm{vec}(\tilde{\mathbf{H}}') = \left[\begin{array}{cccccccc} \mathbf{h}_1^{1T} & \ldots & \mathbf{h}_1^{UT} & \ldots & \mathbf{h}_1^{AT} & \ldots & \mathbf{h}_U^{AT} \end{array} \right]^\mathrm{T}$ denotes a $UAL \times 1$ vector formed by channel input responses and $\tilde{\mathbf{w}}'$ represents the receiver noise vector $AN_c \times 1$.

There are two effects existing due to CFO. One is the rotation and attenuation of the useful signal and the other is the phase offset added into the channel. Both are given in (3.7).

The objective is to estimate the unknowns, based on received $\tilde{\mathbf{y}}'$,

1. ν
2. $\mathbf{h}_a^u = \left[\begin{array}{cccc} h_a^u[0] & \ldots & h_a^u[L-1] \end{array} \right]^T$ for each user and antenna at the BS.

3.3 Derivation of the OFDM-SDMA System Model with CFO

In 3.3.1 is depicted the case of U user terminals transmitting and a BS equipped with A antennas, with the impact of CFO $\Delta f^{R,T}$ normalized to sub-carrier spacing B_{SC}.
Then, if we denote as $\mathbf{h}_a^u = \left[\begin{array}{cccc} h_a^u[0] & \ldots & h_a^u[L-1] \end{array} \right]^T$ the channel from the u-th user to the a-th antenna and $y_a[m]$ the output at the a-th antenna at time instant m for $m = 0, \ldots, N_c + L - 1$, the channel output will be

$$y_a[m] = e^{j\Delta\phi^{R,T}[m]} \sum_{u=1}^{U} \sum_{l=0}^{L-1} h_a^u[l] x^u[m-l] + w_a[m], \tag{3.9}$$

where $w_a[m]$ refers to additive white Gaussian noise at the a-th antenna of the receiver at time instant m and $\Delta\phi^{R,T}$ consists of two terms where the first is responsible for the phase rotation error between the users transmitting and the receiver while the second implies the phase noise. In the previous chapter, there is an analytic definition of $\Delta\phi^{R,T}$ for the case of multiple users and antennas at the BS.

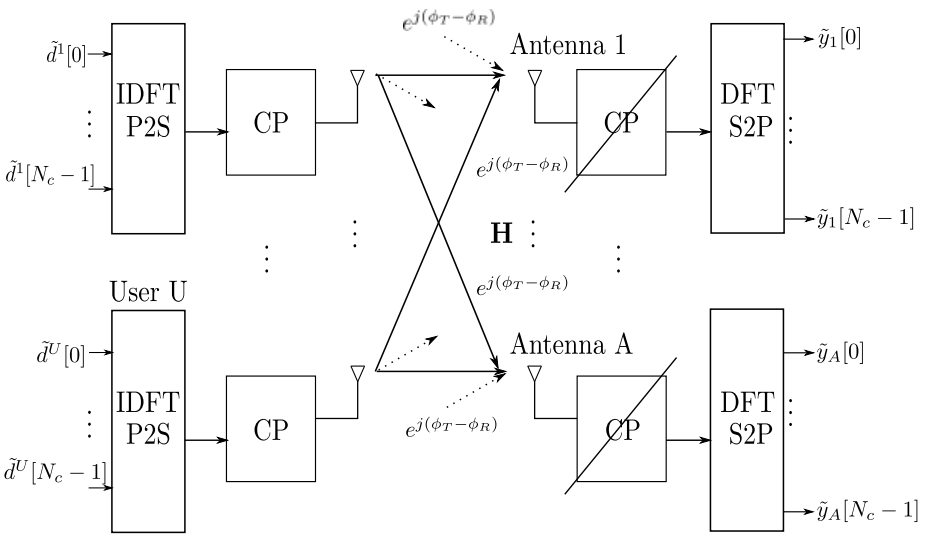

Figure 3.3.1: OFDM-SDMA block diagram with CFO.

After removing the cyclic prefix, at the a-th antenna we get

$$\mathbf{y}'_a = \mathbf{\Gamma}(\nu) \sum_{u=1}^{U} \mathbf{h}_a^u \otimes_{N_c} \mathbf{d}^u + \mathbf{w}_a \tag{3.10}$$

where $\mathbf{\Gamma}(\nu) = \mathrm{diag}(1, \mathrm{e}^{\mathrm{j}\Delta\phi^{\mathrm{R,T}}[1]}, \mathrm{e}^{\mathrm{j}\Delta\phi^{\mathrm{R,T}}[2]}, \ldots, \mathrm{e}^{\mathrm{j}\Delta\phi^{\mathrm{R,T}}[\mathrm{N_c}-1]})$ is the link CFO matrix.
Applying DFT at (3.10) we derive

$$\begin{aligned}
\mathrm{DFT}(\mathbf{y}'_{\mathrm{a}}) = \tilde{\mathbf{y}}'_{\mathrm{a}} &= \mathrm{DFT}(\mathbf{\Gamma}(\nu) \sum_{\mathrm{u=1}}^{\mathrm{U}} \mathbf{h}_{\mathrm{a}}^{\mathrm{u}} \otimes_{\mathrm{N_c}} \mathbf{d}^{\mathrm{u}} + \mathbf{w}_{\mathrm{a}}) = \mathrm{DFT}(\mathbf{\Gamma}(\nu) \sum_{\mathrm{u=1}}^{\mathrm{U}} \mathbf{h}_{\mathrm{a}}^{\mathrm{u}} \otimes_{\mathrm{N_c}} \mathbf{d}^{\mathrm{u}}) + \mathrm{DFT}(\mathbf{w}_{\mathrm{a}}) \\
&= \mathbf{F}(\mathbf{\Gamma}(\nu) \sum_{u=1}^{U} \mathbf{h}_a^u \otimes_{N_c} \mathbf{d}^u) + \mathbf{F}\mathbf{w}_a = \mathbf{F}\mathbf{\Gamma}(\nu) \underbrace{\mathbf{F}^H\mathbf{F}}_{=\mathbf{I}} (\sum_{u=1}^{U} \mathbf{h}_a^u \otimes_{N_c} \mathbf{d}^u) + \mathbf{F}\mathbf{w}_a \\
&= \mathbf{F}\mathbf{\Gamma}(\nu)\mathbf{F}^H (\sum_{u=1}^{U} \tilde{\mathbf{h}}_a^u \odot \tilde{\mathbf{d}}^u) + \mathbf{F}\mathbf{w}_a = \mathbf{F}\mathbf{\Gamma}(\nu)\mathbf{F}^H (\sum_{u=1}^{U} \tilde{\mathbf{D}}'^u \mathbf{F_L} \mathbf{h}_a^u) + \mathbf{F}\mathbf{w}_a \\
&= \mathbf{F}\mathbf{\Gamma}(\nu) (\sum_{u=1}^{U} \underbrace{\mathbf{F}^H \tilde{\mathbf{D}}'^u \mathbf{F_L}}_{=\mathbf{A_u}} \mathbf{h}_a^u) + \mathbf{F}\mathbf{w}_a = \mathbf{F}\mathbf{\Gamma}(\nu) \sum_{u=1}^{U} \mathbf{A_u} \mathbf{h}_a^u + \mathbf{F}\mathbf{w}_a
\end{aligned} \tag{3.11}$$

where $\mathbf{F}$, $\mathbf{\Gamma}(\nu)$, $\tilde{\mathbf{D}}'^u$ and $\mathbf{F}_L$ have been defined in the previous section.
Consequently, in the frequency domain at the a-th antenna we get

$$\tilde{\mathbf{y}}'_a = \mathbf{F}\mathbf{\Gamma}(\nu) \sum_{u=1}^{U} \mathbf{A_u} \mathbf{h}_a^u + \mathbf{F}\mathbf{w}_a. \tag{3.12}$$

Making use of equation (3.12) we derive (3.6)

$$\begin{aligned}
\begin{bmatrix} \tilde{\mathbf{y}'}_1 \\ \vdots \\ \tilde{\mathbf{y}'}_A \end{bmatrix} = \tilde{\mathbf{y}}' &= \underbrace{(\mathbf{I}_{A\times A} \otimes \mathbf{F})}_{\tilde{\mathbf{F}}} \underbrace{(\mathbf{I}_{A\times A} \otimes \mathbf{\Gamma}(\nu))}_{\tilde{\mathbf{\Gamma}}(\nu)} \begin{bmatrix} \sum_{u=1}^{U} \mathbf{A_1} \mathbf{h}_1^u \\ \vdots \\ \sum_{u=1}^{U} \mathbf{A_u} \mathbf{h}_A^u \end{bmatrix} + \begin{bmatrix} \tilde{\mathbf{w}}_1 \\ \vdots \\ \tilde{\mathbf{w}}_A \end{bmatrix} \\
&= \tilde{\mathbf{F}}\tilde{\mathbf{\Gamma}}(\nu) \underbrace{(\mathbf{I}_{A\times A} \otimes \begin{bmatrix} \mathbf{A}_1 & \dots & \mathbf{A}_U \end{bmatrix})}_{\tilde{\mathbf{A}}} \begin{bmatrix} \mathbf{h}_1^1 \\ \vdots \\ \mathbf{h}_1^A \\ \vdots \\ \mathbf{h}_1^U \\ \vdots \\ \mathbf{h}_U^A \end{bmatrix} + \begin{bmatrix} \tilde{\mathbf{w}}_1 \\ \vdots \\ \tilde{\mathbf{w}}_A \end{bmatrix} \\
&= \tilde{\mathbf{F}}\tilde{\mathbf{\Gamma}}(\nu)\tilde{\mathbf{A}}\mathbf{h} + \tilde{\mathbf{w}}' \qquad (3.13)
\end{aligned}$$

where $\mathbf{F}$, $\mathbf{\Gamma}(\nu)$ and $\mathbf{A}_u$ have been defined before.

As a result, we understand from the above equations that (3.6) holds.

Chapter 4

Time Synchronization

This chapter is going to emphasize on packet synchronization problems [2] that we came up with, during our study of both OFDM SISO and MIMO links. Therefore, we suggest simple and efficient solutions.
The problem in general refers to how can we derive a symbol-spaced output sequence out of a sampled case of the noisy output waveform that we get on the receiver.

4.1 Packet Synchronization

Assume now that we take under consideration the simple OFDM SISO case, which is depicted in 4.1.1, where one user transmits 4-QAM modulated symbols $\tilde{\mathbf{d}} = \begin{bmatrix} \tilde{d}[0] & \dots & \tilde{d}[N_c-1] \end{bmatrix}^T$. After taking IDFT of the data, inserting cyclic prefix and passing them through a square root raised cosine filter $g_T(t)$ at the transmitter we get

$$x'(t) = x(t) \star g_T(t) = \sum_{n=0}^{N_c+L-2} x[n] g_T(t - nT) \tag{4.1}$$

where $T = \text{over} \times \text{T}_\text{s}$ with T_s denoting the symbol period, over the oversampling rate, $x[n]$ i.i.d with zero mean and variance $\mathbf{E}[|x|^2] = \sigma_x^2$, $g_T(t)$, $g_R(t)$ square root raised cosine filters are being used both in the transmitter and the receiver and as far as the transmission channel is concerned we discern two cases.

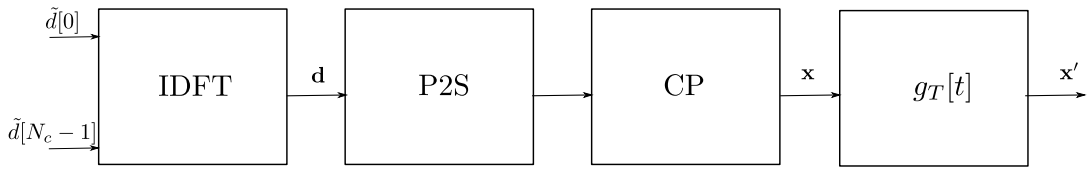

Figure 4.1.1: OFDM SISO Transmitter block diagram.

4.1.1 Ideal Channels

In this case, the transmitted waveforms pass through an ideal channel $c(t)$ which does not introduce a delay or amplitude scaling and then through the matched filter $g_R(t)$ at the receiver.

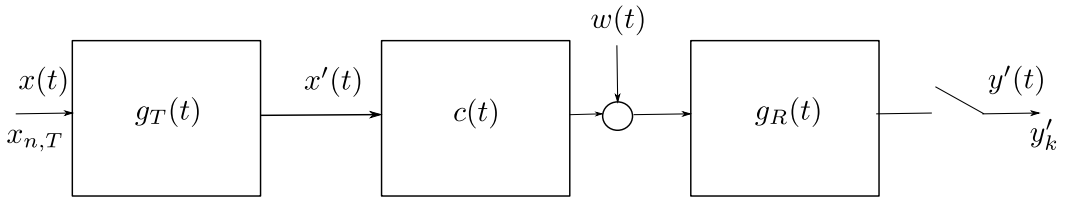

Figure 4.1.2: Composite Channel.

At the receiver we get

$$\begin{aligned} y(t) &= x'(t) \star c(t) + w(t) = x(t) \star g_T(t) \star c(t) + w(t) \\ &= x(t) \star g_T(t) + w(t) = \sum_{n=0}^{N_c+L-2} x[n] g_T(t - nT) + w(t) \\ &= x'(t) + w(t) \end{aligned} \tag{4.2}$$

where $w(t)$ is additive white Gaussian noise with zero mean and variance $\mathbf{E}[|w|^2] = \sigma_w^2$.
The output of the square root raised cosine filter $g_R(t)$ we use at the receiver is

$$\begin{aligned} y'(t) &= y(t) \star g_R(t) = (x'(t) + w(t)) \star g_R(t) \\ &= x'(t) \star g_R(t) + w(t) \star g_R(t) \\ &= x(t) \star g_T(t) \star g_R(t) + w(t) \star g_R(t) \end{aligned} \tag{4.3}$$

In order to avoid intersymbol interference (ISI), we assume that the composite channel response, satisfies Nyquist condition,

$$g(t) = g_T(t) \star c(t) \star g_R(t) = g_T(t) \star g_R(t) \tag{4.4}$$

Consequently (4.3) can be rewritten as

$$y'(t) = x(t) \star g(t) + w(t) \star g_R(t). \tag{4.5}$$

Our main objective is to reconstruct the input sequence. We observe that if we take samples from $y'(t)$ over $N_c + L - 1$ time instants $t = kT$ where $k = 0, \ldots, N_c + L - 2$ we can reconstruct the input sequence.

The output power can be computed as

$$\begin{aligned}\mathbf{E}[y'^2(t)] = \mathbf{E}[&\sum_{n=0}^{N_c+L-2} x[n]g(t-nT) \sum_{m=0}^{N_c+L-2} x[m]g(t-mT)]+ \\ &+ \mathbf{E}[\sum_{n=0}^{N_c+L-2} w[n]g_R(t-nT) \sum_{m=0}^{N_c+L-2} w[m]g_R(t-mT)] \\ &= \sigma_x^2 \sum_{n=0}^{N_c+L-2} g^2(t-nT) + \sigma_w^2 \sum_{n=0}^{N_c+L-2} g_R^2(t-nT). \end{aligned} \tag{4.6}$$

We derive (as it is pictured in 4.1.3) that $\mathbf{E}[y(t)^2]$ is maximized at N_c+L-1 points $t=kT$ for $k=0,\ldots,N_c+L-2$ at which points we have to take samples from $y(t)$ in order to get $x'[k]$'s.

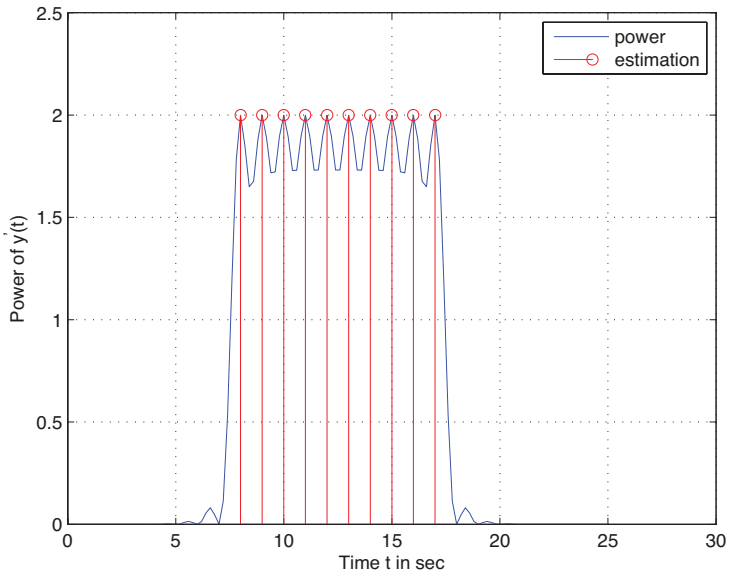

Figure 4.1.3: Power of $y'(t)$, for $N_c=10$, $T=1$, over $=5$ and $\sigma_x^2=2$.

We also have to note that until now we have assumed that the channel does not introduce any delay. The fact that at the time instants $k+iT$, $k=0,\ldots,N_c+L-2$ we get $x'[i]$'s is because of our conversion of the composite channel into causal.

This coincidence indicates that we can create all the length-(N_c+L-2) possible symbol-spaced subsequences, compute their energy and assume as estimation of the output packet the subsequence with the maximum energy.

When the channel inserts unknown delay τ, the output we get would be $y'(t-\tau)$. Therefore we have to take samples at $t=kT+\tau$, $k=0,\ldots,N_c+L-2$ time instants. Obviously in order to achieve this we should know τ. Easily we understand that the $kT+\tau$ time instants would

be the ones where the power of $y'(t-\tau)$ gets maximized.
Consequently we can make use of the deduction above, which indicates that we hold as a good estimation of the output packet the symbol-spaced subsequence with the maximum energy.

In the sequel, if we consider the case of OFDM-SDMA systems, where each of the multiple users $u = 1, \ldots, U$ transmit QAM modulated symbols $\tilde{\mathbf{d}}^u = \left[\begin{array}{ccc} \tilde{d}^u[0] & \ldots & \tilde{d}^u[N_c-1] \end{array} \right]^T$, the waveforms which pass through the ideal channel are expressed as

$$x'^u(t) = x^u(t) \star g_T(t) = \sum_{n=0}^{N_c+L-2} x^u[n] g_T(t-nT) \tag{4.7}$$

where $x^u[n]$ i.i.d with zero mean and variance $\mathbf{E}[|x^u|^2] = \mathbf{E}[|x|^2] = \sigma_x^2 = 2$ are the transmitted data with added cyclic prefix.
Subsequently for a number $a = 1, \ldots, A$ antennas at the receiver, at the a-th antenna we get

$$\begin{aligned} y_a(t) = \sum_{u=1}^{U} x^u(t) \star g_T(t) + w_a(t) &= \sum_{u=1}^{U} \sum_{n=0}^{N_c+L-2} x^u[n] g_T(t-nT) + w_a(t) \\ &= \sum_{u=1}^{U} x'^u(t) + w_a(t) \end{aligned} \tag{4.8}$$

where $w_a(t)$ is white Gaussian noise added by the a-th antenna of the base station with zero mean and variance $\mathbf{E}[|w_a|^2] = \sigma_{w_a}^2$.
In the sequel, received data pass through a square root raised cosine filter $g_R(t)$ and at the a-th antenna we get

$$\begin{aligned} y'_a(t) &= \sum_{u=1}^{U} x^u(t) \star g_T(t) \star g_R(t) + w_a(t) \star g_R(t) \\ &= \sum_{u=1}^{U} \sum_{n=0}^{N_c+L-2} x^u[n] g(t-nT) + \sum_{n=0}^{N_c+L-2} w_a[n] g_R(t-nT) \end{aligned} \tag{4.9}$$

where $g(t) = g_T(t) \star g_R(t)$ from (4.4).
Computing the output power

$$\begin{aligned} \mathbf{E}[y'^2_a(t)] = \mathbf{E}[&\sum_{u=1}^{U} \sum_{n=0}^{N_c+L-2} x^u[n] g(t-nT) \sum_{u=1}^{U} \sum_{m=0}^{N_c+L-2} x^u[m] g(t-mT)] + \\ &+ \mathbf{E}[\sum_{n=0}^{N_c+L-2} w_a[n] g_R(t-nT) \sum_{m=0}^{N_c+L-2} w_a[m] g_R(t-mT)] \\ &= \sum_{u=1}^{U} \sigma_x^2 \sum_{n=0}^{N_c+L-2} g^2(t-nT) + \sigma_{w_a}^2 \sum_{n=0}^{N_c+L-2} g_R^2(t-nT), \end{aligned} \tag{4.10}$$

we understand that taking samples from $y'_a(t)$ at time instants $t = kT$, $k = 0, \ldots, N_c + L - 2$ – where $\mathbf{E}[y'^2_a(t)]$ is maximized (4.1.4) – will give us $\sum_{u=1}^{U} x^u[k]$, which reconstruct the input

sequence given by the sum of users U transmitting.
We therefore create all the possible symbol-spaced subsequences length-$N_c + L - 1$, compute their energy and assume as estimation of the output packet at the a-th antenna of the receiver the subsequence with the maximum energy.

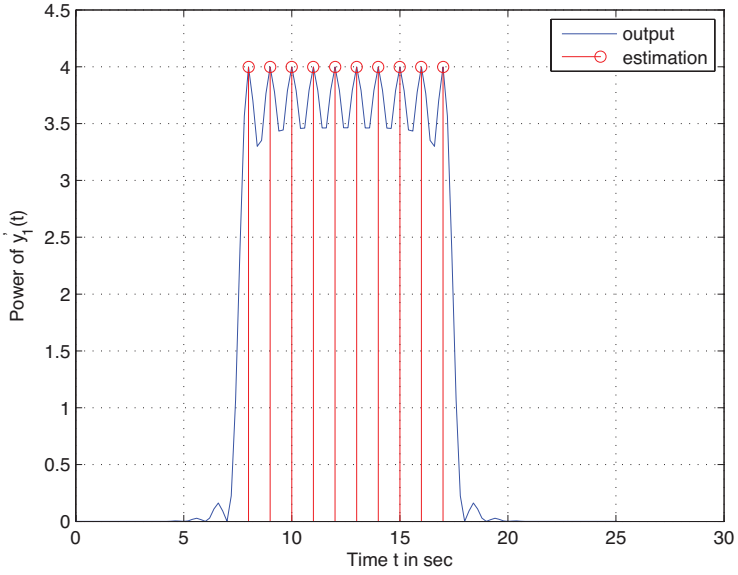

Figure 4.1.4: Power of $y_1'(t)$, at the first antenna of the BS, $U = 2$ users, $N_c = 10$, $T = 1$, over $= 5$ and $\sigma_{x_1}^2 = \sigma_{x_2}^2 = 2$.

4.1.2 Non-Ideal Channels

In the case of non-ideal channels and an OFDM SISO system, which is illustrated in 4.1.2, except that $c(t)$ is not an ideal channel the transmitted waveforms $x'(t) = \sum_{n=0}^{N_c+L-2} x[n]g_T(t - nT)$ are convolved with a frequency-selective channel

$$c(t) = \sum_i c[i]\delta(t - t_i), \quad t_i > 0. \tag{4.11}$$

Under these conditions, at the receiver we get $y(t) = x'(t) \star c(t) + w(t)$ while after filtering using a square root raised cosine pulse $g_R(t)$ we finally get

$$\begin{aligned} y'(t) = y(t) \star g_R(t) &= x'(t) \star c(t) \star g_R(t) + w(t) \star g_R(t) \\ &= x(t) \star g_T(t) \star c(t) \star g_R(t) + w(t) \star g_R(t) \end{aligned} \tag{4.12}$$

where $w(t)$ is additive white Gaussian noise at the receiver.

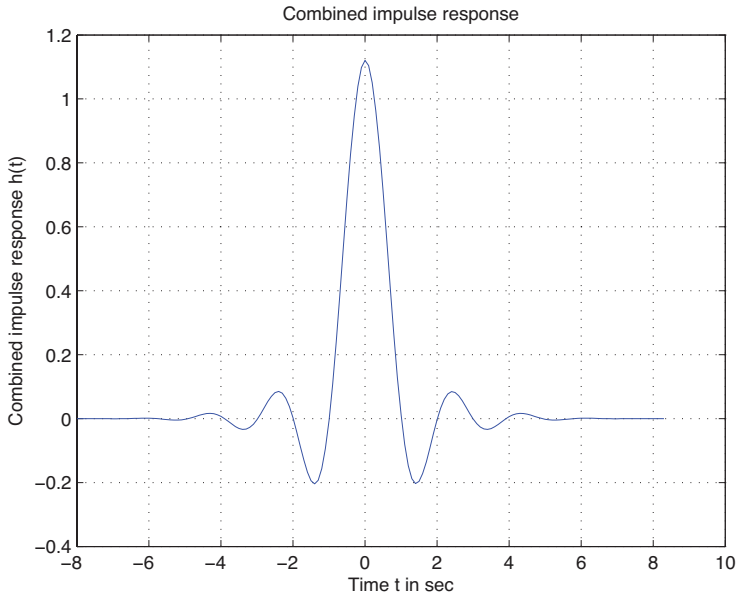

Figure 4.1.5: Composite channel.

The composite channel is depicted in 4.1.5, assuming that $T = 1$ sec and can be written as

$$h(t) = g_T(t) \star c(t) \star g_R(t) \underbrace{=}_{(4.4)} \sum_i c[i] g(t - t_i) \tag{4.13}$$

where $g(t)$ is the corresponding raised cosine pulse (derived from the convolution of the square root raised cosine $g_T(t)$ and $g_R(t)$ at the transmitter and receiver respectively). We observe that the channel is non-causal. As well as in the case of non-causal discrete channel we can always assume that $h(t)$ is causal, as it is illustrated in 4.1.6. Assume now, that the non-zero part of $h(t)$ has L symbol periods (LT_s sec) duration. At 4.1.6, it can be seen that channel's response duration is ~ 16.5 sec. However because of the fact that there are certain long but very small tails at the front and the back part of the channel, we can say that the important part of the channel has smaller length (specifically for this case from ~ 5 sec to ~ 13 sec).

The output of the channel after being filtered by $g_R(t)$ is

$$y'(t) = \sum_{n=0}^{N_c+L-2} x[n] h(t - nT) + \sum_{n=0}^{N_c+L-2} w[n] g_R(t - nT) \tag{4.14}$$

and has duration $(N_c + 2L - 2)$ symbol periods. Our objective is to compute an estimation for the output packet which consists of $(N_c + 2L - 2)$ properly selected symbol-spaced output samples.

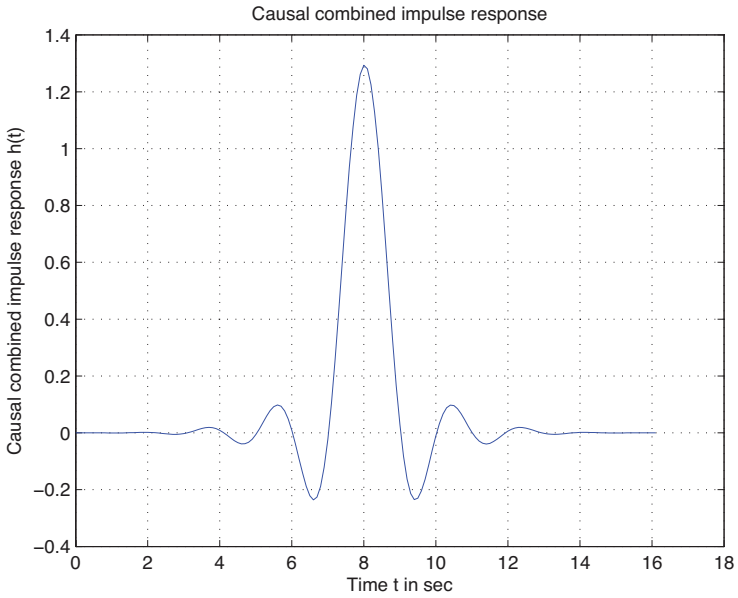

Figure 4.1.6: Causal composite channel.

This can be done if we manage to compute the delay τ and afterwards take samples over $t_k = kT + \tau$ time instants where $k = 0, \ldots, N_c + 2L - 2$.
Consequently, ignoring additive white Gaussian noise at the ouput we get

$$\begin{aligned} y'^{\tau}_k &= y'(kT+\tau) = \sum_{n=0}^{N_c+L-2} x[n]h((k-n)T+\tau) \\ &= \sum_{n=0}^{N_c+L-2} x[n]h^{\tau}_{k-n} = \sum_{m=0}^{L} h^{\tau}_m x[k-m] \end{aligned} \tag{4.15}$$

where $h^{\tau}_m = h[mT + \tau]$ and $m = 0, \ldots, L$.
The $\{y'^{\tau}_k\}_{k=0}^{N_c+L-2}$'s are our estimation for the ouput packet and $\{h^{\tau}_k\}_{k=0}^{L}$ is the discrete equivalent channel.

Having at our disposal the oversampled waveform

$$\mathcal{Y} = \{y'[0], y'[T_s], y'[2T_s], \ldots, y'[(N_c + 2L - 2)T]\} \tag{4.16}$$

or else the oversampled packet, and the only known parameter is the start of the symbol-spaced packet which is at positions $d = d[1], \ldots, d[2]$ then we can create all the length-$(N_c + 2L - 2)$ possible symbol-spaced subsequences, calculate each one's energy

$$\mathcal{E}[d] = \sum_{i=d}^{d+N_c+2L-3} \mathcal{Y}[i]^2, \quad d = d[1], \ldots, d[2] \tag{4.17}$$

and find the position $d^{\star}$ in which $\mathcal{E}[d]$ gets maximized. In that case, $\tau = d^{\star}T_s$ and the estimation for the output packet would be

$$\{y'[0] = y'[d^{\star}T_s], y'[1] = y'[T + d^{\star}T_s], \ldots, y'[N_c + 2L - 3] = y'[(N_c + 2L - 3)T + d^{\star}T_s]\}$$

while for the discrete equivalent channel we get

$$\{h[0] = h[d^{\star}T_s], h[1] = h[T + d^{\star}T_s], \ldots, h[L-1] = h[(L-1)T + d^{\star}T_s]\}.$$

In 4.1.7, we demonstrate the analog output $y'(t)$ and the estimation of the output packet.

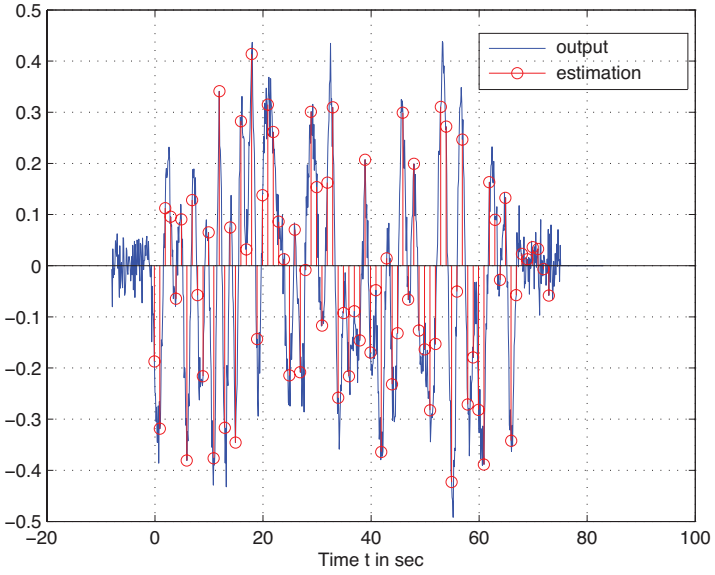

Figure 4.1.7: Analog output and estimation of the output packet (based on energy).

In 4.1.8, we have implemented the combined analog and discrete equivalent channel, having assumed channel length L = 8 (much smaller than the total channel length which includes tails).

In 4.1.9, the symbol spaced output y'_k is illustrated simultaneously with the convolution between channel's input x_k and discrete channel h_k. The reason why there is a little difference between the two graphics is because of the fact that the analog channel's duration is more than $L = 8$ symbol periods. Assuming discrete equivalent channel length-L we "lose" the small contribution of the tails of the analog channel.

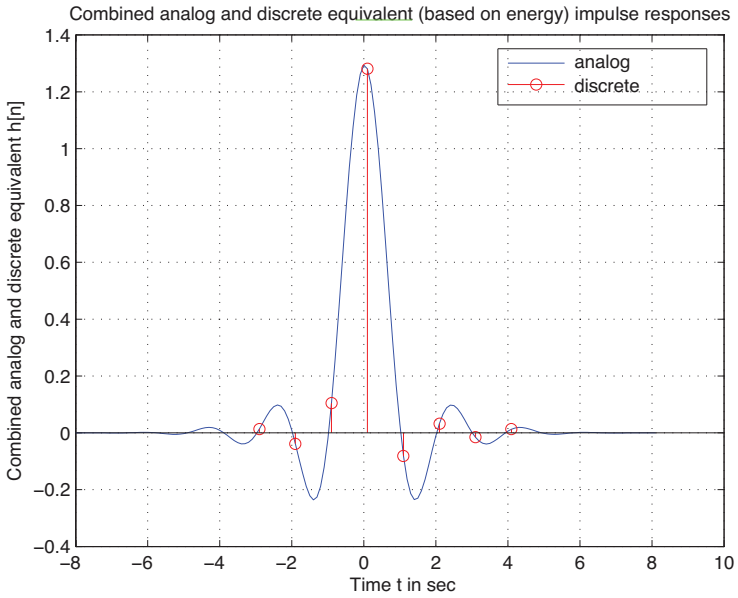

Figure 4.1.8: Analog and discrete equivalent channel (based on energy).

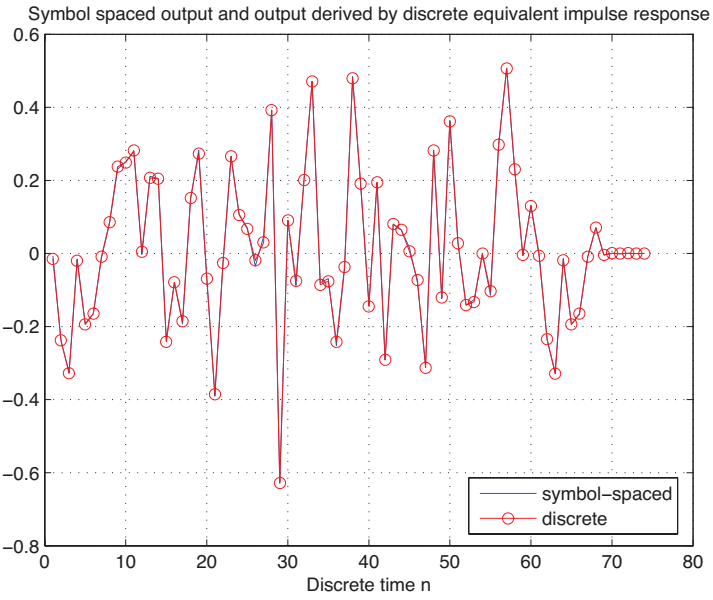

Figure 4.1.9: Symbol-spaced output estimation and convolution between discrete input and discrete equivalent channel (estimation based on energy).

As far as the case of OFDM-SMDA systems is concerned the transmitted waveforms from each user $u = 1, \ldots, U$ with added cyclic prefix $x'^u[t] = \sum_{n=0}^{N_c+L-2} x^u[n] g_T(t - nT)$ pass through a

frequency-selective channel

$$c_a^u[t] = \sum_i c_a^u[i]\delta[t - t_i], \quad t_i > 0 \tag{4.18}$$

where $a = 1, \ldots, A$ is the number of antennas at the base station (BS).
At the a-th antenna at the receiver we get $y_a(t) = \sum_{u=1}^{U} x'^u(t) \star c_a^u(t) + w_a(t)$ while after matched filtering we get

$$\begin{aligned} y'_a(t) = y_a(t) \star g_R(t) &= \sum_{u=1}^{U} x'^u(t) \star c_a^u(t) \star g_R(t) + w_a(t) \star g_R(t) \\ &= \sum_{u=1}^{U} x^u(t) \star g_T(t) \star c_a^u(t) \star g_R(t) + w_a(t) \star g_R(t) \end{aligned} \tag{4.19}$$

where $w_a(t)$ is white Gaussian noise which is added by the ath antenna of the receiver.

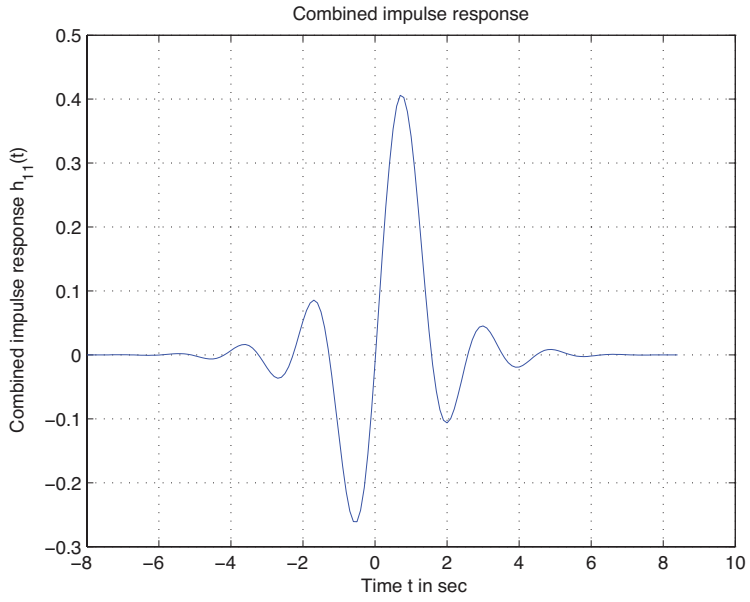

Figure 4.1.10: Composite channel.

The composite channel from the u-th user to the a-th antenna of the BS can be written as

$$h_a^u(t) = \sum_i c_a^u[i] g(t - t_i) \tag{4.20}$$

where $g(t)$ is the corresponding raised cosine pulse. Given in 4.1.10 an implementation for the composite channel of the first user and antenna at the BS, in a supposed 2×2 OFDM-SDMA system, we observe that the channel is non-causal. At 4.1.11 we can assume that $h_1^1(t)$ is causal

and we also notice that the important part of the channel (for this case from ~ 5 sec to ~ 13 sec) has smaller length comparing to the small tails at the front and the back of it.

Channel's output at the a-th antenna in more detail is

$$y'_a[t] = \sum_{u=1}^{U} \sum_{n=0}^{N_c+L-2} x^u[n] h_a^u[t - nT] + \sum_{n=0}^{N_c+L-2} w_a[n] g_R(t - nT) \tag{4.21}$$

and has duration $(N_c + 2L - 2)$ symbol periods. Our objective remains the same and goals to a proper estimation for the output packet for each of the A antennas of the receiver.

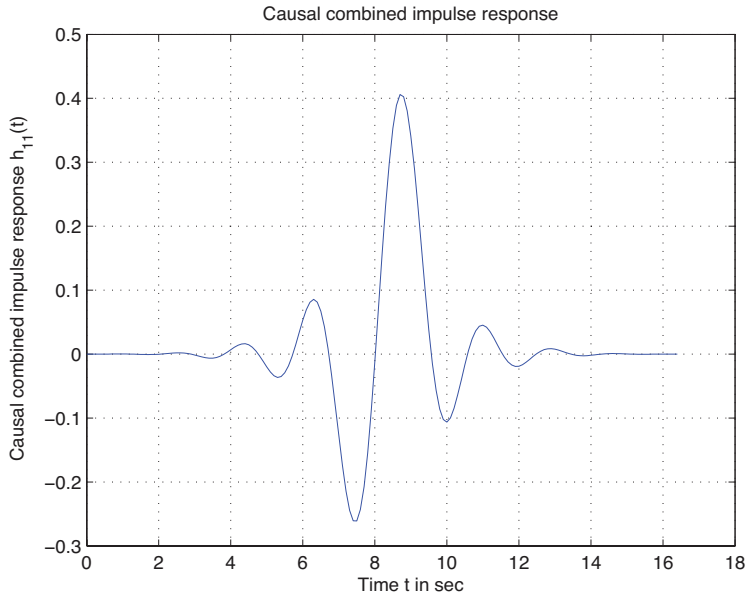

Figure 4.1.11: Causal composite channel.

As it has been mentioned above this can be done if we take samples over $t_k = kT + \tau$ time instants where $k = 0, \ldots, N_c + 2L - 2$

$$\begin{aligned} y'^{\,\tau}_{a\,k} &= y'_a(kT + \tau) = \sum_{u=1}^{U} \sum_{n=0}^{N_c+L-2} x^u[n] h_a^u((k-n)T + \tau) \\ &= \sum_{u=1}^{U} \sum_{n=0}^{N_c+L-2} x^u[n] h^{u\tau}_{a\,k-n} = \sum_{u=1}^{U} \sum_{m=0}^{L} h^{u\tau}_{a\,m} x^u[k-m] \end{aligned} \tag{4.22}$$

where $h^{u\tau}_{a\,m} = h_a^u[mT + \tau]$ for $m = 0, \ldots, L$ and we have also ignored the presence of noise at the receiver.
The $\{y'^{\,\tau}_{ak}\}_{k=0}^{N_c+L-2}$'s are our estimation for the ouput packet at the a-th antenna and $\{h^{u\tau}_{ak}\}_{k=0}^{L}$ is the discrete equivalent channel from the u-th user to the a-th antenna at the BS.

Having at our disposal the oversampled waveform

$$\mathcal{Y}_a = \{y'_a[0], y'_a[T_s], y'_a[2T_s], \ldots, y'_a[(N_c + 2L - 2)T]\} \tag{4.23}$$

or else the oversampled packet received at the a-th antenna, and the only known parameter is the start of the symbol-spaced packet which is at positions $d_a = d_a[1], \ldots, d_a[2]$ then we can create all the length-$(N_c + 2L - 2)$ possible symbol-spaced subsequences, calculate each one's energy

$$\mathcal{E}_a[d_a] = \sum_{i=d_a}^{d_a+N_c+2L-3} \mathcal{Y}_a[i]^2, \quad d_a = d_a[1], \ldots, d_a[2] \tag{4.24}$$

and find the position $d^\star$ in which $\sum_{a=1}^{A} \mathcal{E}_a[d_a]$ gets maximized. In that case $\tau = d^\star T_s$ and the estimation for the output packet at the a-th antenna would be

$$\{y'_a[0] = y'_a[d^\star T_s], y'_a[1] = y'_a[T + d^\star T_s], \ldots, y'_a[N_c + 2L - 3] = y'_a[(N_c + 2L - 3)T + d^\star T_s]\}$$

while for the discrete equivalent channel from the u-th user to the a-th antenna we get

$$\{h^u_a[0] = h^u_a[d^\star T_s], h^u_a[1] = h^u_a[T + d^\star T_s], \ldots, h^u_a[L - 1] = h_a[(L - 1)T + d^\star T_s]\}.$$

In 4.1.12, is depicted the analog output $y'_1(t)$ at the first antenna of the base station, and the estimation of the ouput packet, if we assume that we have to deal with a MIMO system having two users transmitting and two antennas at the BS.

In 4.1.13, the combined analog and discrete equivalent channel are designed in the same plot for channel length $L = 8$.

In 4.1.14, the symbol spaced y'_{1_k} is simultaneously plotted with the convolution between the transmitted data of the first user, x^1_k and discrete channel h^1_{1k}. The reason why there is a little difference between the two plots is again because of the fact that $L = 8 <$ channel's duration and subsequently we "lose" the contribution of channel's tails.

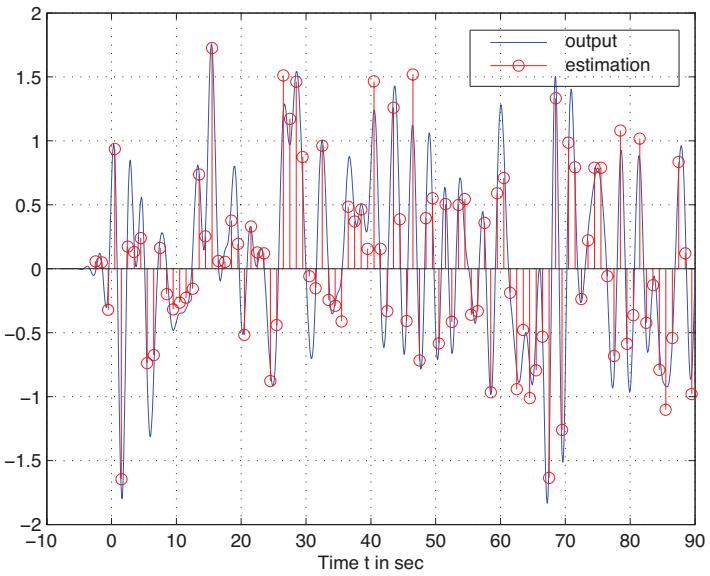

Figure 4.1.12: Analog output and estimation of the output packet at the 1st antenna (based on energy).

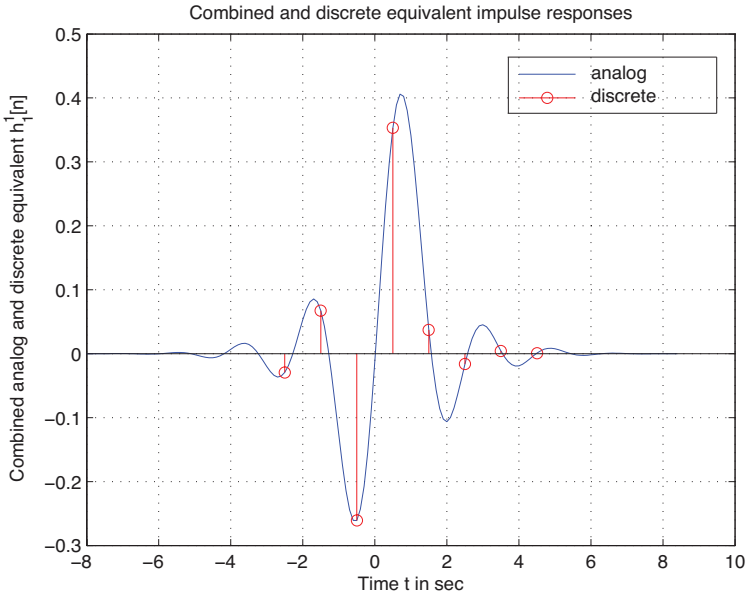

Figure 4.1.13: Analog and discrete equivalent channel $h_1^1[n]$ (based on energy).

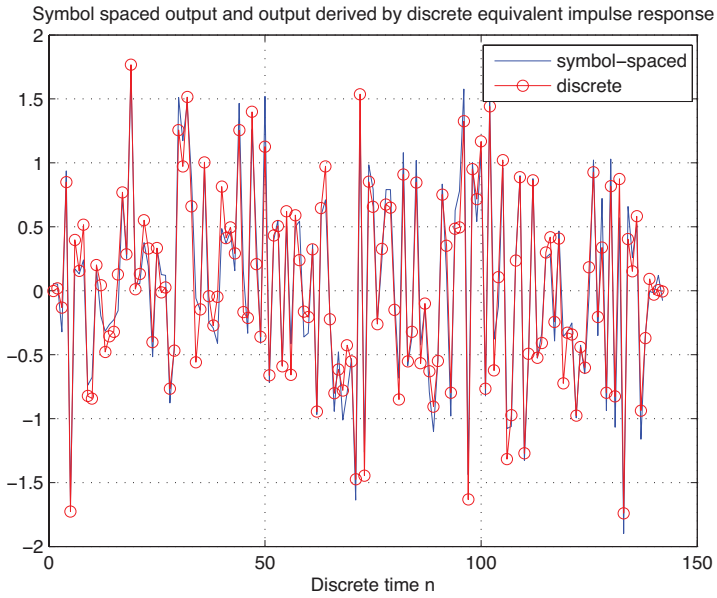

Figure 4.1.14: Symbol-spaced output estimation and convolution between discrete input and discrete equivalent channel (estimation based on energy).

4.2 Impact of CFO on Time Synchronization

In order to make our problem more challenging we also have to study the case of estimating the ouput packet without ignoring the presence of carrier frequency offset $\Delta f^{R,T}$ between the transmitter and the receiver. More specifically, we are going to report only the case of studying an OFDM-SDMA system with U users and A antennas at the receiver
Assuming that there is CFO the channel ouput we get at the a-th antenna at time instant m, for $m = 0, \ldots, N_c + L - 1$ would be the one we described in the previous chapter

$$y'_a[m] = e^{j\Delta\phi^{R,T}[m]} \sum_{u=1}^{U} \sum_{l=0}^{L-1} h_a^u[l] x^u[m-l] + w_a[m], \qquad m = 0, \ldots, N_c + L - 1, \tag{4.25}$$

where $w_a[m]$ refers to white Gaussian noise which is added at the a-th antenna of the receiver at time instant m and $\Delta\phi^{R,T}[m] = 2\pi\Delta\nu^{R,T}\frac{m}{N_c} + \phi^{R,T}$ with CFO $\Delta f^{R,T}$ being normalized to sub-carrier spacing B_{SC}, $(\Delta\nu^{R,T} = \Delta f^{R,T}/B_{SC})$.
As a result, if we take samples over $t_k = kT + \tau$ time instants, where $k = 0, \ldots, N_c + 2L - 2$, at the a-th antenna we get

$$\begin{aligned} y'^{\tau}_{ak} &= y'_a[kT+\tau] = e^{j\Delta\phi^{R,T}[kT+\tau]} \sum_{u=1}^{U} \sum_{n=0}^{N_c+L-2} x^u[n] h_a^u[(k-n)T+\tau] \\ &= e^{j\Delta\phi_k^{(R,T)^\tau}} \sum_{u=1}^{U} \sum_{n=0}^{N_c+L-2} x^u[n] h^{u\tau}_{ak-n} = e^{j\Delta\phi_k^{(R,T)^\tau}} \sum_{u=1}^{U} \sum_{m=0}^{L} h^{u\tau}_{am} x^u[k-m] \end{aligned} \tag{4.26}$$

where $h_{am}^{u\tau} = h_a^u[mT + \tau]$ and $m = 0, \ldots, L$.
Consequently, if at the a-th antenna of the receiver we get the oversampled waveform

$$\mathcal{Y}'_a = \{y'_a[0], y'_a[T_s], y'_a[2T_s], \ldots, y'_a[(N_c + 2L - 2)T]\}, \tag{4.27}$$

the energy of all possible symbol-spaced subsequences which we can create if the start of the symbol-spaced packet is known would be

$$\mathcal{E}_a[d_a] \;=\; \sum_{i=d_a}^{d_a+N_c+2L-3} \mathcal{Y}'_a[i]^2 = \sum_{i=d_a}^{d_a+N_c+2L-3} e^{j\Delta\phi^{R,T}[i]^2} \mathcal{Y}_a[i]^2, \tag{4.28}$$

where $d_a = d_a[1], \ldots, d_a[2]$ is one of the positions we assume to be the start of the packet and $\mathcal{Y}_a$ is given from (4.23).

Therefore the position $d^\star$ at which

$$\begin{aligned} \sum_{a=1}^{A} \sum_{i=d_a}^{d_a+N_c+2L-2} |\mathcal{E}_a[d_a]| &= \sum_{a=1}^{A} \sum_{i=d_a}^{d_a+N_c+2L-2} \underbrace{|e^{j\Delta\phi^{R,T}[i]}|^2}_{=1} \mathcal{Y}_a[i]^2 \\ &= \sum_{a=1}^{A} \sum_{i=d_a}^{d_a+N_c+2L-2} \mathcal{Y}_a[i]^2 \end{aligned} \tag{4.29}$$

gets maximized can be used in order to estimate the output packet as we did in the case of not having CFO.

Chapter 5

Joint Frequency Offset and Channel Estimation

In this chapter, a brief description about the methods of channel estimation will be given, along with a detailed report of the method we selected to use in this thesis.

Additionally, we explain the source of carrier frequency offset between a transmitter and a receiver and finally we present the maximum likelihood estimator we used in this thesis for achieving optimal joint channel and frequency offset estimation.

5.1 Channel Estimation

Channel estimation is the process of estimating the effect of the physical medium on the input sequence (transmitted data). The primary importance of channel estimation is that allows the receiver to take into account the effect of channel on the transmitted signal, secondly channel estimation is essential for removing ISI, noise rejection techniques etc. In wideband mobile communication systems, a dynamic estimation of the channel is essential before the demodulation of OFDM signals because the radio channel is time-varying and frequency selective.

There are two main types of channel estimation methods, namely blind methods and training sequence methods. In blind methods, mathematical or statistical properties of transmitted data are used. In training sequence methods or non-blind methods, the transmitted data and training sequences known to the receiver are embedded into the frame and sent through the channel.

In 5.1.1 is depicted the packet structure, indicating that the length of the training sequence is equal to the transmitted data, a method which is computationally simpler compared to blind methods.

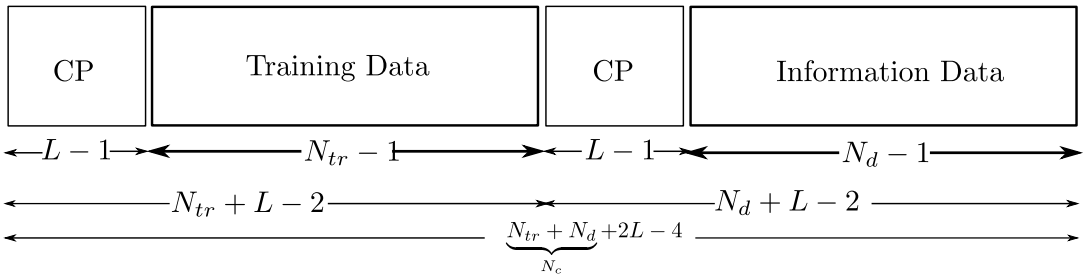

Figure 5.1.1: Transmitted Packet Structure.

The transmitter periodically inserts a number of symbols before the data symbols from which the receiver derives the channel and carrier frequency offset estimation. Although training sequence method is much less computationally intensive than the blind methods, the channel bandwidth is not put into effective use by the transmission of training sequences. The above procedure can be easily summarized in 5.1.2.

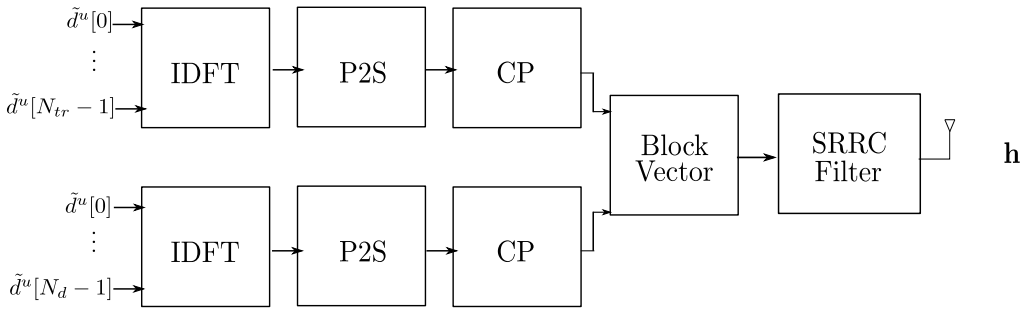

Figure 5.1.2: u-th User Block Diagram.

It is generally preferable to estimate the channel after converting the received signal to frequency domain so as to reduce or eliminate the risk of compounded error.
Consequently, in our case after OFDM modulation of the data and training symbols of each user on frequency domain sub-channels, they will be scaled by different sub-channel frequency response coefficients after passing through the multipath channel. For coherent detection, these sub-channel frequency responses are to be estimated. The way of performing frequency domain channel estimation in our thesis is illustrated in 5.1.3.

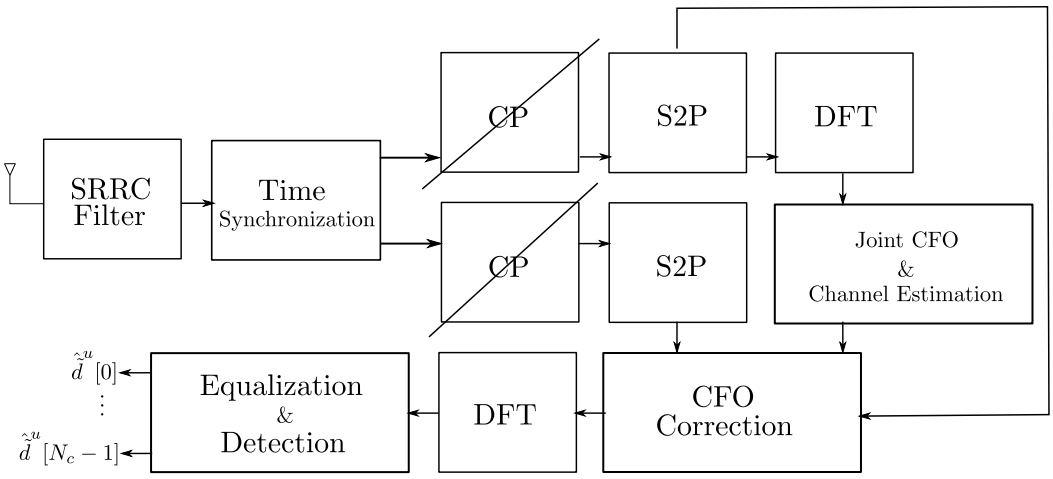

Figure 5.1.3: Receiver a-th Antenna Block Diagram.

5.1.1 Channel Estimation Ignoring Frequency Offset

In this subsection, we focus on studying the non-realistic case of OFDM-SDMA systems, without the impact of carrier frequency offset $\Delta f^{R,T}$ and more specifically we will apply Maximum Likelihood channel estimation using training symbols.
As we have seen in Chapter 3, the ideal frequency domain signal model for each training sub-carrier $n = 0, \ldots, N_{tr} - 1$ is given by

$$\underbrace{\begin{bmatrix} \tilde{y}_1[n] \\ \vdots \\ \tilde{y}_A[n] \end{bmatrix}}_{\tilde{\mathbf{y}}[n]} = \underbrace{\begin{bmatrix} \tilde{h}_1^1[n] & \ldots & \tilde{h}_1^U[n] \\ \vdots & \ddots & \vdots \\ \tilde{h}_A^1[n] & \ldots & \tilde{h}_A^U[n] \end{bmatrix}}_{\tilde{\mathbf{H}}[n]} \underbrace{\begin{bmatrix} \tilde{d}^1[n] \\ \vdots \\ \tilde{d}^U[n] \end{bmatrix}}_{\tilde{\mathbf{d}}[n]} + \underbrace{\begin{bmatrix} \tilde{w}_1[n] \\ \vdots \\ \tilde{w}_A[n] \end{bmatrix}}_{\tilde{\mathbf{w}}[n]}, \tag{5.1}$$

where $N_{tr} = N_d$, N_d is the number of data sub-carriers, $N_{tr} + N_d = N_c$, U is the number of users transmitting and A the number of antennas at the BS.
Generalizing the equation above, for all training sub-carriers, we get

$$\tilde{\mathbf{y}}'_{tr} = \tilde{\mathbf{H}}'_{tr}\tilde{\mathbf{d}}'_{tr} + \tilde{\mathbf{w}}'_{tr} \tag{5.2}$$

where

1. $\tilde{\mathbf{y}}'_{tr} = \begin{bmatrix} \tilde{\mathbf{y}}[0]^T & \tilde{\mathbf{y}}[1]^T & \ldots & \tilde{\mathbf{y}}[N_{tr}-1]^T \end{bmatrix}^T$ denotes the $N_{tr}A \times 1$ received MIMO OFDM training vector.

2. $\tilde{\mathbf{H}}'_{tr} = \mathrm{diag}(\tilde{\mathbf{H}}[0], \tilde{\mathbf{H}}[1], \ldots, \tilde{\mathbf{H}}[\mathrm{N_{tr}} - 1])$ denotes a $N_{tr}A \times N_{tr}U$ block diagonal matrix.

3. $\tilde{\mathbf{d}}'_{tr} = \begin{bmatrix} \tilde{\mathbf{d}}[0]^T & \tilde{\mathbf{d}}[1]^T & \ldots & \tilde{\mathbf{d}}[N_{tr}-1]^T \end{bmatrix}^T$ denotes the $N_{tr}U \times 1$ transmitted MIMO OFDM training vector.

4. Additionally, the $N_{tr}A \times 1$ vector, $\tilde{\mathbf{w}}'_{tr}$, vector represents the receiver noise.

We observe that (5.2) can be rewritten as

$$\tilde{\mathbf{y}}'_{tr} = \tilde{\mathbf{F}}_{tr}\tilde{\mathbf{A}}_{tr}\mathbf{h}_{tr} + \tilde{\mathbf{w}}'_{tr} \tag{5.3}$$

where $\tilde{\mathbf{F}}_{tr} = \mathbf{I}_{A\times A} \otimes \mathbf{F}_{tr}$ with $\mathbf{F}_{tr}$ denoting a $N_{tr} \times N_{tr}$ DFT matrix.
Moreover, $\tilde{\mathbf{A}}_{tr} = \mathbf{I}_{A\times A} \otimes \begin{bmatrix} \mathbf{A}_{1tr} & \dots & \mathbf{A}_{Utr} \end{bmatrix}$ where $\mathbf{A}_{utr} = {\mathbf{F}_{tr}}^H \tilde{\mathbf{D}}'_{utr} \mathbf{F}_{\mathbf{L}tr}$

1. $\tilde{\mathbf{D}}'_{utr} = \mathrm{diag}(\tilde{\mathbf{d}}_{\mathrm{utr}})$ denotes a $N_{tr} \times N_{tr}$ diagonal matrix having main diagonal the training symbols of the u-th user.

2. $\mathbf{F}_{Ltr}$, denotes a $N_{tr} \times L$ DFT matrix.

Finally, $\mathbf{h}_{tr} = \mathrm{vec}(\tilde{\mathbf{H}}'_{\mathrm{tr}})$, denotes a $UAL \times 1$ vector given by the vectorization of the matrix $\tilde{\mathbf{H}}'_{tr}$ containing the channel coefficients in the frequency domain.

Given equation (5.3), we define $\mathbf{B} = \tilde{\mathbf{F}}_{tr}\tilde{\mathbf{A}}_{tr}$. Furthermore, for a value $\mathbf{h}_{tr}$ the vector $\tilde{\mathbf{y}}'_{tr}$ in (5.3) is Gaussian with mean $\mathbf{B}$ and covariance matrix $\sigma_N^2\mathbf{I}_{N_{tr}}$ where $\mathbf{I}_{N_{tr}}$ is the $N_{tr} \times N_{tr}$ identity matrix. Thus, the likelihood function for the parameter $\mathbf{h}_{tr}$ takes the form

$$\Lambda(\tilde{\mathbf{y}}'_{tr}; \breve{\mathbf{h}}_{tr}) = \frac{1}{\pi(\sigma^2_{N_{tr}})^{N_{tr}}} \exp\{-\frac{1}{\sigma^2_{N_{tr}}}[\tilde{\mathbf{y}}'_{tr} - \mathbf{B}\breve{\mathbf{h}}_{tr}]^H[\tilde{\mathbf{y}}'_{tr} - \mathbf{B}\breve{\mathbf{h}}_{tr}]\} \tag{5.4}$$

where $\breve{\mathbf{h}}_{tr}$ is a trial value.
Maximum likelihood estimate maximizes the likelihood function $\Lambda(\tilde{\mathbf{y}}'_{tr}; \breve{\mathbf{h}}_{tr})$. Therefore, we get

$$\hat{\mathbf{h}}_{ML}(\tilde{\mathbf{y}}'_{tr}) = \underset{\mathbf{h}_{tr}\in\mathcal{C}^L}{\arg\max}\, \Lambda(\tilde{\mathbf{y}}'_{tr}; \breve{\mathbf{h}}_{tr}). \tag{5.5}$$

Since the logarithm is a monotone function i.e. $z_1 < z_2$ if and only if $\ln(z_1) < \ln(z_2)$, we can equivalently obtain the ML estimate by maximizing the log-likelihood function

$$\begin{aligned} \hat{\mathbf{h}}_{ML}(\tilde{\mathbf{y}}') &= \underset{\mathbf{h}_{tr}\in\mathcal{C}^L}{\arg\max} \ln(\Lambda(\tilde{\mathbf{y}}'_{tr}; \breve{\mathbf{h}}_{tr})) \\ &= \underset{\mathbf{h}_{tr}\in\mathcal{C}^L}{\arg\max} -[\tilde{\mathbf{y}}'_{tr} - \mathbf{B}\breve{\mathbf{h}}_{tr}]^H[\tilde{\mathbf{y}}'_{tr} - \mathbf{B}\breve{\mathbf{h}}_{tr}] \\ &= \underset{\mathbf{h}_{tr}\in\mathcal{C}^L}{\arg\max} -\|\tilde{\mathbf{y}}'_{tr} - \mathbf{B}\breve{\mathbf{h}}_{tr}\|^2 \end{aligned} \tag{5.6}$$

which is equivalent to

$$\hat{\mathbf{h}}_{ML}(\tilde{\mathbf{y}}'_{tr}) = \underset{\mathbf{h}_{tr}\in\mathcal{C}^L}{\arg\min} \|\tilde{\mathbf{y}}'_{tr} - \mathbf{B}\breve{\mathbf{h}}_{tr}\|^2. \tag{5.7}$$

Under these conditions, $\Lambda(\tilde{\mathbf{y}}_{tr}; \breve{\mathbf{h}}_{tr})$ gets minimized when

$$\nabla_{\breve{\mathbf{h}}_{tr}}[\|\tilde{\mathbf{y}}'_{tr} - \mathbf{B}\breve{\mathbf{h}}_{tr}\|^2] = 0 \tag{5.8}$$

and solving for $\breve{\mathbf{h}}_{tr}$ gives us

$$\hat{\mathbf{h}}_{ML} = (\mathbf{B}^H\mathbf{B})^{-1}\mathbf{B}^H\tilde{\mathbf{y}}'_{tr}. \tag{5.9}$$

For a proof of (5.9) see the Appendix.
By substituting $\mathbf{B} = \tilde{\mathbf{F}}_{tr}\tilde{\mathbf{A}}_{tr}$ in equation (5.9), we get

$$\hat{\mathbf{h}}_{ML} = (\tilde{\mathbf{A}}^H_{tr} \underbrace{\tilde{\mathbf{F}}^H_{tr}\tilde{\mathbf{F}}_{tr}}_{=\mathbf{I}_{N_{tr}\times N_{tr}}} \tilde{\mathbf{A}}_{tr})^{-1}\tilde{\mathbf{A}}^H_{tr}\tilde{\mathbf{F}}^H_{tr}\tilde{\mathbf{y}}'_{tr} = (\tilde{\mathbf{A}}^H_{tr}\tilde{\mathbf{A}}_{tr})^{-1}\tilde{\mathbf{A}}^H_{tr}\tilde{\mathbf{F}}^H_{tr}\tilde{\mathbf{y}}'_{tr} \tag{5.10}$$

which gives the channel responses ML estimation, in the case we ignore the presence of CFO.

5.2 Frequency Offset

A major disadvantage of OFDM-SDMA systems compared with single carrier systems is the sensitivity to frequency offset. In general, frequency offset is defined as the difference between the nominal and actual output frequency.

The uncertainty in carrier frequency is mainly due to a difference in the frequencies of the local oscillator in the transceivers. This difference gives rise to a shift in the frequency domain and is also referred to as frequency offset. The process of demodulation of the OFDM modulated signal of each user with an offset in the carrier frequency can cause large bit error rate and degrade the performance of our system. Therefore it is essential to estimate and eliminate the impact of the frequency offset.

As it was also mentioned above, where we studied the impact of CFO in the OFDM-SDMA system model, we assume a single local oscillator for the total number of users and a different one for the BS.

Frequency offset is denoted as $\Delta f^{R,T}$ between the u-th user and the a-th antenna at the receiver and does not vary between the number of users U or between the A antennas at the BS, as it is also pictured in 3.3.1.
Then, the OFDM signals generated by each user $u = 1, \ldots, U$ can be expressed as

$$x'^{u}[n] = e^{j\phi^{T}[n]} x^{u}[n] \qquad n = 0, \ldots, N_c + L - 1. \tag{5.11}$$

The received signal at the a-th antenna at the receiver, for $n = 0, \ldots, N_c + L - 1$ is expressed as

$$y_a[n] = \sum_{u=1}^{U} h_a^u[n] \star (e^{j(\phi^{T}[n] - \phi^{R}[n])} x^u[n]) + w_a[n] = \sum_{u=1}^{U} h_a^u[n] \star (e^{j\Delta\phi^{R,T}[n]} x^u[n]) + w_a[n] \tag{5.12}$$

where $\Delta\phi^{R,T}$ implies the phase rotation error between the up and the down conversion process on the link between the u-th user and a-th antenna at the receiver and can be also defined as a linear phase process if we take into consideration only the CFO impact

$$\Delta\phi^{R,T}[n] = 2\pi\Delta\nu^{R,T}\frac{n}{N_c} + \phi^{R,T} \tag{5.13}$$

where $\Delta\nu^{R,T}$ is the normalized CFO to sub-carrier spacing B_{SC} and ϕ refers to phase noise.

Because of the fact that we assumed that $\Delta f^{R,T}$ does not differ from user to user, and subsequently the same applies to ϕ and $\Delta\phi^{R,T}$ which is a function of $\Delta f^{R,T}$ we can rewrite (5.12) as

$$y_a[n] = e^{j\Delta\phi^{R,T}[n]} \sum_{u=1}^{U} h_a^u[n] \star x^u[n] + w_a[n] \tag{5.14}$$

It is remarked, that the effect of frequency offset is a translation of these frequency responses of each sub-channel which results in loss of orthogonality between the sub-carriers and leads to inter-carrier interference (ICI).

5.3 Maximum Likelihood (ML) Estimation

In this section, we will take under consideration the system model we derived in Chapter 3 with the impact of CFO in OFDM-SDMA systems and we are going to apply joint channel and carrier frequency offset estimation for each user using the ML estimator and our training sub-carriers $n = 0, \ldots, N_{tr} - 1$ known to the receiver.
ML is known to provide a consistent approach to parameter estimation problems and become minimum variance unbiased with the increase of the size of samples. However, ML estimates can be sensitive to starting values and can also be heavily biased for small size of samples.

In the presence of CFO, the contribution of the u-th user to the training symbol $y_a[n]$ that the BS receives on the nth sub-carrier ($n = 0, \ldots, N_{tr} - 1$) at the a-th antenna during an OFDM symbol is expressed as

$$\tilde{\mathbf{y}}'_{tr} = \tilde{\mathbf{F}}_{tr}\tilde{\mathbf{\Gamma}}_{tr}\tilde{\mathbf{A}}_{tr}\mathbf{h}_{tr} + \tilde{\mathbf{w}}'_{tr}, \tag{5.15}$$

where $\tilde{\mathbf{F}}_{tr}$, $\tilde{\mathbf{A}}_{tr}$ and $\mathbf{h}_{tr}$ have been defined in the subsection above where we described ML channel estimation without the impact of CFO. As far as the received MIMO OFDM $N_{tr}A \times 1$ vector is concerned $\tilde{\mathbf{y}}'_{tr} = \left[\ \tilde{\mathbf{y}}[0]^T \quad \tilde{\mathbf{y}}[1]^T \quad \ldots \quad \tilde{\mathbf{y}}[N_{tr} - 1^T]\ \right]^T$, while the $N_{tr}A \times 1$ vector $\tilde{\mathbf{w}}'_{tr}$ represents the receiver noise. Finally, $\tilde{\mathbf{\Gamma}}_{tr} = \mathbf{I}_{A\times A} \otimes \mathbf{\Gamma}_{tr}(\nu)$ denotes a $N_{tr}A \times N_{tr}A$ block diagonal matrix having as main diagonal, $N_{tr} \times N_{tr}$ diagonal $\mathbf{\Gamma}_{tr}(\nu)$ matrices where

$$\mathbf{\Gamma}_{tr}(\nu) = \mathrm{diag}(1, \mathrm{e}^{\mathrm{j}\Delta\phi^{\mathrm{R,T}}[1]}, \mathrm{e}^{\mathrm{j}\Delta\phi^{\mathrm{R,T}}[2]}, \ldots, \mathrm{e}^{\mathrm{j}\Delta\phi^{\mathrm{R,T}}[\mathrm{N_{tr}}-1]}) \tag{5.16}$$

is the link CFO matrix, defined relatively to our training symbols N_{tr}.

At this point, it is also essential to remind that $\Delta\phi^{R,T}$ which is defined above is a function of ν which describes the normalized CFO to sub-carrier spacing B_{SC}.

For a given pair of $(\mathbf{h}_{tr}, \nu)$ the vector $\tilde{\mathbf{y}}'_{tr}$ in (5.15) is Gaussian with mean $\tilde{\mathbf{F}}_{tr}\tilde{\mathbf{\Gamma}}_{tr}\tilde{\mathbf{A}}_{tr}\mathbf{h}_{tr}$ and covariance matrix $\sigma_N^2\mathbf{I}_{N_{tr}}$ where $\mathbf{I}_{N_{tr}}$ is the $N_{tr} \times N_{tr}$ identity matrix. Thus, the likelihood function for the parameters $(\mathbf{h}_{tr}, \nu)$ takes the form

$$\Lambda(\tilde{\mathbf{y}}'_{tr}; \breve{\mathbf{h}}_{tr}, \breve{\nu}) = \frac{1}{(\pi\sigma^2_{N_{tr}})^{N_{tr}}} \exp\{-\frac{1}{\sigma^2_{N_{tr}}}[\tilde{\mathbf{y}}'_{tr} - \tilde{\mathbf{F}}_{tr}\breve{\tilde{\mathbf{\Gamma}}}_{tr}\tilde{\mathbf{A}}_{tr}\breve{\mathbf{h}}_{tr}]^H[\tilde{\mathbf{y}}'_{tr} - \tilde{\mathbf{F}}_{tr}\breve{\tilde{\mathbf{\Gamma}}}_{tr}\tilde{\mathbf{A}}_{tr}\breve{\mathbf{h}}_{tr}]\} \tag{5.17}$$

where $\breve{\mathbf{h}}_{tr}$ and $\breve{\nu}$ are trial values of $\mathbf{h}_{tr}$ and ν respectively, $\breve{\tilde{\mathbf{\Gamma}}}_{tr} = \mathbf{I}_{A\times A} \otimes \breve{\mathbf{\Gamma}}(\nu)$ where

$$\breve{\mathbf{\Gamma}}(\nu) = \mathrm{diag}(1, \mathrm{e}^{\mathrm{j}2\pi\breve{\Delta\phi}^{\mathrm{R,T}}[1]}, \mathrm{e}^{\mathrm{j}2\pi\breve{\Delta\phi}^{\mathrm{R,T}}[2]}, \ldots, \mathrm{e}^{\mathrm{j}2\pi\breve{\Delta\phi}^{\mathrm{R,T}}[\mathrm{N_{tr}}-1]})$$

and $\Delta\phi^{R,T}[n] = 2\pi\Delta\breve{\nu}^{R,T}\frac{n}{N_{tr}} + \phi^{R,T}$, where $n = 0, \ldots, N_{tr} - 1$.

As indicated in (5.17), two possible approaches may be taken to estimate ν according to the ML criterion. One is the Bayesian approach which consists of modelling of $\breve{\mathbf{h}}_{tr}$ as a random vector with some probability density $p(\breve{\mathbf{h}}_{tr})$ and computing the average of $\Lambda(\tilde{\mathbf{y}}'_{tr}; \breve{\mathbf{h}}_{tr}, \breve{\nu})$ with respect to $p(\breve{\mathbf{h}}_{tr})$. This gives the marginal likelihood of ν, from which the desired estimate of ν is obtained looking for the location of the maximum. The alternative approach, which we are going to follow, aims at maximizing $\Lambda(\tilde{\mathbf{y}}'_{tr}; \breve{\mathbf{h}}_{tr}, \breve{\nu})$ over $\breve{\mathbf{h}}_{tr}$ and $\breve{\nu}$. The location of the maximum

gives the joint ML estimates of $\mathbf{h}_{tr}$ and ν.

ML estimate maximizes the likelihood function $\Lambda(\tilde{\mathbf{y}}'_{tr}; \breve{\mathbf{h}}_{tr}, \breve{\nu})$. Therefore keeping $\breve{\nu}$ fixed and letting $\breve{\mathbf{h}}_{tr}$ vary we get

$$\hat{\mathbf{h}}_{ML}(\tilde{\mathbf{y}}'_{tr}, \breve{\nu}) = \arg\max_{\mathbf{h}_{tr} \in \mathcal{C}^L} \Lambda(\tilde{\mathbf{y}}'_{tr}; \breve{\mathbf{h}}_{tr}, \breve{\nu}). \tag{5.18}$$

Since the logarithm is a monotone function i.e. $z_1 < z_2$ if and only if $\ln(z_1) < \ln(z_2)$, we can equivalently obtain the ML estimate by maximizing the log-likelihood function

$$\begin{aligned}
\hat{\mathbf{h}}_{ML}(\tilde{\mathbf{y}}'_{tr}, \breve{\nu}) &= \arg\max_{\mathbf{h}_{tr} \in \mathcal{C}^L} \ln(\Lambda(\tilde{\mathbf{y}}'_{tr}; \breve{\mathbf{h}}_{tr}, \breve{\nu})) \\
&= \arg\max_{\mathbf{h}_{tr} \in \mathcal{C}^L} -[\tilde{\mathbf{y}}'_{tr} - \tilde{\mathbf{F}}_{tr}\breve{\tilde{\mathbf{\Gamma}}}_{tr}\tilde{\mathbf{A}}_{tr}\breve{\mathbf{h}}_{tr}]^H[\tilde{\mathbf{y}}'_{tr} - \tilde{\mathbf{F}}_{tr}\breve{\tilde{\mathbf{\Gamma}}}_{tr}\tilde{\mathbf{A}}_{tr}\breve{\mathbf{h}}_{tr}] \\
&= \arg\max_{\mathbf{h}_{tr} \in \mathcal{C}^L} -\|\tilde{\mathbf{y}}'_{tr} - \tilde{\mathbf{F}}_{tr}\breve{\tilde{\mathbf{\Gamma}}}_{tr}\tilde{\mathbf{A}}_{tr}\breve{\mathbf{h}}_{tr}\|^2
\end{aligned} \tag{5.19}$$

which is equivalent to

$$\hat{\mathbf{h}}_{ML}(\tilde{\mathbf{y}}'_{tr}, \breve{\nu}) = \arg\min_{\mathbf{h}_{tr} \in \mathcal{C}^L} \|\tilde{\mathbf{y}}'_{tr} - \tilde{\mathbf{F}}_{tr}\breve{\tilde{\mathbf{\Gamma}}}_{tr}\tilde{\mathbf{A}}_{tr}\breve{\mathbf{h}}_{tr}\|^2. \tag{5.20}$$

Under these conditions, for a fixed $\breve{\nu}$, $\Lambda(\tilde{\mathbf{y}}'_{tr}; \breve{\mathbf{h}}_{tr}, \breve{\nu})$ gets simultaneously minimized when

$$\nabla_{\breve{\mathbf{h}}_{tr}}[\|\tilde{\mathbf{y}}'_{tr} - \tilde{\mathbf{F}}_{tr}\breve{\tilde{\mathbf{\Gamma}}}_{tr}\tilde{\mathbf{A}}_{tr}\breve{\mathbf{h}}_{tr}\|^2] = 0 \tag{5.21}$$

and solving for $\breve{\mathbf{h}}_{tr}$ gives us

$$\hat{\mathbf{h}}_{ML} = (\tilde{\mathbf{A}}_{tr}^H\tilde{\mathbf{A}}_{tr})^{-1}\tilde{\mathbf{A}}_{tr}^H\breve{\tilde{\mathbf{\Gamma}}}_{tr}^H\tilde{\mathbf{F}}_{tr}^H\tilde{\mathbf{y}}'_{tr}. \tag{5.22}$$

For a proof of (5.22) see the Appendix.
Next, substituting (5.21) into (5.17) and varying $\breve{\nu}$ we get

$$\hat{\nu}_{ML}(\tilde{\mathbf{y}}'_{tr}) = \arg\max_{\breve{\nu}} \Lambda(\tilde{\mathbf{y}}'_{tr}; \breve{\mathbf{h}}_{tr}, \breve{\nu}) \tag{5.23}$$

which is equivalent to

$$\begin{aligned}
\hat{\nu}_{ML}(\tilde{\mathbf{y}}'_{tr}) &= \arg\max_{\breve{\nu}} \ln(\Lambda(\tilde{\mathbf{y}}'_{tr}; \breve{\mathbf{h}}_{tr}, \breve{\nu})) \\
&= \arg\max_{\breve{\nu}} -\|\tilde{\mathbf{y}}'_{tr} - \tilde{\mathbf{F}}_{tr}\breve{\tilde{\mathbf{\Gamma}}}_{tr}\tilde{\mathbf{A}}_{tr}\breve{\mathbf{h}}_{tr}\|^2 \\
&= \arg\max_{\breve{\nu}} -\|\tilde{\mathbf{y}}'_{tr} - \tilde{\mathbf{F}}_{tr}\breve{\tilde{\mathbf{\Gamma}}}_{tr}\underbrace{\tilde{\mathbf{A}}_{tr}(\tilde{\mathbf{A}}_{tr}^H\tilde{\mathbf{A}}_{tr})^{-1}\tilde{\mathbf{A}}_{tr}^H}_{=\mathbf{P}}\breve{\tilde{\mathbf{\Gamma}}}_{tr}^H\tilde{\mathbf{F}}_{tr}^H\tilde{\mathbf{y}}'_{tr}\|^2 \\
&= \arg\max_{\breve{\nu}} -\|\tilde{\mathbf{y}}'_{tr} - \tilde{\mathbf{F}}_{tr}\breve{\tilde{\mathbf{\Gamma}}}_{tr}\mathbf{P}\breve{\tilde{\mathbf{\Gamma}}}_{tr}^H\tilde{\mathbf{F}}_{tr}^H\tilde{\mathbf{y}}'_{tr}\|^2 \\
&= \arg\min_{\breve{\nu}} \|\tilde{\mathbf{y}}'_{tr} - \tilde{\mathbf{F}}_{tr}\breve{\tilde{\mathbf{\Gamma}}}_{tr}\mathbf{P}\breve{\tilde{\mathbf{\Gamma}}}_{tr}^H\tilde{\mathbf{F}}_{tr}^H\tilde{\mathbf{y}}'_{tr}\|^2
\end{aligned} \tag{5.24}$$

where $\mathbf{P} = \tilde{\mathbf{A}}_{tr}(\tilde{\mathbf{A}}_{tr}^H\tilde{\mathbf{A}}_{tr})^{-1}\tilde{\mathbf{A}}_{tr}^H$ is the projection matrix. It is also known that $\mathbf{P}^2 = \mathbf{P}$ and $\mathbf{P}^H = \mathbf{P}$ as properties of the projection matrix $\mathbf{P}$.

Consequently, for a fixed $\breve{\mathbf{h}}_{tr}$, the ML estimate $\hat{\nu}_{ML}(\tilde{\mathbf{y}}'_{tr})$ is expressed as

$$\hat{\nu}_{ML}(\tilde{\mathbf{y}}'_{tr}) = \arg\min_{\breve{\nu}}[\tilde{\mathbf{y}'}_{tr}^H\tilde{\mathbf{y}}'_{tr} - \tilde{\mathbf{y}'}_{tr}^H\tilde{\mathbf{F}}_{tr}\breve{\tilde{\mathbf{\Gamma}}}_{tr}\mathbf{P}\breve{\tilde{\mathbf{\Gamma}}}_{tr}^H\tilde{\mathbf{F}}_{tr}^H\tilde{\mathbf{y}}'_{tr}] \tag{5.25}$$

which is equivalent to maximizing

$$g(\breve{\nu}) = \tilde{\mathbf{y}'}_{tr}^H\tilde{\mathbf{F}}_{tr}\breve{\tilde{\mathbf{\Gamma}}}_{tr}\mathbf{P}\breve{\tilde{\mathbf{\Gamma}}}_{tr}^H\tilde{\mathbf{F}}_{tr}^H\tilde{\mathbf{y}}'_{tr}. \tag{5.26}$$

For a proof of (5.25) see the Appendix.
In summary, the ν-estimator reads

$$\hat{\nu} = \arg\max_{\breve{\nu}}\{g(\breve{\nu})\}. \tag{5.27}$$

Notice that (5.26) may be put in the form [6]

$$g(\breve{\nu}) = -\rho(0) + 2\Re\{\sum_{m=0}^{N_{tr}-1}\rho(m)e^{-j2\pi m\breve{\nu}}\}, \tag{5.28}$$

where $\Re\{\cdot\}$ denotes the real part of the enclosed quantity, $\rho(m)$ is a weighted correlation of the data

$$\rho(m) = \sum_{k=m}^{N_{tr}-1}[\mathbf{P}]_{k-m,k}\tilde{\mathbf{F}}_{tr}^H\tilde{\mathbf{y}}'_{tr}\tilde{\mathbf{y}'}_{tr}^H\tilde{\mathbf{F}}_{tr} \tag{5.29}$$

and $[\mathbf{P}]_{i,j}$ is the (i, j)-entry of $\mathbf{P}$.

Some remarks of interest as follows:

1. From equations (5.21), (5.26) and (5.27), it appears that the estimates ν and $\mathbf{h}$ are decoupled, meaning that the former can be computed first and then exploited to get the latter. Actually, the estimate of $\mathbf{h}_{tr}$ is obtained by setting $\breve{\nu} = \hat{\nu}$ into (5.21)

$$\hat{\mathbf{h}}_{ML} = (\tilde{\mathbf{A}}_{tr}^H\tilde{\mathbf{A}}_{tr})^{-1}\tilde{\mathbf{A}}_{tr}^H\tilde{\mathbf{\Gamma}}_{tr}^H\tilde{\mathbf{F}}_{tr}^H\tilde{\mathbf{y}}'_{tr}. \tag{5.30}$$

   This result coincides with the classical channel estimate ignoring carrier frequency offset at (5.10) obtained for $\nu = 0$, save that the signal samples $\tilde{\mathbf{y}}'_{tr}[n]$ for $n = 0, \ldots, N_{tr} - 1$ are counter rotated to compensate for the frequency offset.

2. If $\tilde{\mathbf{A}}_{tr}$ is square ($N_{tr} = UL$) and non-singular, then from (5.3) one sees that $\mathbf{P} = \mathbf{I}_{N_{tr}}$ and the right-hand side of (5.26) becomes independent of $\breve{\nu}$. In these conditions maximizing $g(\breve{\nu})$ is meaningless. Physically, this means that the UL data $\tilde{\mathbf{y}}'_{tr}$ are insufficient to estimate the $L + 1$ parameters $(\mathbf{h}_{tr}, \nu)$.

Chapter 6

CFO Correction and Equalization

In this chapter we are going to implement symbol by symbol detection algorithms for OFDM-SDMA systems after firstly compensating the carrier frequency offset between the transmitter and the receiver which has been estimated in the previous chapter.

6.1 CFO Correction

Symbol detection is possible when an estimate $\hat{\nu}$ of the frequency offset ν and an estimate $\hat{\mathbf{h}}$ of the channel response $\mathbf{h}$ are available. These unknown parameters are estimated in the previous chapter and are also assumed to be constant for a minimum time interval.

After obtaining the estimate $\hat{\mathbf{h}}$ of $\mathbf{h} = \text{vec}(\tilde{\mathbf{H}}')$ which denotes a $UAL \times 1$ vector where U is the number of users and A is the number of antennas at the BS and contains the channel input responses, we will then take the discete fourier transform of each length-L estimate in order to get

$$\hat{\tilde{\mathbf{h}}}_a^u = \sum_{l=0}^{L-1} \hat{h}_a^u[l] e^{\frac{-j2\pi ln}{N_c}}, \quad n = 0, \ldots, N_c - 1 \tag{6.1}$$

where $\hat{\tilde{\mathbf{h}}}_{\mathbf{a}}^{\mathbf{u}}$ is the channel estimation for the u-th user and a-th antenna in the frequency domain.

Additionally we have to correct the carrier frequency offset $\Delta\phi^{R,T}$ at the output of each antenna taking advantage of our estimate $\hat{\nu}$. As a result, we have to premultiply each time domain output vector, after cyclic prefix removal, at the a-th antenna $\mathbf{y}'_a = \mathbf{\Gamma}(\nu) \sum_{u=1}^{U} \mathbf{h}_a^u \otimes_{N_c} \mathbf{d}^u + \mathbf{w}_a$ where $\mathbf{\Gamma}(\nu) = \{1, e^{j\Delta\phi^{R,T}[1]}, e^{j\Delta\phi^{R,T}[2]}, \ldots, e^{j\Delta\phi^{R,T}[N_c-1]}\}$ with the matrix

$$\mathbf{\Gamma}'(\hat{\nu}) = \text{diag}(1, \mathrm{e}^{\mathrm{j}\hat{\Delta\phi}^{\mathrm{R,T}}[1]}, \mathrm{e}^{\mathrm{j}\hat{\Delta\phi}^{\mathrm{R,T}}[2]}, \ldots, \mathrm{e}^{\mathrm{j}\hat{\Delta\phi}^{\mathrm{R,T}}[\mathrm{N_c}-1]}) \tag{6.2}$$

where $\Delta\phi^{R,T}[m] = 2\pi\Delta\hat{\nu}\frac{m}{N_c} + \phi^{R,T} \quad m = 0, \ldots, N_c - 1$ and $\hat{\nu}$ has been estimated in the previous chapter, based on the training sub-carriers, remains common for the following data sub-carriers and also between all the users.

Finally, we get

$$\hat{\mathbf{y}}'_a = \mathbf{\Gamma}'(\hat{\nu})\mathbf{y}'_a = \underbrace{\mathbf{\Gamma}'(\hat{\nu})\mathbf{\Gamma}(\nu)}_{\mathbf{I}} \sum_{u=1}^{U} \hat{\mathbf{h}}_a^u \otimes_{N_c} \mathbf{d}^u + \mathbf{w}_a$$
$$= \sum_{u=1}^{U} \hat{\mathbf{h}}_a^u \otimes_{N_c} \mathbf{d}^u + \mathbf{w}_a \tag{6.3}$$

Note that $\mathbf{\Gamma}'(\hat{\nu})\mathbf{\Gamma} = \mathbf{I}$ only in the ideal case where the frequency offset is estimated without any error.
We understand that $\hat{\mathbf{y}}_a$ is the system output at the a-th antenna after carrier frequency offset correction.
If we then apply Discrete Fourier Transform to equation (6.3) we get

$$\mathrm{DFT}(\hat{\mathbf{y}}'_{\mathrm{a}}) = \mathrm{DFT}(\sum_{\mathrm{u=1}}^{\mathrm{U}} \hat{\mathbf{h}}_{\mathrm{a}}^{\mathrm{u}} \otimes_{\mathrm{N_c}} \mathbf{d}^{\mathrm{u}} + \mathbf{w}_{\mathrm{a}}) = \mathrm{DFT}(\sum_{\mathrm{u=1}}^{\mathrm{U}} \hat{\mathbf{h}}_{\mathrm{a}}^{\mathrm{u}} \otimes_{\mathrm{N_c}} \mathbf{d}^{\mathrm{u}}) + \mathrm{DFT}(\mathbf{w}_{\mathrm{a}}))$$
$$= \sum_{u=1}^{U} \hat{\tilde{\mathbf{h}}}_a^u \odot \tilde{\mathbf{d}}^u + \tilde{\mathbf{w}}_a. \tag{6.4}$$

It is obvious, that convolution in time domain becomes equivalent with multiplication in the frequency domain. As a result, (6.4) can be rewritten for each sub-carrier n as it follows

$$\underbrace{\begin{bmatrix} \hat{\tilde{y}}_1[n] \\ \vdots \\ \hat{\tilde{y}}_A[n] \end{bmatrix}}_{\hat{\tilde{\mathbf{y}}}[n]} = \underbrace{\begin{bmatrix} \hat{\tilde{h}}_1^1[n] & \dots & \hat{\tilde{h}}_1^U[n] \\ \vdots & \ddots & \vdots \\ \hat{\tilde{h}}_A^1[n] & \dots & \hat{\tilde{h}}_A^U[n] \end{bmatrix}}_{\hat{\tilde{\mathbf{H}}}[n]} \underbrace{\begin{bmatrix} \tilde{d}^1[n] \\ \vdots \\ \tilde{d}^U[n] \end{bmatrix}}_{\tilde{\mathbf{d}}[n]} + \underbrace{\begin{bmatrix} \tilde{w}_1[n] \\ \vdots \\ \tilde{w}_A[n] \end{bmatrix}}_{\tilde{\mathbf{w}}[n]}, \quad n = 0, \dots, N_c - 1 \tag{6.5}$$

Generalizing the above we get the following signal system model

$$\hat{\tilde{\mathbf{y}}}' = \hat{\tilde{\mathbf{H}}}'\tilde{\mathbf{d}}' + \tilde{\mathbf{w}}' \tag{6.6}$$

which coincides with the system model, presented in Chapter 3 where OFDM-SDMA systems without the impact of CFO, were considered. The only difference is that we take advantage of the channel coefficients estimated above.

6.2 Zero Forcing (ZF) Detector

Zero-Forcing (ZF) scheme is used in order to separate the signals received from the U users, based on the channel knowledge obtained by frequency domain Maximum Likelihood channel estimator.

As a consequence, the zero-forcing multi-user signal detector calculates an estimate $\hat{\tilde{\mathbf{d}}}[n] = \begin{bmatrix} \hat{\tilde{d}}^1[n] & \dots & \hat{\tilde{d}}^U[n] \end{bmatrix}^T$ of the transmitted signal from each user $\tilde{\mathbf{d}}[n] = \begin{bmatrix} \tilde{d}^1[n] & \dots & \tilde{d}^U[n] \end{bmatrix}^T$

per sub-carrier by multiplying the received output with the inverse channel coefficients matrix for each sub-carrier $n = 0, \ldots, N_c - 1$, which has been estimated and described above $\hat{\tilde{\mathbf{H}}}[n]$

$$\hat{\tilde{\mathbf{d}}}[n] = \hat{\tilde{\mathbf{H}}}[n]^{-1}\hat{\tilde{\mathbf{y}}}[n]. \tag{6.7}$$

Considering the above, we manage to eliminate the intersymbol interference (ISI), by taking into consideration each user's channel estimated impulse response. Nonetheless, the ZF detector can fully suppress multi-user interference.
The ZF detector in OFDM-SDMA systems has also an advantage over the orthogonal frequency division multiple access (OFDMA) systems in terms of the interaction of CFO impacts among users, because in the uplink OFDMA systems, each of all users occupies different sub-carriers, and ICI directly leads to multi-user signal interference [8].

6.3 Least Squares (LS) Detector

In this case, the optimization interval of Least Squares detector spans the entire hyperplane $\tilde{d}$. The least squares (LS) receiver is given by

$$\breve{\tilde{\mathbf{d}}}[n] = \arg\min_{\tilde{\mathbf{d}}} \|\hat{\tilde{\mathbf{H}}}[n]\tilde{\mathbf{d}}[n] - \hat{\tilde{\mathbf{y}}}[n]\|_2^2, \quad n = 0, \ldots, N_c - 1, \tag{6.8}$$

which constitutes a least squares problem.
Under these conditions, the quantity above gets minimized when

$$\nabla_{\tilde{\mathbf{d}}}[\|\hat{\tilde{\mathbf{H}}}[n]\tilde{\mathbf{d}}[n] - \hat{\tilde{\mathbf{y}}}[n]\|_2^2] = 0 \tag{6.9}$$

and solving for $\breve{\tilde{\mathbf{d}}}$ gives us for each subcarrier n

$$\hat{\tilde{\mathbf{d}}}_{LS}[n] = (\hat{\tilde{\mathbf{H}}}^H[n]\hat{\tilde{\mathbf{H}}}[n])^{-1}\hat{\tilde{\mathbf{H}}}^H[n]\hat{\tilde{\mathbf{y}}}[n] \tag{6.10}$$

For a proof of (6.10) see the Appendix.
A remark of interest here is that Least Squares detector coincides with the Zero Forcing detector if we proceed with some calculations at (6.9)

$$\begin{aligned}\hat{\tilde{\mathbf{d}}}_{LS}[n] = (\hat{\tilde{\mathbf{H}}}^H[n]\hat{\tilde{\mathbf{H}}}[n])^{-1}\hat{\tilde{\mathbf{H}}}^H[n]\hat{\tilde{\mathbf{y}}}[n] &= \hat{\tilde{\mathbf{H}}}[n]^{-1}\underbrace{\hat{\tilde{\mathbf{H}}}^H[n]^{-1}\hat{\tilde{\mathbf{H}}}^H[n]}_{=\mathbf{I}}\hat{\tilde{\mathbf{y}}}[n] \\ &= \hat{\tilde{\mathbf{H}}}[n]^{-1}\hat{\tilde{\mathbf{y}}}[n]\end{aligned} \tag{6.11}$$

which confirms (6.7).

6.4 Maximum Likelihood (ML) Detector

In this thesis, we assume i.i.d. AWGN on all antennas. The optimal multi-user detector for each carrier is given by maximum likelihood (ML) detector which minimizes the log-likelihood function $\Lambda(\tilde{\mathbf{d}}[n])$ for each given by

$$\Lambda(\tilde{\mathbf{d}}[n]) = \|\hat{\tilde{\mathbf{H}}}[n]\tilde{\mathbf{d}}[n] - \hat{\tilde{\mathbf{y}}}[n]\|_2^2, \quad n = 0, \ldots, N_c - 1, \tag{6.12}$$

over the set of possible constellation points $\tilde{d}$ which are in the set $\tilde{d}_{ML} = \{1+j, 1-j, -1+j, -1-j\}^U$ for 4-QAM.
The ML detector is thus given by

$$\hat{\tilde{\mathbf{d}}}_{GLRT}[n] = \underset{\tilde{\mathbf{d}} \in \tilde{d}_{ML}}{\arg\min} \|\hat{\tilde{\mathbf{H}}}[n]\tilde{\mathbf{d}}[n] - \hat{\tilde{\mathbf{y}}}[n]\|_2^2 \tag{6.13}$$

and denotes the generalized-likelihood-ratio-test (GLRT) detection of $\tilde{\mathbf{d}}$. As is well known, the main disadvantage of the ML detector is its complexity: the number of points in $\tilde{d}_{ML}$ grows exponentially with the number of users U and the constellation order.

We remind that $\hat{\tilde{\mathbf{H}}}[n]$ denotes an $A \times U$ matrix containing each estimated channel's impulse response in the frequency domain for the nth sub-carrier.
To sum up, the ML multiuser signal detector for each sub-carrier $n = 0, \ldots, N_c - 1$ is given by an exhaustive search among all 4^U data sequences where $\tilde{d}_{ML} \in \{\pm 1 \pm j\}^U$ in order to find the one that minimizes the quantity above in (6.13).

Some remarks of interest as follows:

1. When the number of sub-carriers N_c is large, transmit samples $\tilde{d}[n], (n = 0, \ldots, N_c - 1)$ can be modelled as complex Gaussian via the central limit theorem (CLT).

2. When the number of paths is large, the received OFDM signal at the A antennas, $\hat{\tilde{\mathbf{y}}}$ may also be modelled as a complex Gaussian.

Chapter 7

Software Defined Radio

In this chapter, firstly we are going to describe and analyze what exactly a Software-Defined Radio system (SDR) is, and secondly how can we take advantage of such systems in order to implement a real-time wireless communication system.

7.1 Introduction to SDR

Software Defined Radio (SDR) is where all the signal manipulations and processing works in radio communication are done in software instead of hardware. In other words, SDR is a radio communication system where components that have been typically implemented in hardware (e.g. mixers, filters, amplifiers, modulators/demodulators, detectors) are instead implemented by means of software on a personal computer or embedding computing devices. This provides the SDR huge flexibility with respect to operating frequencies, supported protocols and waveforms meaning that virtually anything can be implemented.

A basic SDR system may consist of a personal computer equipped with a sound card, or other analog-to-digital converter, preceded by some form of RF front end. Significant amounts of signal processing are handed over to the general-purpose processor, rather than being done in special-purpose hardware. Such a design produces a radio which can receive and transmit widely different radio protocols (sometimes referred to as waveforms) based solely on the software used.

As a result, in SDR, signal will be processed in digital domain instead of analog domain as in the conventional radio. The digitization work will be done by a device called the Analog to Digital Converter (ADC). Fig. 7.1.1 depicts the concept of Software Defined Radio. This figure shows that the ADC process is taking place after the Front End circuit. Front End is used to down convert the signal to the lower frequency called an Intermediate Frequency (IF) ; this is needed due to the limitation of the speed of current Commercial of the Shelf (COTS) ADC. The ADC will digitize signal and pass it to the baseband processor for further processes; demodulation, channel coding, source coding and etc. In conventional radio, all these processes are done in hardware.

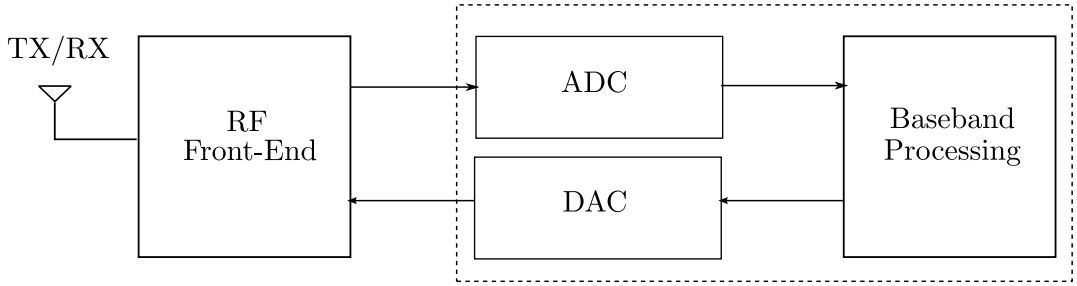

Figure 7.1.1: Software Defined Radio Block Diagram.

In general, Software Defined Radio (SDR) is defined as a software based communication platform which characteristics can be reconfigured and modified to perform different functions at different times.

The device we use so as to transmit and receive waveforms is called Universal Software Radio Peripheral (USRP). At this time there are two versions of this device, USRP1 and USRP2. In the following sections of this chapter we will describe some of the basic characteristics of USRP1, which are essential to know when you program applications at GNU radio environment.

7.2 USRP

The Universal Software Radio Peripheral (USRP) provides relatively cheap hardware for building a software defined radio testbed. It has an open design, with schematics and drivers freely available. In general, USRP is a flexible low-cost platform for SDRs developed by Matt Ettus [7]. USRP consists of two main boards; a motherboard on which can be plugged in up to 4 expansion cards called daughterboards. The motherboard consists of four 12-bit Analog to Digital Converter (ADC), four 14-bit Digital to Analog Converter (DAC), a programmable USB 2.0 controller for communication between USRP and GNU Radio and an FPGA for implementing four Digital Down Converter (DDC) and high rate signal processing. There are also four slots on the motherboard which are used to connect the daughterboards with the motherboard. The reason why it has been designed in this way is to offer practicality to whoever want to set up his own communication system and also want to work on a range of different frequencies. This convenience is offered by the wide range of daughterboards each of which can be chosen in order to fulfil anyone's requirements. In our thesis we are going to use only daughterboards which operate at the range of 2.4 GHz.

7.2.1 RF Front-End, AD and DA Converters

The daughterboard is acting as the RF front-end of the SDR. More specifically in order to create our complete radio system we used RFX2400 frontend daughterboards which have designed to operate at the band of 2.4GHz. This band consists of a continuous spectrum area of 100MHz, having as lower bound 2.4GHz, and also is one of the frequency areas belonging to the ISM

band. Over the daughterboard there are surface mounted connectors, labeled RX, TX/RX meant for a receiver and a transceiver respectively.

As far as the transmitter is concerned, the baseband analog signal it gets from the motherboard is then modulated in a central frequency of our choice. Transmitter's output is then directed to a switch which can be software programmed whether we want to transmit or receive a waveform. Additionally the baseband signal with the aid of the daughterboard's ADC (Analog to Digital Converter) is afterwards sampled with rate 64 MSPS (Mega Symbols per second) and identically quantized at 12bit. At this point we have to mention that the representation quality of a signal majorly depends on the thresholds range. Consequently, the best way to customize the quantizer to the received signal is by putting a Programmable Gain Amplifier (PGA) before the ADC in order to achieve adaptivity of the thresholds. Actually this solution is a compromise between the need for big dynamic range and precision in sampling.

On the other hand the receiver consists of an oscillator which frequency can be programmed and a mixer which is used for mixing this frequency with the received signal. This type of receiver is called direct conversion because of the fact that converts our signal from its frequency directly to baseband.
The baseband signal is then converted into analog form by using the daughterboard's DAC (Digital to Analog Converter) which operates at 128 MSPS (Mega Symbols per second) and has 14bit precision. In actual fact, DAC produces two analog baseband signals, I and Q respectively, which phases have a difference of 90 degrees. As a result, we can demodulate them without provoking interference between them. We can also imagine I and Q analog signals as the real and imaginary part of a complex signal which are then sent for sampling to the motherboard.

7.2.2 FPGA, USRP and GNU Radio

As it was mentioned in the first section of this chapter, a personal computer which is connected via USB cable with the USRP is essential for programming a real-time communication system. Unfortunately USB port has maximum transfer rate 32Mbyte/sec while the USRP at a transceiver mode has to send and receive

$$(64\text{MSPS} \times 12\frac{\text{bit}}{\text{Sample}} + 128\text{MSPS} \times 14\frac{\text{bit}}{\text{Sample}}) \times 2 = 640\frac{\text{Mbyte}}{\text{sec}}.$$

Consequently, the USRP's Field Programmable Gate Array (FPGA) will convert 12 and 14bit into the nearest multiple of 8bit so as the PC to be able to deal with them.
FPGA consists of two digital filters, the decimation and the interpolation. The first receives ADC samples with rate 64MSPS and oversamples with a factor called decimation rate which always has to be a multiple of 2 and also between 4 and 256. The interpolation filter is responsible for oversampling the samples coming from the PC with a factor called interpolation rate, having as ultimate goal to reach the sampling rate of the DAC. However, because of the interpolation rate and the transfer rate that USB uses, the final transfer rate will be the product of those two rates, which makes the use of a buffer necessary.
It is also worth mentioning that the maximum output power of the DAC chip used in the USRP is 10mW, while the Programmable Gain Amplifier (PGA) on the receiver side of the USRP can

give gain up to 20dB.
Nevertheless, the existence of buffers shouldn't evoke negligence of the rate we use, because either the buffer may be full and accordingly have a lossy sample transfer or the buffer may be empty. Then the FPGA will not have any samples to send and we will have underflow which is denoted as uU at the terminal window of our application.
Another reason why we may lose samples is either because of the way the USB functions or because of the connectivity between a PC and peripheral devices such as the USRP. In the first case, USB sends packets and not bitstreams, as a consequence, samples should be stored in a buffer until they are going to be sent to the PC. In the second case, the relationship between the PC and the USRP is the one between master and slave, which means that only the first gives permission for the start of a transaction. Consequently, if the PC does not read fast enough the samples sent by the FPGA, the buffer will overflow.

GNU Radio is an open source software toolkit which consists of signal processing blocks library and the glue to tie these blocks together for building and deploying SDRs. The signal processing blocks are written in C++ while python is used as a scripting language to tie the blocks together to form the flow graph. Simplified Wrapper and Interface Generator (SWIG) is used as the interface compiler which allows the integration between C++ and Python language. Fig. 7.2.1 shows the structure of GNU Radio and USRP SDR.
The USRP will digitize the inflow data from the air and passing it to the GNU Radio through the USB interface. GNU Radio will then further process the signal by demodulating and filtering until the signal is translated to a packet or a stream of data.
GNU radio is a free software development toolkit that provides the signal processing runtime and processing blocks to implement software radios using readily-available, low-cost external RF hardware and commodity processors.
GNU radio applications are primarily written using the Python programming language, while the supplied, performance-critical signal path is implemented in C++.

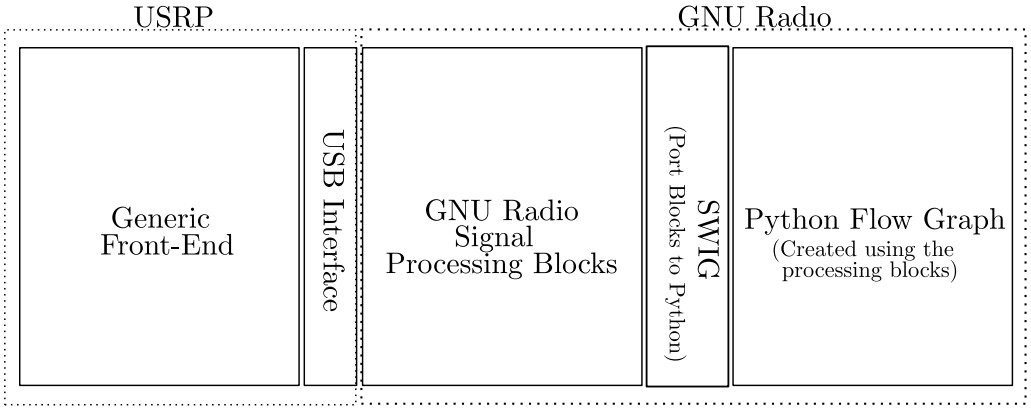

Figure 7.2.1: GNU Radio Components.

7.3 Experimental Setup

Our implementation of a real time OFDM-SDMA wireless communication system, consisting of $U = 2$ user terminals and a base station with $A = 2$ antennas in SDR, utilizing GNU Radio, demanded the existence of 2 USRPs, 4 RFX2400 daughterboards, 2 power adapters, 2 USB cables and 2 computers equipped with GNU radio.

The PC with USRP A acts as the receiver while the PC and USRP B acts as the transmitter. The RFX2400 which were used for our experiment can cover frequencies from 2.3GHz to 2.9GHz as it has been also mentioned above. The experiments were conducted indoor. However, there was a neighboring access point to consider which can interfere with the USRP frequencies. Therefore the access point frequency was set to operate at 5.0GHz to avoid the interference and jamming with the USRP which was set to 2.45GHz.

The aim of these experiments was to implement an SDR testbed using the USRPs and study more thoroughly OFDM-SDMA systems. In particular, we transmitted OFDM 4-QAM modulated symbols from USRP B using its both daughterboards so as to simulate two different users, and then process the data at the receiver.

However, data to be transmitted should have a particular position at the symbol sequence so as to be read efficiently by the USRPs. Moreover, after implementing in Matlab all the necessary steps required for transmitting OFDM modulated symbols, we have to separate the real from the imaginary part and consecutively place each antenna's symbols over a period of time (called interleaving process). In the meantime, the python code is executed and enables transmission from both antennas.

On the other hand, in order to make reception possible using two antennas, a corresponding python code is executed at the receiver which has been constructed with the aid of GNU Radio Companion (GRC). GRC gives us the potential to form flow graphs which are then connected together and generate a python code. Then, our packetizer at the receiver, reads the data stored at the FIFO and recognizes, after separating from noise packets, the transmitted packets by computing the energy of two consecutive data sequences. In the sequel, each packet undergoes processing which includes joint channel and frequency offset estimation (CFO) algorithms. CFO correction and finally detection algorithms for the received symbols were applied and tested while they are also reported in more detail in the previous chapters.

Chapter 8

Simulations and Experimental Results

In this chapter, we will report some significant experimental results, concerning OFDM-SDMA systems and the Bit Error Rate (BER) with respect to Signal to Noise Ratio (SNR) during a number of transmissions either by using results taken from our SDR testbed located at an indoor environment or by attempting to simulate all the above in Matlab.

In Table 8.1, we report the parameters used for the specific case study which consists of a basestation equipped with two antennas and up to two simultaneously or not transmitting users.

Number of training sub-carriers	$N_{tr} = 200$
Number of data sub-carriers	$N_d = 200$
Cyclic prefix length	$L = 1$
Number of antennas	$A = 2$
Number of users	$U = 2$
Samping rate	over = 10
SRRC roll-off factor	$k = 0.5$
Number of transmissions	maxiters = 3000
SNR values range	$10 < \text{SNR} < 20$
Carrier frequency	2.45 GHz
Modulation order	4-QAM
CFO Range	$[-1/2 : 1/4000 : (1/2 - 1/4000)]$
FFT size	$N_f = 4 * 1024$
Transmitter's amplitude range	$[200, 14000]$

Table 8.1: OFDM-SDMA Case-Study Specification.

8.1 Simulations

In this section, we evaluate the system performance under various Signal to Noise Ratio values. Therefore, we consider a set-up with two users ($U = 2$) and two antennas at the basestation

$(A = 2)$, where we continuously increase the SNR values for a number of $p = 2000$ transmissions considering each value while the channels remain constant for the total number of transmissions, in an attempt to simulate AWGN channels.

Given the values of SNR for each iteration we can easily compute noise's variance at each of the antennas at the base station by firstly computing the total power of the noiseless output

$$P_a = \mathbf{E}[y'^2_a[k]] = \frac{\sum_{k=0}^{N_{tr}+L-2} |\sum_{u=1}^{U} \sum_{n=0}^{N_{tr}+L-2} x^u[n] h^u_a[(k-n)]|^2}{N_{tr}+L-2} \tag{8.1}$$

where $a = 1, \ldots, A$ and $u = 1, \ldots, U$ denotes the number of antennas and users respectively, while $k = 0, \ldots, N_{tr} + L - 2$, and $h^u_a[k]$ is the discrete equivalent channel for the u-th user and a-th antenna at time instant k. We have to emphasize here that $y'_a[k]$ denotes the noiseless channel output at the a-th antenna at time instant k.
Then, it is obvious from the definition of Signal to Noise Ratio that at k time instants

$$\mathrm{SNR} = \frac{\mathcal{E}[\mathrm{y'^2_a[k]}]}{\mathbf{E}[\mathrm{w^2_a[k]}]} \qquad \mathrm{k} = 0, \ldots, \mathrm{N_{tr}} + \mathrm{L} - 2 \tag{8.2}$$

where $\mathbf{E}[w^2_a[k]] = \sigma^2_{w_a} \underbrace{|G_R(F)|^2}_{=1} = \sigma^2_{w_a}$ because of the fact that $g_T(t) = g_R(t)$ and $g_T(t) = g_T(-t)$ ($g_T(t)$ even) as a square root raised cosine pulse.

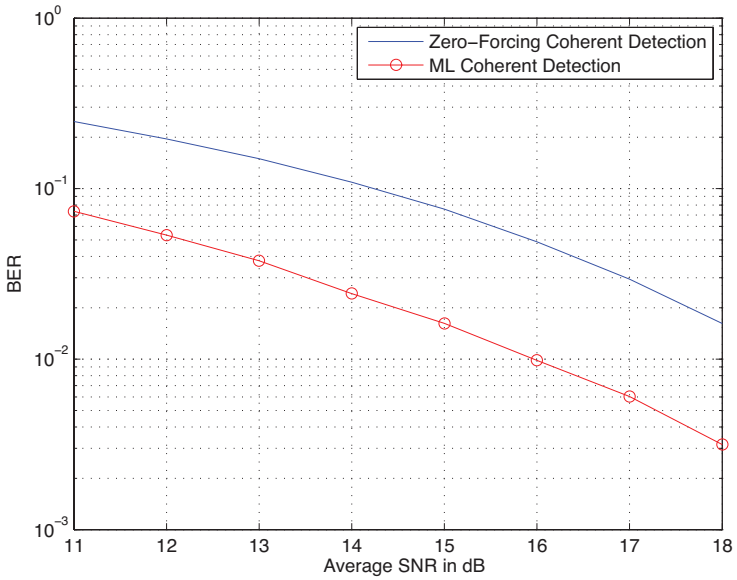

Figure 8.1.1: BER versus average SNR for OFDM-SDMA for U=2 and A=2.

Consequently, for noise's variance at the a-th antenna we get

$$\sigma^2_{w_a} = \frac{\mathcal{E}[y'^2_a[k]]}{\mathrm{SNR}} \tag{8.3}$$

and finally we create in Matlab w_1 and w_2 vectors which denote additive Gaussian noise for each antenna at the receiver.
The simulation parameters are listed in Table 8.1. Within this simulation set-up we compare the introduced ML and ZF schemes with CFO compensation and correction at the receiver as well as ML channel estimation using the training sub-carriers.

In 8.1.1, the bit error rate degradation for a flat fading channel is pictured, whereas the normalized CFO for this case, remains constant.

In real time cellular mobile networks the user terminals can pre-compensate its coarse CFOs such that only residual frequency offsets occur at the receiver sides. In the case of ML detection scheme we observe that system's performance increases with the disadvantage of a high complexity effort.

8.2 Experimental Results

Consider now the case where the experimental setup described above in Chapter 7 is used. A several amount of experiments has been carried out in an indoor environment, without any presence of movement between the transmitter and the receiver.

Moreover, we have experimented with different values of amplitude in means of scaling the oversampled transmitted waveforms for both of the users, as well as also with the location of the receiver relatively to the transmitter, in order to achieve transmissions at low SNR and evaluate the bit error rate degradation of the real-time system's perfrormance.

Taking under consideration the definition of Signal to Noise Ratio, for each one of the transmissions we can define at the receiver a ratio between the power of the received useful signal to the power of noise in the frequency domain which can give us measurements about the SNR at the base station.

As far as the power of the useful signal is concerned, we take advantage of our channel estimation for each sub-carrier $n = 0, \ldots, N_{tr} - 1$, $\hat{\tilde{\mathbf{H}}}[n]$, and our training symbols for both of the users $\tilde{\mathbf{d}}[n]$. Consequently, the power of the useful signal is

$$\mathbf{P} = \mathbf{E}[\|\hat{\tilde{\mathbf{H}}}[n]\tilde{\mathbf{d}}[n]\|^2] = \mathbf{E}[\tilde{\mathbf{d}}[n]^H \hat{\tilde{\mathbf{H}}}^H[n]\hat{\tilde{\mathbf{H}}}[n]\tilde{\mathbf{d}}[n]]. \tag{8.4}$$

We observe that

$$\begin{aligned}\hat{\tilde{\mathbf{H}}}^H[n]\hat{\tilde{\mathbf{H}}}[n] &= \begin{bmatrix} \hat{\tilde{h}}_1^{1\,H}[n] & \ldots & \hat{\tilde{h}}_A^{1\,H}[n] \\ \vdots & \ddots & \vdots \\ \hat{\tilde{h}}_1^{U\,H}[n] & \ldots & \hat{\tilde{h}}_A^{U\,H}[n] \end{bmatrix} \begin{bmatrix} \hat{\tilde{h}}_1^1[n] & \ldots & \hat{\tilde{h}}_1^U[n] \\ \vdots & \ddots & \vdots \\ \hat{\tilde{h}}_A^1[n] & \ldots & \hat{\tilde{h}}_A^U[n] \end{bmatrix} \\ &= \begin{bmatrix} \hat{\tilde{h}}_1^{1\,H}[n]\hat{\tilde{h}}_1^1[n] + \cdots + \hat{\tilde{h}}_A^{1\,H}[n]\hat{\tilde{h}}_A^1[n] & \ldots & \hat{\tilde{h}}_1^{1\,H}[n]\hat{\tilde{h}}_1^U[n] + \cdots + \hat{\tilde{h}}_A^{1\,H}[n]\hat{\tilde{h}}_A^U[n] \\ \vdots & \ddots & \vdots \\ \hat{\tilde{h}}_1^{U\,H}[n]\hat{\tilde{h}}_1^1[n] + \cdots + \hat{\tilde{h}}_A^{U\,H}[n]\hat{\tilde{h}}_A^1[n] & \ldots & \hat{\tilde{h}}_1^{U\,H}[n]\hat{\tilde{h}}_1^U[n] + \cdots + \hat{\tilde{h}}_A^{U\,H}[n]\hat{\tilde{h}}_A^U[n] \end{bmatrix}. \end{aligned} \tag{8.5}$$

As a result, from (8.4) we get

$$\mathbf{P} = \mathbf{E}[\begin{bmatrix} \tilde{d^1}^H[n] & \dots & \tilde{d^U}^H[n] \end{bmatrix} \hat{\tilde{\mathbf{H}}}^H[n]\hat{\tilde{\mathbf{H}}}[n] \begin{bmatrix} \tilde{d^1}[n] \\ \vdots \\ \tilde{d^U}[n] \end{bmatrix}]$$

$$= \mathbf{E}[\begin{bmatrix} \tilde{d^1}^H[n] \sum_{a=1}^{A} \|\hat{\tilde{h}}_a^1[n]\|^2 + \tilde{d^U}^H[n] \sum_{a=1}^{A} \hat{\tilde{h}}_a^U{}^H[n]\hat{\tilde{h}}_a^1[n] \\ \vdots \\ \tilde{d^1}^H[n] \sum_{a=1}^{A} \hat{\tilde{h}}_a^1{}^H[n]\hat{\tilde{h}}_a^U[n] + \tilde{d^U}^H[n] \sum_{a=1}^{A} \|\hat{\tilde{h}}_a^U[n]\|^2 \end{bmatrix}^T \begin{bmatrix} \tilde{d^1}[n] \\ \vdots \\ \tilde{d^U}[n] \end{bmatrix}]$$

$$= \mathbf{E}[\|\tilde{d^1}[n]\|^2\|\hat{\tilde{h}}_1^1[n]\|^2 + \dots + \|\tilde{d^1}[n]\|^2\|\hat{\tilde{h}}_A^1[n]\|^2 + \dots + \|\tilde{d^U}[n]\|^2\|\hat{\tilde{h}}_1^U[n]\|^2 + \dots + \|\tilde{d^1}[n]\|^2\|\hat{\tilde{h}}_A^U[n]\|^2] \tag{8.6}$$

for the case study of $u = 1, \dots, U$ users and $a = 1, \dots, A$ antennas at the basestation. We also have to note above that $\|\tilde{d^1}[n]\|^2 = \|\tilde{d^U}[n]\|^2 = \|\tilde{d}[n]\|^2 = 2$ as our users will transmit 4-QAM symbol sequences, while $\mathbf{E}[\hat{\tilde{h}}_a^u{}^H[n]\hat{\tilde{h}}_{a'}^{u'}[n]] = 0$ when $u' \neq u$ because of the fact that each user's channels are i.i.d and uncorrelated.
In our system set-up for $U = 2$ and $A = 2$ we get

$$\mathbf{P} = \mathbf{E}[\|\tilde{d}[n]\|^2(\|\hat{\tilde{h}}_1^1[n]\|^2 + \|\hat{\tilde{h}}_2^1[n]\|^2 + \|\hat{\tilde{h}}_1^2[n]\|^2 + \|\hat{\tilde{h}}_2^2[n]\|^2)] = \sum_{a=1}^{2} \frac{\sum_{n=0}^{N_{tr}-1} |\tilde{d}[n]|^2 (\sum_{u=1}^{2} \|\hat{\tilde{h}}_a^u[n]\|^2)}{N_{tr}}$$

Moreover, the power of noise at the base station for $a = 1, \dots, A$ antennas for each sub-carrier $n = 0, \dots, N_{tr} - 1$ is

$$\begin{aligned} \mathbf{P}_{\tilde{w}} = \mathbf{E}[\|\tilde{\mathbf{w}}[n]\|^2] = \mathbf{E}[\tilde{\mathbf{w}}^H[n]\tilde{\mathbf{w}}[n]] &= \mathbf{E}[\begin{bmatrix} \tilde{w}_1^H[n] & \dots & \tilde{w}_A^H[n]] \end{bmatrix} \begin{bmatrix} \tilde{w}_1[n] \\ \vdots \\ \tilde{w}_A[n] \end{bmatrix} \\ &= \mathbf{E}[\tilde{w}_1^H[n]\tilde{w}_1[n] + \dots + \tilde{w}_A^H[n]\tilde{w}_A[n]] \\ &= \mathbf{E}[\|\tilde{w}_1\|^2[n]] + \dots + \mathbf{E}[\|\tilde{w}_A\|^2[n]] \end{aligned} \tag{8.7}$$

where the power of noise at the a-th antenna $\mathbf{E}[\|\tilde{w}_a\|^2]$ is computed based on the difference between the received signal at the a-th antenna of the receiver and the expected one which is expressed in terms of the channels estimation in the frequency domain $\hat{\tilde{\mathbf{H}}}[n]$ and our training symbols $\tilde{\mathbf{d}}[n]$ for each sub-carrier n.
More analytically the power of noise at the a-th antenna can be expressed as

$$\mathbf{P}_{\tilde{w}_a} = \mathbf{E}[\|\tilde{w}_a[n]\|^2] = \frac{\sum_{n=0}^{N_{tr}-1} (\hat{\tilde{y}}_a[n] - \breve{\tilde{y}}_a[n])^2}{N_{tr}} \tag{8.8}$$

where $\breve{\tilde{y}}_a[n] = \begin{bmatrix} \hat{\tilde{h}}_a^1[n] & \dots & \hat{\tilde{h}}_a^U[n] \end{bmatrix} \begin{bmatrix} \tilde{d^1}[n] \\ \vdots \\ \tilde{d^U}[n] \end{bmatrix}$ denotes the expected received output at the a-th antenna for $n = 0, \dots, N_{tr} - 1$.

Generalizing all the above, relatively to the power of noise we get

$$\mathbf{P}_{\tilde{w}} = \mathbf{E}[\sum_{a=1}^{A} \|\tilde{w}_a[n]\|^2] = \sum_{a=1}^{A} \underbrace{\frac{\sum_{n=0}^{N_{tr}-1} (\hat{\tilde{\mathbf{y}}}[n] - \hat{\tilde{\mathbf{H}}}[n]\tilde{\mathbf{d}}[n])^2}{N_{tr}}}_{=\mathbf{E}[\|\tilde{w}_a[n]\|^2]} \tag{8.9}$$

In our case study specification for two users transmitting and one basestation equipped with two antennas playing the role of the receiver we get

$$\mathbf{P}_{\tilde{w}} = \sum_{a=1}^{2} \frac{\sum_{n=0}^{N_{tr}-1} (\hat{\tilde{y}}_a[n] - \breve{\tilde{y}}_a[n])^2}{N_{tr}}, \qquad n = 0, \ldots, N_{tr} - 1 \tag{8.10}$$

where $\breve{\tilde{y}}_a[n] = \begin{bmatrix} \hat{\tilde{h}}_a^1[n] & \hat{\tilde{h}}_a^2[n] \end{bmatrix} \begin{bmatrix} \tilde{d}^1[n] \\ \tilde{d}^2[n] \end{bmatrix}$ denotes the expected received signal at the a-th antenna of the basestation.

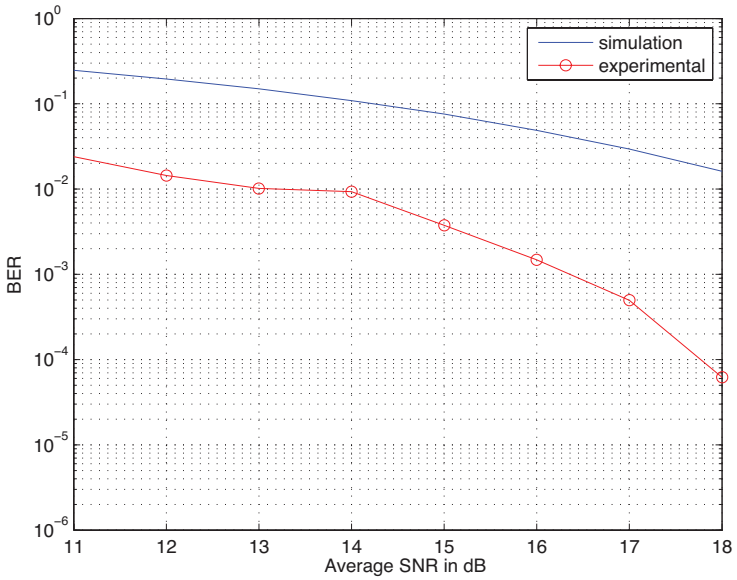

Figure 8.2.1: BER versus average SNR for OFDM-SDMA for U=2 and A=2.

Therefore, we can define the Signal to Noise Ratio in our experiments for measuring system's performance as the ratio

$$\mathrm{SNR}_{\mathrm{avg}} = \frac{\mathbf{E}_{\mathrm{p}}[\mathbf{P}]}{\mathbf{E}_{\mathrm{p}}[\mathbf{P}_{\tilde{\mathrm{w}}}]} = \frac{\sum_{\mathrm{a}=1}^{2} \frac{\sum_{\mathrm{n}=0}^{\mathrm{N_{tr}}-1} |\tilde{\mathrm{d}}[\mathrm{n}]|^2 (\sum_{\mathrm{u}=1}^{2} \|\hat{\tilde{\mathrm{h}}}_{\mathrm{a}}^{\mathrm{u}}[\mathrm{n}]\|^2)}{\mathrm{N_{tr}}}}{\sum_{\mathrm{a}=1}^{2} \frac{\sum_{\mathrm{n}=0}^{\mathrm{N_{tr}}-1} (\hat{\tilde{\mathrm{y}}}_{\mathrm{a}}[\mathrm{n}] - \breve{\tilde{\mathrm{y}}}_{\mathrm{a}}[\mathrm{n}])^2}{\mathrm{N_{tr}}}} \tag{8.11}$$

over the total number p of transmissions.

The experimental parameters are listed in Table 8.1. In addition, this experimental set-up does not consider a constant value for carrier frequency offset. Actually, carrier frequency offset between the receiver and the transmitter changes in respect to the location of the basestation relatively to the transmitter as well as with the presence of movement or not between them.

In 8.2.1, the bit error rate degradation for a flat fading channel is pictured, in combination with the simulation results given above where ZF detection scheme has been used, taking also under consideration non-constant CFO which is corrected efficiently at the receiver.

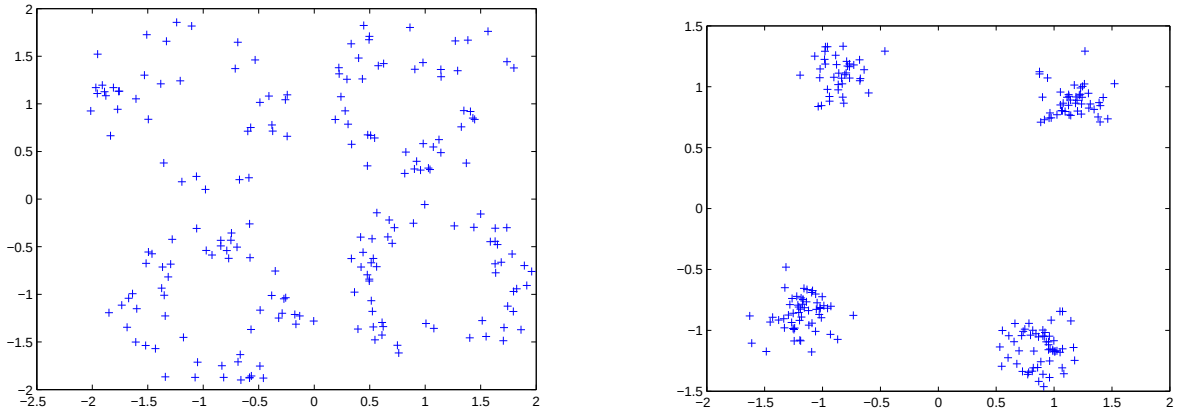

Figure 8.2.2: Scatterplot of the received symbols in the case of non-synchronized users for channel length $L = 1$ and $L = 3$ from left to right respectively.

In 8.2.2, we expected that in the case of dealing with $U = 2$ users which transmit with a time offset of over time instants, we could get the same results as in the case of synchronized multi-users if the channel's length L increased in the order of 2. In our implementation 8.2.2, the results pictured, come from an experiment where the channel length was firstly set to $L = 1$ where each user's symbols were not easily separated, while when we increased the channel length to $L = 3$ we get successul detection of our 4-QAM transmitted symbols at the BS.

Chapter 9

Conclusion and Future Work

This thesis project gave us a good knowledge of both OFDM and OFDM-SDMA systems, a good experimental backend throughout our implementation in SDR using the USRP.

In this thesis we presented how to cope with either synchronous or asynchronous multi-user MIMO systems. We have shown the complete system model for SISO, SIMO and MIMO systems, which we used for further evaluation of signal detection and carrier frequency offset compensation processes. We have also investigated the performance degradation of uplink OFDM-SDMA systems due to CFO and how this can be optimized using joint maximum likelihood channel and CFO estimation in the frequency domain before multi-user detection.

However, except simulating matlab codes for our study, we managed to implement all the above, by developing a SDR testbed consisted of two USRPs. As a result, we took advantage of the open source software toolkit called GNU Radio and became able to implement a real-time multi-user MIMO system with all the necessary signal processing blocks deployed.

9.1 Future Work

In the future it would be interesting to study different modulation methods, e.g.: 16-QAM, 64-QAM as well as channel coding. In means of improving the system performance in such practical systems more work needs to be done on channel coding (FEC) and signal modulation methods.

Finally it would be interesting to investigate the case where each of the multiple users transmitting, introduces a different carrier frequency offset and how can this directly affect our system's performance.

Appendix

Proof of (5.9)

We observe that

$$\begin{aligned}\|\tilde{\mathbf{y}}'_{tr} - \mathbf{B}\breve{\mathbf{h}}_{tr}\|^2 &= [\tilde{\mathbf{y}}'_{tr} - \mathbf{B}\breve{\mathbf{h}}_{tr}]^H[\tilde{\mathbf{y}}'_{tr} - \mathbf{B}\breve{\mathbf{h}}_{tr}] \\ &= [\tilde{\mathbf{y}'}^H_{tr}\tilde{\mathbf{y}}'_{tr} - \tilde{\mathbf{y}'}^H_{tr}\mathbf{B}\breve{\mathbf{h}}_{tr} - \breve{\mathbf{h}}^H_{tr}\mathbf{B}^H\tilde{\mathbf{y}}'_{tr} + \breve{\mathbf{h}}^H_{tr}\mathbf{B}^H\mathbf{B}\breve{\mathbf{h}}_{tr}].\end{aligned}$$

Substituting the above in (5.8), gives us

$$\begin{aligned}&\nabla_{\breve{\mathbf{h}}_{tr}}[\tilde{\mathbf{y}'}^H_{tr}\tilde{\mathbf{y}}'_{tr} - \tilde{\mathbf{y}'}^H_{tr}\mathbf{B}\breve{\mathbf{h}}_{tr} - \breve{\mathbf{h}}^H_{tr}\mathbf{B}^H\tilde{\mathbf{y}}'_{tr} + \breve{\mathbf{h}}^H_{tr}\mathbf{B}^H\mathbf{B}\breve{\mathbf{h}}_{tr}] = 0 \\ &\implies \nabla_{\breve{\mathbf{h}}_{tr}}[\tilde{\mathbf{y}'}^H_{tr}\tilde{\mathbf{y}}'_{tr}] - \nabla_{\breve{\mathbf{h}}_{tr}}[\tilde{\mathbf{y}'}^H_{tr}\mathbf{B}\breve{\mathbf{h}}_{tr}] - \nabla_{\breve{\mathbf{h}}_{tr}}[\breve{\mathbf{h}}^H_{tr}\mathbf{B}^H\tilde{\mathbf{y}}'_{tr}] + \nabla_{\breve{\mathbf{h}}_{tr}}[\breve{\mathbf{h}}^H_{tr}\mathbf{B}^H\mathbf{B}\breve{\mathbf{h}}_{tr}] = 0 \\ &\implies -\tilde{\mathbf{y}'}^H_{tr}\mathbf{B} - \mathbf{B}^H\tilde{\mathbf{y}}'_{tr} + 2\breve{\mathbf{h}}^H_{tr}\mathbf{B}^H\mathbf{B} = 0 \\ &\implies -2\tilde{\mathbf{y}'}^H_{tr}\tilde{\mathbf{B}} + 2\breve{\mathbf{h}}^H_{tr}\mathbf{B}^H\mathbf{B} = 0 \\ &\implies \breve{\mathbf{h}}^H_{tr}\mathbf{B}^H\mathbf{B} = \tilde{\mathbf{y}'}^H_{tr}\mathbf{B} \\ &\implies \hat{\mathbf{h}}_{ML} = (\mathbf{B}^H\mathbf{B})^{-1}\mathbf{B}^H\tilde{\mathbf{y}}'_{tr},\end{aligned}$$

hence (**??**) is obtained.

□

Proof of (5.22)

We observe that

$$\begin{aligned}\|\tilde{\mathbf{y}}'_{tr} - \tilde{\mathbf{F}}_{tr}\tilde{\breve{\mathbf{\Gamma}}}_{tr}\tilde{\mathbf{A}}_{tr}\breve{\mathbf{h}}_{tr}\|^2 &= [\tilde{\mathbf{y}}'_{tr} - \tilde{\mathbf{F}}_{tr}\tilde{\breve{\mathbf{\Gamma}}}_{tr}\tilde{\mathbf{A}}_{tr}\breve{\mathbf{h}}_{tr}]^H[\tilde{\mathbf{y}}'_{tr} - \tilde{\mathbf{F}}_{tr}\tilde{\breve{\mathbf{\Gamma}}}_{tr}\tilde{\mathbf{A}}_{tr}\breve{\mathbf{h}}_{tr}] \\ &= [\tilde{\mathbf{y}'}^H_{tr}\tilde{\mathbf{y}}'_{tr} - \tilde{\mathbf{y}'}^H_{tr}\tilde{\mathbf{F}}_{tr}\tilde{\breve{\mathbf{\Gamma}}}_{tr}\tilde{\mathbf{A}}_{tr}\breve{\mathbf{h}}_{tr} + \breve{\mathbf{h}}^H_{tr}\tilde{\mathbf{A}}^H_{tr}\tilde{\breve{\mathbf{\Gamma}}}^H_{tr}\tilde{\mathbf{F}}^H_{tr}\tilde{\mathbf{y}}'_{tr} + \\ &\quad + \breve{\mathbf{h}}^H_{tr}\tilde{\mathbf{A}}^H_{tr}\tilde{\breve{\mathbf{\Gamma}}}^H_{tr}\tilde{\mathbf{F}}^H_{tr}\tilde{\mathbf{F}}\tilde{\breve{\mathbf{\Gamma}}}_{tr}\tilde{\mathbf{A}}_{tr}\breve{\mathbf{h}}_{tr}].\end{aligned}$$

Substituting the above in (5.21), gives us

$$\begin{aligned}
&\nabla_{\check{\mathbf{h}}_{tr}}[\tilde{\mathbf{y}'}_{tr}^{H}\tilde{\mathbf{y}}'_{tr} - \tilde{\mathbf{y}'}_{tr}^{H}\tilde{\mathbf{F}}_{tr}\breve{\tilde{\mathbf{\Gamma}}}_{tr}\tilde{\mathbf{A}}_{tr}\check{\mathbf{h}}_{tr} + \check{\mathbf{h}}_{tr}^{H}\tilde{\mathbf{A}}_{tr}^{H}\breve{\tilde{\mathbf{\Gamma}}}_{tr}^{H}\tilde{\mathbf{F}}_{tr}^{H}\tilde{\mathbf{y}}'_{tr} + \check{\mathbf{h}}_{tr}^{H}\tilde{\mathbf{A}}_{tr}^{H}\breve{\tilde{\mathbf{\Gamma}}}_{tr}^{H}\tilde{\mathbf{F}}_{tr}^{H}\tilde{\mathbf{F}}_{tr}\breve{\tilde{\mathbf{\Gamma}}}_{tr}\tilde{\mathbf{A}}_{tr}\check{\mathbf{h}}_{tr}] = 0\\
&\implies \nabla_{\check{\mathbf{h}}_{tr}}[\tilde{\mathbf{y}'}_{tr}^{H}\tilde{\mathbf{y}}'_{tr}] - \nabla_{\check{\mathbf{h}}_{tr}}[\tilde{\mathbf{y}'}_{tr}^{H}\tilde{\mathbf{F}}_{tr}\breve{\tilde{\mathbf{\Gamma}}}_{tr}\tilde{\mathbf{A}}_{tr}\check{\mathbf{h}}_{tr}] + \nabla_{\check{\mathbf{h}}_{tr}}[\check{\mathbf{h}}_{tr}^{H}\tilde{\mathbf{A}}_{tr}^{H}\breve{\tilde{\mathbf{\Gamma}}}_{tr}^{H}\tilde{\mathbf{F}}_{tr}^{H}\tilde{\mathbf{y}}'_{tr}]+\\
&+ \nabla_{\check{\mathbf{h}}_{tr}}[\check{\mathbf{h}}_{tr}^{H}\tilde{\mathbf{A}}_{tr}^{H}\breve{\tilde{\mathbf{\Gamma}}}_{tr}^{H}\tilde{\mathbf{F}}_{tr}^{H}\tilde{\mathbf{F}}_{tr}\breve{\tilde{\mathbf{\Gamma}}}_{tr}\tilde{\mathbf{A}}_{tr}\check{\mathbf{h}}_{tr}] = 0\\
&\implies -\tilde{\mathbf{y}'}_{tr}^{H}\tilde{\mathbf{F}}_{tr}\breve{\tilde{\mathbf{\Gamma}}}_{tr}\tilde{\mathbf{A}}_{tr} - \tilde{\mathbf{A}}_{tr}^{H}\breve{\tilde{\mathbf{\Gamma}}}_{tr}^{H}\tilde{\mathbf{F}}_{tr}\tilde{\mathbf{y}}'_{tr} + 2\check{\mathbf{h}}_{tr}^{H}\tilde{\mathbf{A}}_{tr}^{H}\breve{\tilde{\mathbf{\Gamma}}}_{tr}^{H}\underbrace{\tilde{\mathbf{F}}_{tr}^{H}\tilde{\mathbf{F}}_{tr}}_{=\mathbf{I}}\breve{\tilde{\mathbf{\Gamma}}}_{tr}\tilde{\mathbf{A}}_{tr}\check{\mathbf{h}}_{tr} = 0\\
&\implies -2\tilde{\mathbf{y}'}_{tr}^{H}\tilde{\mathbf{F}}_{tr}\breve{\tilde{\mathbf{\Gamma}}}_{tr}\tilde{\mathbf{A}}_{tr} + 2\check{\mathbf{h}}_{tr}\tilde{\mathbf{A}}_{tr}^{H}\underbrace{\breve{\tilde{\mathbf{\Gamma}}}_{tr}^{H}\breve{\tilde{\mathbf{\Gamma}}}_{tr}}_{=\mathbf{I}}\tilde{\mathbf{A}}_{tr} = 0\\
&\implies \check{\mathbf{h}}_{tr}^{H}\tilde{\mathbf{A}}_{tr}^{H}\tilde{\mathbf{A}}_{tr} = \tilde{\mathbf{y}'}_{tr}^{H}\tilde{\mathbf{F}}_{tr}\breve{\tilde{\mathbf{\Gamma}}}_{tr}\tilde{\mathbf{A}}_{tr}\\
&\implies \hat{\mathbf{h}}_{ML} = \frac{\tilde{\mathbf{A}}_{tr}^{H}\breve{\tilde{\mathbf{\Gamma}}}_{tr}^{H}\tilde{\mathbf{F}}_{tr}^{H}}{(\tilde{\mathbf{A}}_{tr}^{H}\tilde{\mathbf{A}}_{tr})}\tilde{\mathbf{y}}'_{tr}\\
&\implies \hat{\mathbf{h}}_{ML} = (\tilde{\mathbf{A}}_{tr}^{H}\tilde{\mathbf{A}}_{tr})^{-1}\tilde{\mathbf{A}}_{tr}^{H}\breve{\tilde{\mathbf{\Gamma}}}_{tr}^{H}\tilde{\mathbf{F}}_{tr}^{H}\tilde{\mathbf{y}}'_{tr}.
\end{aligned}$$

hence (5.22) is obtained.

□

Proof of (5.25)

The ML estimate $\hat{\nu}_{ML}(\tilde{\mathbf{y}}'_{tr})$ minimizes $\|\tilde{\mathbf{y}}'_{tr} - \tilde{\mathbf{F}}_{tr}\breve{\tilde{\mathbf{\Gamma}}}_{tr}\mathbf{P}\breve{\tilde{\mathbf{F}}}_{tr}^{H}\tilde{\mathbf{y}}'_{tr}\|^2$ which is equivalent to

$$\begin{aligned}
\hat{\nu}_{ML}(\tilde{\mathbf{y}}'_{tr}) &= \arg\min_{\breve{\nu}}\|\tilde{\mathbf{y}}'_{tr} - \tilde{\mathbf{F}}_{tr}\breve{\tilde{\mathbf{\Gamma}}}_{tr}\mathbf{P}\breve{\tilde{\mathbf{\Gamma}}}_{tr}^{H}\tilde{\mathbf{F}}_{tr}^{H}\tilde{\mathbf{y}}'_{tr}\|^2\\
&= \arg\min_{\breve{\nu}}[\tilde{\mathbf{y}}'_{tr} - \tilde{\mathbf{F}}_{tr}\breve{\tilde{\mathbf{\Gamma}}}_{tr}\mathbf{P}\breve{\tilde{\mathbf{\Gamma}}}_{tr}^{H}\tilde{\mathbf{F}}_{tr}^{H}\tilde{\mathbf{y}}'_{tr}]^{H}[\tilde{\mathbf{y}}'_{tr} - \tilde{\mathbf{F}}_{tr}\breve{\tilde{\mathbf{\Gamma}}}_{tr}\mathbf{P}\breve{\tilde{\mathbf{\Gamma}}}_{tr}^{H}\tilde{\mathbf{F}}_{tr}^{H}\tilde{\mathbf{y}}'_{tr}]\\
&= \arg\min_{\breve{\nu}}[\tilde{\mathbf{y}'}_{tr}^{H}\tilde{\mathbf{y}}'_{tr} - \tilde{\mathbf{y}}_{tr}^{H}\tilde{\mathbf{F}}_{tr}\breve{\tilde{\mathbf{\Gamma}}}_{tr}\mathbf{P}\breve{\tilde{\mathbf{\Gamma}}}_{tr}^{H}\tilde{\mathbf{F}}_{tr}^{H}\tilde{\mathbf{y}}'_{tr} - \tilde{\mathbf{y}'}_{tr}^{H}\tilde{\mathbf{F}}_{tr}\breve{\tilde{\mathbf{\Gamma}}}_{tr}\mathbf{P}^{H}\breve{\tilde{\mathbf{\Gamma}}}_{tr}^{H}\tilde{\mathbf{F}}_{tr}^{H}\tilde{\mathbf{y}}'_{tr}+\\
&+ \tilde{\mathbf{y}'}_{tr}^{H}\tilde{\mathbf{F}}_{tr}\breve{\tilde{\mathbf{\Gamma}}}_{tr}\mathbf{P}^{H}\breve{\tilde{\mathbf{\Gamma}}}_{tr}^{H}\underbrace{\tilde{\mathbf{F}}_{tr}^{H}\tilde{\mathbf{F}}_{tr}}_{=\mathbf{I}_{N_{tr}\times N_{tr}}}\breve{\tilde{\mathbf{\Gamma}}}_{tr}\mathbf{P}\breve{\tilde{\mathbf{\Gamma}}}_{tr}^{H}\tilde{\mathbf{F}}_{tr}^{H}\tilde{\mathbf{y}}'_{tr}]\\
&= \arg\min_{\breve{\nu}}[\tilde{\mathbf{y}'}_{tr}^{H}\tilde{\mathbf{y}}'_{tr} - 2\tilde{\mathbf{F}}_{tr}\breve{\tilde{\mathbf{\Gamma}}}_{tr}\mathbf{P}\breve{\tilde{\mathbf{\Gamma}}}_{tr}^{H}\tilde{\mathbf{F}}_{tr}^{H}\tilde{\mathbf{y}}'_{tr} + \tilde{\mathbf{y}'}_{tr}^{H}\tilde{\mathbf{F}}_{tr}\breve{\tilde{\mathbf{\Gamma}}}_{tr}\mathbf{P}^{H}\underbrace{\breve{\tilde{\mathbf{\Gamma}}}_{tr}^{H}\breve{\tilde{\mathbf{\Gamma}}}_{tr}}_{=\mathbf{I}_{N_{tr}\times N_{tr}}}\mathbf{P}\breve{\tilde{\mathbf{\Gamma}}}_{tr}^{H}\tilde{\mathbf{F}}_{tr}^{H}\tilde{\mathbf{y}}'_{tr}]\\
&= \arg\min_{\breve{\nu}}[\tilde{\mathbf{y}'}_{tr}^{H}\tilde{\mathbf{y}}'_{tr} - 2\tilde{\mathbf{y}'}_{tr}^{H}\tilde{\mathbf{F}}_{tr}\breve{\tilde{\mathbf{\Gamma}}}_{tr}\mathbf{P}\breve{\tilde{\mathbf{\Gamma}}}_{tr}^{H}\tilde{\mathbf{F}}_{tr}^{H}\tilde{\mathbf{y}}'_{tr} + \tilde{\mathbf{y}'}_{tr}^{H}\tilde{\mathbf{F}}_{tr}\breve{\tilde{\mathbf{\Gamma}}}_{tr}\mathbf{P}^{H}\mathbf{P}\breve{\tilde{\mathbf{\Gamma}}}_{tr}^{H}\tilde{\mathbf{F}}_{tr}^{H}\tilde{\mathbf{y}}'_{tr}]\\
&= \arg\min_{\breve{\nu}}[\tilde{\mathbf{y}'}_{tr}^{H}\tilde{\mathbf{y}}'_{tr} - 2\tilde{\mathbf{y}}_{tr}^{H}\tilde{\mathbf{F}}_{tr}\breve{\tilde{\mathbf{\Gamma}}}_{tr}\mathbf{P}\breve{\tilde{\mathbf{\Gamma}}}_{tr}^{H}\tilde{\mathbf{F}}_{tr}^{H}\tilde{\mathbf{y}}'_{tr} + \tilde{\mathbf{y}'}_{tr}^{H}\tilde{\mathbf{F}}_{tr}\breve{\tilde{\mathbf{\Gamma}}}_{tr}\underbrace{\mathbf{P}\mathbf{P}}_{=\mathbf{P}^2}\breve{\tilde{\mathbf{\Gamma}}}_{tr}^{H}\tilde{\mathbf{F}}_{tr}^{H}\tilde{\mathbf{y}}'_{tr}]\\
&\underbrace{=}_{\mathbf{P}^2=\mathbf{P}} \arg\min_{\breve{\nu}}[\tilde{\mathbf{y}'}_{tr}^{H}\tilde{\mathbf{y}}'_{tr} - 2\tilde{\mathbf{y}'}_{tr}^{H}\tilde{\mathbf{F}}_{tr}\breve{\tilde{\mathbf{\Gamma}}}_{tr}\mathbf{P}\breve{\tilde{\mathbf{\Gamma}}}_{tr}^{H}\tilde{\mathbf{F}}_{tr}^{H}\tilde{\mathbf{y}}'_{tr} + \tilde{\mathbf{y}'}_{tr}^{H}\tilde{\mathbf{F}}_{tr}\breve{\tilde{\mathbf{\Gamma}}}_{tr}\mathbf{P}\breve{\tilde{\mathbf{\Gamma}}}_{tr}^{H}\tilde{\mathbf{F}}_{tr}^{H}\tilde{\mathbf{y}}'_{tr}]\\
&= \arg\min_{\breve{\nu}}[\tilde{\mathbf{y}'}_{tr}^{H}\tilde{\mathbf{y}}'_{tr} - \tilde{\mathbf{y}'}_{tr}^{H}\tilde{\mathbf{F}}_{tr}\breve{\tilde{\mathbf{\Gamma}}}_{tr}\mathbf{P}\breve{\tilde{\mathbf{\Gamma}}}_{tr}^{H}\tilde{\mathbf{F}}_{tr}^{H}\tilde{\mathbf{y}}'_{tr}]
\end{aligned}$$

hence the $\hat{\nu}$-estimator expressed in (5.25) is obtained.

□

Proof of (5.25)

We observe that

$$\begin{aligned}\|\hat{\tilde{\mathbf{H}}}[n]\tilde{\mathbf{d}}[n]-\hat{\tilde{\mathbf{y}}}[n]\|^2 &= [\hat{\tilde{\mathbf{H}}}[n]\tilde{\mathbf{d}}[n]-\hat{\tilde{\mathbf{y}}}[n]]^H[\hat{\tilde{\mathbf{H}}}[n]\tilde{\mathbf{d}}[n]-\hat{\tilde{\mathbf{y}}}[n]]\\ &= [\tilde{\mathbf{d}}^H[n]\hat{\tilde{\mathbf{H}}}^H[n]\hat{\tilde{\mathbf{H}}}[n]\tilde{\mathbf{d}}[n]-\hat{\tilde{\mathbf{y}}}^H[n]\hat{\tilde{\mathbf{H}}}[n]\tilde{\mathbf{d}}[n]-\tilde{\mathbf{d}}^H[n]\hat{\tilde{\mathbf{H}}}^H[n]\hat{\tilde{\mathbf{y}}}[n]+\\ &= +\hat{\tilde{\mathbf{y}}}^H[n]\hat{\tilde{\mathbf{y}}}[n]]\end{aligned}$$

Substituting the above in (6.9), gives us

$$\begin{aligned}&\nabla_{\tilde{\mathbf{d}}}[\tilde{\mathbf{d}}^H[n]\hat{\tilde{\mathbf{H}}}^H[n]\hat{\tilde{\mathbf{H}}}[n]\tilde{\mathbf{d}}[n]-\hat{\tilde{\mathbf{y}}}^H[n]\hat{\tilde{\mathbf{H}}}[n]\tilde{\mathbf{d}}[n]-\tilde{\mathbf{d}}^H[n]\hat{\tilde{\mathbf{H}}}^H[n]\hat{\tilde{\mathbf{y}}}[n]+\hat{\tilde{\mathbf{y}}}^H[n]\hat{\tilde{\mathbf{y}}}[n]]=0\\ &\implies \nabla_{\tilde{\mathbf{d}}}[\tilde{\mathbf{d}}^H[n]\hat{\tilde{\mathbf{H}}}^H[n]\hat{\tilde{\mathbf{H}}}[n]\tilde{\mathbf{d}}[n]]-\nabla_{\tilde{\mathbf{d}}}[\hat{\tilde{\mathbf{y}}}^H[n]\hat{\tilde{\mathbf{H}}}[n]\tilde{\mathbf{d}}[n]]-\nabla_{\tilde{\mathbf{d}}}[\tilde{\mathbf{d}}^H[n]\hat{\tilde{\mathbf{H}}}^H[n]\hat{\tilde{\mathbf{y}}}[n]]+\nabla_{\tilde{\mathbf{d}}}[\hat{\tilde{\mathbf{y}}}^H[n]\hat{\tilde{\mathbf{y}}}[n]]=0\\ &\implies -\hat{\tilde{\mathbf{y}}}^H[n]\hat{\tilde{\mathbf{H}}}[n]-\hat{\tilde{\mathbf{H}}}^H[n]\hat{\tilde{\mathbf{y}}}[n]+2\tilde{\mathbf{d}}^H[n]\hat{\tilde{\mathbf{H}}}^H[n]\hat{\tilde{\mathbf{H}}}[n]=0\\ &\implies -2\hat{\tilde{\mathbf{y}}}^H[n]\hat{\tilde{\mathbf{H}}}[n]+2\tilde{\mathbf{d}}^H[n]\hat{\tilde{\mathbf{H}}}^H[n]\hat{\tilde{\mathbf{H}}}[n]=0\\ &\implies \tilde{\mathbf{d}}^H[n]\hat{\tilde{\mathbf{H}}}^H[n]\hat{\tilde{\mathbf{H}}}[n]=\hat{\tilde{\mathbf{y}}}^H[n]\hat{\tilde{\mathbf{H}}}[n]\\ &\implies \hat{\tilde{\mathbf{d}}}_{LS}[n]=(\hat{\tilde{\mathbf{H}}}^H[n]\hat{\tilde{\mathbf{H}}}[n])^{-1}\hat{\tilde{\mathbf{H}}}^H[n]\hat{\tilde{\mathbf{y}}}[n]\end{aligned}$$

hence (6.10) is obtained.

□

Bibliography

[1] D. Tse and P. Viswanath "Fundamental of Wireless Communication", *Cambridge University Press*, 2005.

[2] A. P. Liavas, "Introduction in Wireless Communication", *Electronic and Computer Engineering Dept., Technical University of Crete*, Dec. 2009.

[3] J. Bingham, "Multicarrier modulation for data transmission: An Idea whose time has come", *IEEE Commun. Mag.*, vol. 28, pp. 5-14, May 1990.

[4] P. Vandenameele, "Space Division Multiple Access For Wireless Local Area Networks", *Kluwer Academic Publishers*, 2001.

[5] M. Luise and R. Reggiannini, "Carrier frequency acquisition and tracking for OFDM systems", *IEEE Trans. Commun.*, vol. 44, pp. 1590-1598, Nov. 1996.

[6] M. Morelli and U. Mengali "Carrier-frequency estimation for transmissions over selective channels", *IEEE Trans. Commun.*, vol.48, no. 9, pp. 1580-1589, Sep. 2000.

[7] Matt Ettus, Universal software radio peripheral. http://www.ettus.com.

[8] S. Zhou, K. Zhang and Z. Niu "On the Impact of Carrier Frequency Offsets in OFDM/SDMA Systems", *in Proc. ICC 2007.*

[9] S. Thoen, L. Deneire, L. V. der Perre, M. Engels and H. De Man "Constrained Least Squares Detector for OFDM/SDMA Wireless Networks", *IEEE Trans. Wireless Commun.*, vol. 2, no. 1, pp. 129-140, Jan. 2003.

[10] T. Cui and C. Tellambura "Joint Frequency Offset and Channel Estimation for OFDM Systems Using Pilot Symbols and Virtual Carriers", *IEEE Trans. Wireless Commun.*, vol. 6, no. 4, pp. 1193-1202, April 2007.

[11] J. G. Proakis and D. G. Manolakis "Digital Signal Processing - Principles, Algorithms and Applications", *Prentice-Hall International, Inc.*, 1996.

[12] V. Kotzsch, J. Holfeld and G. Fettweis "Joint Detection and CFO Compensation in Asynchronous Multi-User MIMO OFDM Systems",

[13] D. Huang and K. B. Letaief "Carrier Frequency Offset Estimation for OFDM Systems Using Null sub-carriers", *IEEE Trans, Commun.*, vol. 54, no. 5, pp. 813-823, May 2006.

[14] J. Lee, H. -L. Lou, D. Toumpakaris and J. M. Cioffi, "SNR Analysis of OFDM Systems in the Presence of Carrier Frequency Offset for Fading Channels", *IEEE Trans, Wireless Commun.*, vol. 5, no. 12, pp. 3360-3364, 2006.

[15] X. Dai, "Carrier Frequency Offset Estimation for OFDM/SDMA Systems Using Consecutive Pilots", *IEEE Proc. Commun.*, vol. 152, no. 5, pp. 624-632, Oct. 2005.

[16] M. Schellmann and V. Jungnickel, "Multiple CFOs in OFDM-SDMA Uplink: Interference Analysis and Compensation", *EURASIP Journal on Wireless Communications and Networking*, 2009.

[17] B. C. Levy, "Principles of Signal Detection and Parameter Estimation", *Springer Science and Business Media*, 2008.

[18] X. Ma, H. Kobayashi and S. C. Schwartz, "Joint Frequency Offset and Channel Estimation for OFDM", *in Proc. GLOBECOM 2003*, pp. 15-19.

[19] T. Cui and C. Tellambura, "Maximum-Likelihood Carrier Frequency Offset Estimation for OFDM Systems over Frequency-Selective Channels", *in Proc. ICC 2005.*

[20] B. Chen, "Maximum Likelihood Estimation of OFDM Carrier Frequency Offset", *IEEE Signal Processing Lett.*, vol. 9, no. 4, pp. 123-126, April 2002.

[21] E. Blossom, "Exploring GNU Radio" http://www.gnu.org/software/gnuradio/doc/exploring-gnuradio.html

[22] M. Ettus, "USRP User's and Developer's Guide" http://www.olifantasia.com/gnuradio/usrp/files/usrp_guide.pdf.